UNIVERSITÀ DEGLI STUDI
DI GENOVA

ISTITUTO ITALIANO
DI TECNOLOGIA

PHD PROGRAM IN BIOENGINEERING AND ROBOTICS

Understanding motor control in humans to improve rehabilitation robots

Amel Cherif

Thesis submitted for the degree of Doctor of Philosophy (XXXII cycle)

December 2019

Jacopo Zenzeri	Supervisor
Pietro Morasso	Supervisor
Giorgio Cannata	Head of PhD program

Thesis Jury:

Serena Ivaldi, INRIA	External examiner
Yasuyuki Suzuki, Osaka University	External examiner
Maura Casadio, Università di Genova	Internal examiner

Declaration

I hereby declare that except where specific reference is made to the work of others, the contents of this dissertation are original and have not been submitted in whole or in part for consideration for any other degree or qualification in this, or any other university. This dissertation is my own work and contains nothing which is the outcome of work done in collaboration with others, except as specified in the text and Acknowledgements. This dissertation contains fewer than 65,000 words including appendices, bibliography, footnotes, tables and equations and has fewer than 150 figures.

Amel Cherif

December 2019

Acknowledgements

I would like to thank my supervisors, Jacopo Zenzeri and Pietro Morasso who gave me the opportunity to work in an exceptional research environment and guided me over all these years.

I deeply thank Prof. Ian Loram for hosting me in his lab in Manchester and for his precious support through these three years.

Thanks also to Giulio Sandini for coordinating our research department and giving us the opportunity to carry on our activities.

I acknowledge our technical and administrative collaborators from IIT always available whenever needed.

Thanks to all the participants of my studies for their patience and their cooperation.

Grazie alle mie colleghe e amiche del Motor Learning Assistive Rehabilitation Robotics lab: grazie alle vecchiette Maddalena e Francesca con cui ho condiviso 'gioie e dolori' durante tutto questo percorso e alle new entries Giulia A., Giulia B., Giulia P., Valeria e Gaia per la loro positività e solidarietà femminile. Grazie anche ad Anna Vera per avermi dato la possibilità di dare seguito alla sua ricerca.

Grazie a Marcello, per avermi aiutato a 'cacciare i mostri' nascosti nel software del Wristbot e per le nostre pause caffè.

Thanks to the iCub Reddy friends with whom I shared not only the office spaces but the entire 'PhD life'.

Grazie alle mie 'sorelline' Denise e Selene, per esserci sempre state sin dall'infanzia.

Grazie a Massimo per essere al mio fianco e grazie alla mia famiglia, senza la quale non sarei arrivata fin qui.

Publications

Journal articles

P. Morasso, **A. Cherif**, J. Zenzeri. "Quiet standing: The single inverted pendulum model is not so bad after all". PLoS ONE. 2019.

A. Cherif, I. Loram, J. Zenzeri. "Effect of motor and sensory noise in the control of upright standing". Progress in Brain Research. 2019.

R. Iandolo, F. Marini, M. Semprini, M. Laffranchi, M. Mugnosso, **A. Cherif**, L. De Michieli, M. Chiappalone, J. Zenzeri . "Perspectives and challenges in robotic neurorehabilitation". Applied Sciences. 2019.

L. Avanzino[+], **A. Cherif**[+], O. Crisafulli, F. Carbone, J. Zenzeri, P. Morasso, G. Abbruzzese, E. Pelosin, J. Konczak. "Tactile and proprioceptive dysfunction differentiates cervical dystonia with and without tremor". Neurology. 2020.

A. Cherif, I. Loram, J. Zenzeri. "Human balance of an inverted pendulum: force accuracy rather than high stiffness is associated with greater learning and reduced falls". Under review for Scientific Reports

P. Morasso[+], **A. Cherif**[+], J. Zenzeri. "State space intermittent feedback stabilization of a dual balancing task". Under review for Scientific Reports

A. Cherif, J .Zenzeri, I. Loram. "Intermittency in human balance". In preparation for Journal of Physiology.

+equal contribution

Conference proceedings

A. Cherif, J. Zenzeri, P. Morasso. "Preliminary results of a dual balancing task." In Engineering in Medicine and Biology Society (EMBC), 2019 41st Annual International Conference of the IEEE

Other conferences

Congresso Nazionale SIMFER. October 2017. Genova.
Valutazione quantitativa della sensibilità propriocettiva in pazienti affetti da distonia cervicale
A. Cherif, A.V. Cuppone, F. Carbone, O. Crisafulli, A. Ravaschio, G. Abruzzese, P. Morasso, J. Konczak, J. Zenzeri, E. Pelosin and L. Avanzino

PACE Workshop. October 2017. Genova.
Strategies characterization during destabilized standing
A. Cherif, I. Loram, H. Gollee, J. Zenzeri.

Society for Neuroscience 2017. November 2017. Washington DC.
Learning postural balancing in a dynamic destabilizing environment.
A. Cherif, I. Loram, H. Gollee, J. Zenzeri.

Mathematical modeling in motor neuroscience. June 2018. Pavia.
Emergence of multiple postural control strategies in destabilizing environments.
A.Cherif, I. Loram, H. Gollee, J. Zenzeri.

Workshop Innovation in Rehabilitation Technologies. March 2019. Genova.
Robot-based proprioceptive assessment in cervical dystonia patients.
A. Cherif, A.V. Cuppone, F. Carbone, O. Crisafulli, A. Ravaschio, G. Abruzzese, P. Morasso, J. Konczak, J. Zenzeri, E. Pelosin and L. Avanzino.

Society for neural control of movement. April 2019. Toyama.
Stick balancing while standing: an example of dual unstable task control.
A.Cherif, J. Zenzeri, P. Morasso.

IEEE Engineering in Medicine and Biology Society. June 2019. Berlin.
Motor Control Mechanisms in Multi Strategies and Multi Goals Tasks
J. Zenzeri, **A. Cherif**, G. Belgiovine, P. Morasso.

Invited talk

Osaka University. May 2019. Understanding motor control in humans to improve rehabilitation robots.

Abstract

Recent reviews highlighted the limited results of robotic rehabilitation and the low quality of evidences in this field. Despite the worldwide presence of several robotic infrastructures, there is still a lack of knowledge about the capabilities of robotic training effect on the neural control of movement. To fill this gap, a step back to motor neuroscience is needed: the understanding how the brain works in the generation of movements, how it adapts to changes and how it acquires new motor skills is fundamental. This is the rationale behind my PhD project and the contents of this thesis: all the studies included in fact examined changes in motor control due to different destabilizing conditions, ranging from external perturbations, to self-generated disturbances, to pathological conditions.

Data on healthy and impaired adults have been collected and quantitative and objective information about kinematics, dynamics, performance and learning were obtained for the investigation of motor control and skill learning.

Results on subjects with cervical dystonia show how important assessment is: possibly adequate treatments are missing because the physiological and pathological mechanisms underlying sensorimotor control are not routinely addressed in clinical practice. These results showed how sensory function is crucial for motor control.

The relevance of proprioception in motor control and learning is evident also in a second study. This study, performed on healthy subjects, showed that stiffness control is associated with worse robustness to external perturbations and worse learning, which can be attributed to the lower sensitiveness while moving or co-activating. On the other hand, we found that the combination of higher reliance on proprioception with "disturbance training" is able to lead to a better learning and better robustness. This is in line with recent findings showing that variability may facilitate learning and thus can be exploited for sensorimotor recovery.

Based on these results, in a third study, we asked participants to use the more robust and efficient strategy in order to investigate the control policies used to reject disturbances. We found that control is non-linear and we associated this non-linearity with intermittent control. As the name says, intermittent control is characterized by open loop intervals, in which movements are not actively controlled.

We exploited the intermittent control paradigm for other two modeling studies. In these studies we have shown how robust is this model, evaluating it in two complex situations, the coordination of two joints for postural balance and the coordination of two different balancing tasks. It is an intriguing issue, to be addressed in future studies, to consider how learning affects intermittency and how this can be exploited to enhance learning or recovery.

The approach, that can exploit the results of this thesis, is the computational neurorehabilitation, which mathematically models the mechanisms underlying the rehabilitation process, with the aim of optimizing the individual treatment of patients. Integrating models of sensorimotor control during robotic neurorehabilitation, might lead to robots that are fully adaptable to the level of impairment of the patient and able to change their behavior accordingly to the patient's intention. This is one of the goals for the development of rehabilitation robotics and in particular of Wristbot, our robot for wrist rehabilitation: combining proper assessment and training protocols, based on motor control paradigms, will maximize robotic rehabilitation effects.

Contents

List of figures

List of tables

Introduction

Motor and sensory loss or dysfunction, caused by brain injuries or neurological disorders, severely affects the quality of life and may culminate in the inability to perform simple activities of daily living. Unfortunately, such sensorimotor impairments are very common among neurological patients: more than two-thirds of all stroke patients have affected upper limbs and approximately 50% of them suffer from a chronic reduction in arm function. These impairments can also affect the lower limb, compromising, with different degrees of severity, the sensorimotor strategies used by the brain during gait and balance control.

In the last decades, innovative robotic technologies have been developed in order to effectively help both patients and clinicians during the rehabilitation process. The term "robotic technology" in this application domain refers to any mechatronic device with a certain degree of intelligence that can physically intervene on the behavior of the patient, optimizing and speeding up his/her sensorimotor recovery.

However, most of the studies in this field have been focused more on the development of the devices, whereas less effort was made on understanding the causes behind the behavior of the patient and the related possible ways to maximize the degree of intelligence of the robots to promote recovery. As a consequence, unfortunately it is quite common to find patients treated for the symptoms related to their neurological conditions instead of for the root cause of their sensorimotor impairments, obtaining thus poor results.

For these reasons, understanding how the brain controls movements and which the applied mechanisms to learn new skills are is crucial. In fact, a deeper knowledge of the mechanisms underlying motor control and learning in both healthy and pathological condition, would allow the design of more appropriate and effective robot control strategies.

A step forward in this direction was done with the studies collected in this thesis.

One usual paradigm used to study changes in motor control (either adaptation or learning) is to observe human behavior in presence of challenging or destabilizing conditions.

This is also the paradigm exploited in the studies presented below.

The subject of study, in the first works, is postural balance control. The choice of starting with postural control is not accidental: the standing human body can be simply and realistically modeled as an inverted pendulum controlled to maintain the body center of mass (CoM) within the base of support, possibly in one degree of freedom only. This makes postural control easier to isolate and study than the motor control of other body districts.

However quiet standing by itself is something we learn as children and we easily perform as healthy adults. Therefore to make it a good 'learning experimental paradigm' and, in a way, also more similar to real life situations we included different destabilizing disturbances.

After a brief overview of the human sensorimotor system from both a neural and a control perspectives (Chapters 1-2), Chapter 3 describes human behavior in presence of external disturbances. Participants were asked to maintain balance without falling while pushed by externally triggered perturbations.

In particular three studies are presented: the first one gives particular attention to the effect of different levels of noise on motor control strategies. The second one goes deeper in associating different motor control strategies to the level of robustness to perturbations and to the level of learning. The third investigates how postural responses to external stimuli originate and is an additional step forward for the understanding of the nature of motor control and the possible mechanisms behind the differences in control strategies effectiveness. Here some evidences about the intermittent nature of the postural control process are introduced.

Chapter 4 presents two studies where postural control is affected by self-initiated disturbances. The first compares the reliability of single and double inverted pendulum models for quiet standing. The second one describes the effects of a second motor task on postural balance. In this chapter, the complexity of the systems studied starts to gradually increase: first with the evaluation of the double inverted pendulum as model of the standing body and secondly with the inclusion of the effect of upper limbs movements.

Taking into account the evidences present in literature and in the studies of the previous chapter, we tested the robustness of control strategies in more complex paradigms. Finally, we get to the consideration of a very complex system: Chapter 5 shows the effect, on upper limb sensorimotor control, of a disturbance that is internally triggered due to a neurological condition, cervical dystonia. This study looks into sensory function

in both the affected district (the neck) and one unaffected district (the wrist) in subjects with cervical dystonia to determine if different phenotypes of cervical dystonia express different types and levels of somatosensory impairment.

The thesis concludes with a general discussion of the results and the future possible developments on the basis of these results.

In all the studies described in this thesis I directly contributed for experimental protocol design, data collection, data analysis and data interpretation. As regards data collection, it was performed in three different locations. For the studies in Chapter 3, I had the opportunity to perform experiments in the Research Centre for Musculoskeletal Science & Sports Medicine at Manchester Metropolitan University, where I spent 3 months. For studies in Chapter 4, I collected experimental data in the laboratories of Istituto Italiano di Tecnologia. Finally, Chapter 5 is a result of the data I collected in San Martino hospital, in collaboration with neurologists and physiotherapists. The number of participants to each study is variable due to the availability during the limited time abroad or the inclusion criteria for patients.

Chapter 1

Sensorimotor system

1.1 Neural system perspective

Sensorimotor integration is fundamental for motor control. Motor control can be understood as a main feedback loop combining concurrent elements of perception, selection and motor control (van de Kamp *et al.*, 2013*a*) implemented through a range of neural pathways (Figure 1. 2).

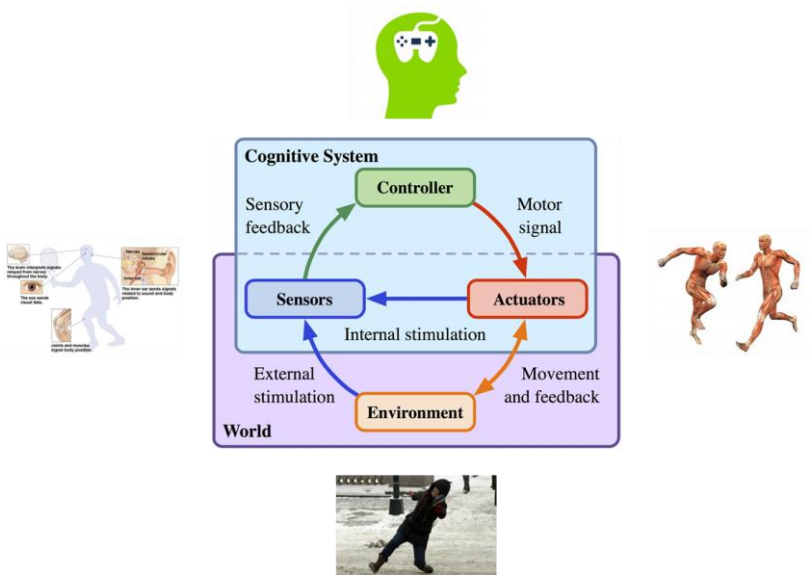

Figure 1. 1 Motor control is the process by which humans and animals use their brain to activate and coordinate muscles and limbs involved in the performance of a motor skill. Fundamentally, it is the integration of sensory information, both about the world and the current state of the body, to determine the appropriate set of muscle forces and joint activations to generate some desired movement or action. This process requires cooperative interaction between the central nervous system and the musculoskeletal system, and is thus a problem of information processing, coordination, mechanics, physics and cognition. Successful motor control is crucial to interact with the world, not only determining action capabilities, but regulating balance and stability as well.

Daily life requires sensory and mechanical engagement with external objects and social engagement with other people: the required configurations are many and unpredictable. Pre-computing motor solutions and storing them in a retrievable fashion is appropriate

when the controlled system and necessary constraints do not change (Arsan *et al.*, 1999). These pre-computed motor solutions, known as motor primitives, are stored within the motor cortex, brain stem and spinal cord. The sensorimotor system retrieves and combines these primitives in the construction of posture and movement (Inzelberg *et al.*, 1995; Roh *et al.*, 2011; Hardwick *et al.*, 2013). However, primitives alone are insufficient. Handling changes requires flexibility for computing new motor solutions in the moment of activity (Bernstein, 1996). Constructing new motor solutions in the moment of activity requires selection, recombination of existing possibilities and temporal inhibition of non-selected alternatives (Frank, 2011).

Thus, the human motor system requires two kinds of loops: a fast loop for implementing pre-computed control, and a slow loop for implementing control which is reconstructed during activity. Both loops require sensory feedback. The human brain receives sensory information through different channels: eyes, ears, skin, muscles, joints and other internal sources. Sensory information is uncertain and potentially ambiguous. However, the human brain has the power of integrating information between sensory modalities and combining them with prior experience to improve sensory accuracy and confidence (Bays & Wolpert, 2007; Fetsch *et al.*, 2009; Kok *et al.*, 2013). Combination of sensory signals and prior expectation occurs centrally in areas including the midbrain and cerebral cortex (Körding & Wolpert, 2006; Berniker & Kording, 2011). For example, the posterior parietal cortex receives input from the three sensory systems that enable localization of the body and external objects in space: the visual system, the auditory system and the somatosensory system. The posterior parietal cortex also receives input from the cerebellum which is increasingly thought to generate expected sensory signals from known motor commands (Figure 1. 3). Much of the output of the posterior parietal cortex goes to areas of the frontal motor cortex (Hardwick et al., 2013). After these integrations, a number of possible movements are available (Cohen & Frank, 2009). Between them, priorities are selected by the slow and fast pathways working together with the optimization pathways such as basal ganglia and cerebellum (Frank, 2011).

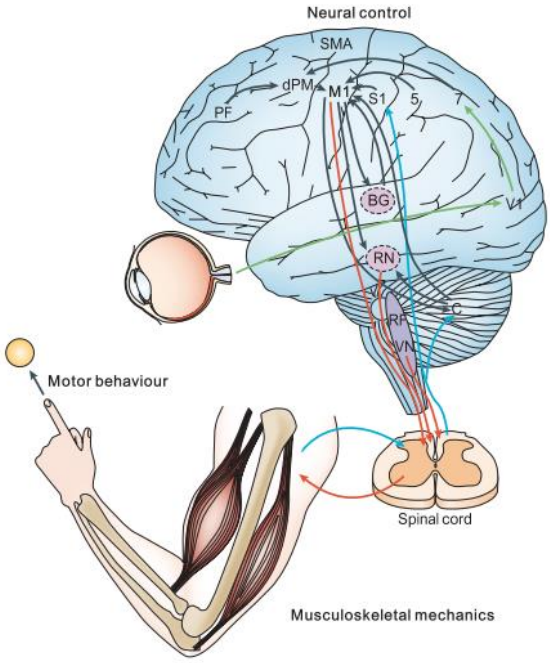

Figure 1. 2 Sensorimotor pathways through the central nervous system. The central nervous system is conventionally viewed as having a hierarchical organization with three levels: the spinal cord, brainstem and cortex. The spinal cord is the lowest level, including motor neurons, the final common pathway for all motor output, and interneurons that integrate sensory feedback from the skin, muscle and joints with descending commands from higher centres. The motor repertoire at this level includes stereotypical multijoint and even multilimb reflex patterns, and basic locomotor patterns. At the second level, brainstem regions such as the reticular formation (RF) and vestibular nuclei (VN) select and enhance the spinal repertoire by improving postural control, and can vary the speed and quality of oscillatory patterns for locomotion. The highest level of control, which supports a large and adaptable motor repertoire, is provided by the cerebral cortex in combination with subcortical loops through the basal ganglia and cerebellum.36 Motor planning and visual feedback are provided through several parietal and premotor regions. The primary motor cortex (M1) contributes the largest number of axons to the corticospinal tract and receives input from other cortical regions that are predominantly involved in motor planning. Somatosensory information is provided through the primary somatosensory cortex (S1), parietal cortex area 5 (5) and cerebellar pathways. The basal ganglia (BG) and cerebellum (C) are also important for motor function through their connections with M1 and other brain regions. RN, Red nucleus; V1, Primary visual cortex; 7, Region of posterior parietal cortex; dPM, Dorsal premotor cortex; SMA, Supplementary motor area; PF, Prefrontal cortex. (Scott, 2004)

Among sensory channels, the somatosensory one (including proprioception) is crucial for motor control. Proprioception provides the sense of relative position and movement of the body parts. The sensory information derives mainly from sensory receptors associated with skeletal striated muscles (spindles, Golgi tendon organs) and is combined with cutaneous receptors signaling skin stretch and pressure (Proske & Gandevia, 2012). The importance of this sense compared to vision and vestibular sensation is demonstrated by the fact that loss of proprioception is instantly devastating for motor and postural control (Cole, 1995).

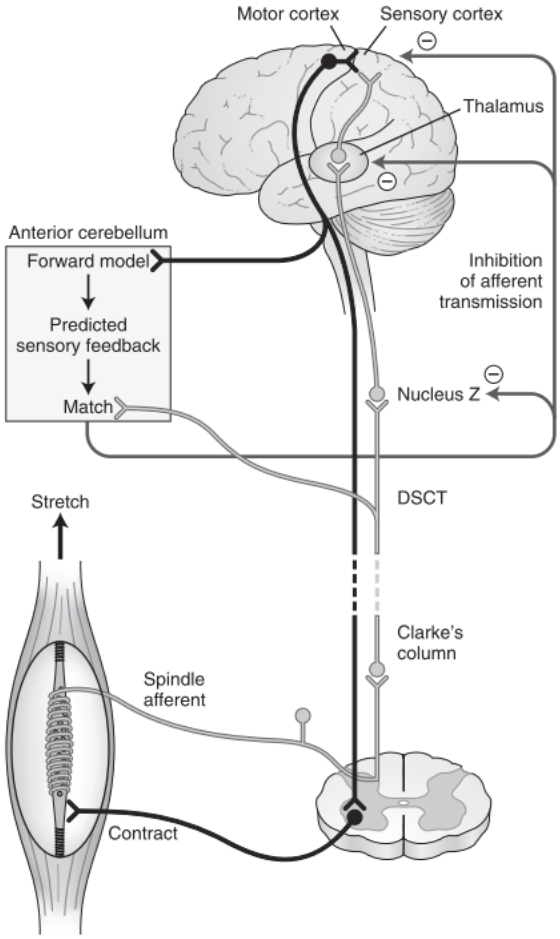

Figure 1. 3 Neural pathways estimating position from sensory and motor information. Integration of muscle spindle afferents with expectations generated from motor output. When the muscle is stretched, spindle impulses travel to sensory areas of the cerebral cortex via Clarke's column, the dorsal spinocerebellar tract (DSCT), Nucleus Z, and the thalamus. Collaterals of DSCT cells project to the anterior cerebellum. When a motor command is generated, it leads to co-activation of skeletomotor and fusimotor neurons. A copy of the motor command is sent to the anterior cerebellum where a comparison takes place between the expected spindle response based on that command and the actual signal provided by the DSCT collaterals. The outcome of the match is used to inhibit reafferent activity, preventing it from reaching the cerebral cortex. Sites of inhibition could be at Nucleus Z, the thalamus, or the parietal cortex itself. (Loram, 2015)

As mentioned above, the motor system operates through fast and slow feedback loops (Yin & Knowlton, 2006; Frank, 2011). The fast loop corresponds to automated, habitual and reflexive control. Although functional, the fast loop alone is not adequate to reject disturbance, is highly variable and is not fully sustained (Marsden *et al.*, 1981). Fully adequate, accurate and sustained control requires the combined operation of both fast and slow feedback loops. The slow loop corresponds to intentional control limited to the low bandwidth of 1–2 Hz. Within this bandwidth there is flexibility within the feedback loop

to reselect the control priorities, goals internal and external constraints at a maximum rate of two to four times per second (Loram *et al.*, 2011).

The motor system receives integrated sensory input from the vestibular nuclei and different sensory areas of the cerebral cortex such as the posterior parietal cortex.

From the selection processes, the motor system also receives the task-related parameters which tell the motor system what kind of coordination, feedback control and muscles synergies to generate. The motor system includes more preliminary organizing function within motor parts of the basal ganglia system, the supplementary motor area, the premotor cortex and cerebellum, and influences muscle activations through the pyramidal and extrapyramidal systems (Kandel *et al.*, 2000).

The pyramidal motor system transmits directly from the motor cortex, through upper motor neurons within the corticospinal tract. Upper motor neurons terminate within the anterior horn of the spinal cord mostly on interneurons and to a lesser extent directly on lower motor neurons. Lower motor neurons directly innervate muscles as motor units. The pyramidal system is concerned specifically with discrete voluntary skilled movements, such as precise movement of the fingers and toes. The more ancient extrapyramidal motor system includes all motor tracts other than the corticospinal (pyramidal) tract, including parts of the rubrospinal, reticulospinal, vestibulospinal and tectospinal tracts. The rubrospinal tract, small in humans compared with primates, is responsible for large muscle movement as well as fine motor control, and it terminates primarily in the cervical spinal cord, suggesting that it functions in upper limb but not in lower limb control. The reticulospinal tract descends from the reticular formation in two tracts, medullary and pontine, to act on the motor neurons supplying the trunk and proximal limb muscles. It functions to coordinate automatic movements of locomotion and posture, facilitate and inhibit voluntary movement and influence muscle tone. The vestibulospinal tract originates in the vestibular nuclei, receives additional input from the vestibulocerebellum, and projects down to the lumbar spinal cord (Loram, 2015).

1.2 Control system perspective

Arguably the first motor control hypothesis was introduced by Merton. This hypothesis, termed the servo-hypothesis, postulated a particular physiological signal as the control variable in the production of voluntary movements. According to Merton's servo-

hypothesis, signals to the system of motoneurons established a desired muscle length, and the tonic stretch reflex acted to make sure that the encoded length was achieved, independently of the external load and its possible changes (Merton, 1953).

In 1959, Matthews (Matthews, 1959) showed that a fixed descending input into the spinal cord (a fixed level of stimulation of the descending pathways) was associated not with a fixed length, or a fixed force, or a fixed level of activation, but with a stable relation between muscle force and length, while muscle activation changed in parallel with the force. Changes in the stimulation level resulted in shifts of the force-length characteristics along the length axis. In other words, muscles behaved like non-linear springs with zero length dependency on the descending signals. These studies were direct precursors of experiments by Feldman and Bizzi that led to the formulation of the Equilibrium Point hypothesis (EP-hypothesis) (Feldman, 1966; Bizzi *et al.*, 1982).

These are some examples of theories that view movements as built on reflexes or feedback control. Feedback control can be seen as a closed loop, since signals from sensors are compared with a desired state (planned movement), represented by a reference signal. The difference, or error signal, is used to adjust the output. The advantage of this kind of control is that it allows for changes in the environment during movement. However, since all signals require a certain time before they reach the relevant brainstem from sensory receptors, this information is always time-delayed (Campbell, 2007). This presence of delay in the feedback loop is crucial, especially because many common tasks are intrinsically unstable. Burdet proposed that, in case of unstable dynamics, the central nervous system reduces the effects of an external disturbance via impedance control. By modulating stiffness, the motor system can exercise control over the delayed response to external perturbations. Although stiffness can be used to deal with some perturbations, it is limited in its flexibility and, because it often requires co-contraction of opposing muscles, it can be an effortful solution to maintain stability (Burdet *et al.*, 2001).

On the other hand, Shadmehr and Mussa Ivaldi laid the basis for the concept of feedforward control (Shadmehr & Mussa-Ivaldi, 1994). The feedforward control acts in advance of certain perturbations and the entire movements pre-planned and executed without on-line corrective responses. This form of control is often referred as open-loop control to emphasize that feedback sensory signals do not directly affect the timing of the current response but possibly of the next one. However, this control it is not sensory

signal independent, because it must rely on a great deal of information, from sensors as well as experience, to operate correctly. However, for a feedforward controller to be useful, it must be able to predict the limb's response, that is it must have an internal model of how the controlled system behaves (Wolpert *et al.*, 1995; Jordan, 1996; Scheidt *et al.*, 2000). The construction of these internal models is strictly related with voluntary control and learning.

In goal-directed movement both feedforward and feedback controls are important. The way in which these two controls interact is still an open question. The continuous paradigm (e.g. servo control, continuous optimal control, closed loop control) has been the mainstay of postural and motor control. The more recently developed intermittent control paradigm (e.g. open loop control) includes and extends the explanatory power of the better known continuous paradigm.

Different versions of intermittent control have been proposed throughout the years. Intermittent control action may be initiated at regular intervals determined by a clock, or at irregular intervals determined by events; an event is typically triggered by an error signal crossing a threshold. Clock-driven control is discussed by (Neilson *et al.*, 1988) and (Gawthrop & Wang, 2007). Event-driven control is used by (Bottaro *et al.*, 2005; Asai *et al.*, 2009; Gawthrop & Wang, 2009). The common feature distinguishing intermittent from continuous control is the open loop interval. The length of the open loop interval gives a trade-off between continuous control (zero open loop intervals) and intermittency. Continuous control maximizes the frequency bandwidth and stability margins at the cost of reduced flexibility, whereas intermittent control allows in the loop optimization and selection at the cost of reduced frequency bandwidth and reduced stability margins. When the flexibility needed is more than tuning parameters in the currently selected fast solution (e.g. if disturbances occur, or if pain occurs, or if an obstacle is presented), it is more economical to select and optimize solutions as required rather than pre-compute and retrievably store solutions for every eventuality. The rationale for intermittent control is that it confers online flexibility and adaptability that has an advantage for performance in daily life activities.

Disturbances affect all aspects of nervous system function and sensorimotor system is not an exception. First our movements are inherently variable. Sensory information is uncertain and potentially ambiguous as well as there is variability in the force that is

produced by human skeletal muscle, attributed to the physiological organization of the pool of motor neurons and their muscle fibers (Faisal *et al.*, 2008).

These kinds of noise are intrinsic in all humans. The studies presented in the following chapters, instead, investigate human behavior in a series of different destabilizing situations, which represent common problems present in our daily life such as standing on a moving bus (external perturbations), phishing on an oscillating boat or holding a dish full of soup (self-generated disturbances), or dealing with neurological conditions (pathological disturbances).

Chapter 2

Sensorimotor learning and recovery

2.1 Sensorimotor learning

Humans show a strong ability to learn a variety of motor skills. Learning such skills involves a number of interacting elements. First, there are different task components that must be learned for skilled performance, including efficient gathering of task-relevant sensory information, decision making and selection of strategies, and the implementation of both predictive (feedforward) and reactive (feedback) control mechanisms. Second, there are different learning processes that apply to these components, which specify how errors and rewards drive learning. Finally, learning is strongly determined by the neural representations of motor memory that influence how we assign credit during learning and how learning generalizes to novel situations.

Focusing on the control mechanisms, as a result of time delays associated with receptor transduction, neural conduction, central processing and muscle activation, skilled action often relies on predictive control. Predictive control requires a forward model, which is a neural simulator that predicts the sensory consequences of an action given the current state and a copy of the motor command (efference copy). These internal models are acquired and supported by new learned mappings between motor and sensory variables (Wolpert *et al.*, 2011).

This is possible because motor learning is dependent upon plasticity in motor areas of the brain (Hebb, 1962; Li *et al.*, 2001; Kelly & Garavan, 2005). The discovery of synaptic plasticity in single neurons was revolutionary, but was far from sufficient to explain motor skills. Recent integrative and multidisciplinary approaches have begun to suggest that essential features of motor skills reside in dynamic interactions between multiple neural networks. Such networks are composed of loop circuits formed by the frontoparietal cortices, the basal ganglia, and the cerebellum (Hikosaka *et al.*, 2002).

2.2 Sensorimotor rehabilitation and robotics

Motor and sensory loss or dysfunction, caused by brain injuries or neurological disorders, severely affects the quality of life and may culminate in the inability of performing simple activities of daily living. Unfortunately, such sensorimotor impairments are very common among neurological patients: more than two-thirds of all stroke patients have affected upper limb (Hatem *et al.*, 2016) and approximately the 50% of them remains with a chronic reduction of arm functions (Broeks *et al.*, 1999). These impairments affect also the lower limb, compromising, with different degrees of severity, the sensorimotor strategies used by the brain during gait and balance control. In order to understand how to recover from these pathological conditions, it is necessary to highlight in which way a specific impairment reflects on the patient behavior. For example, proprioceptive impairments affect movement planning and inter-limb coordination (Winward *et al.*, 1999; Coderre *et al.*, 2010); paresis affects movements in accuracy, temporal efficiency and efficacy (Lang *et al.*, 2013); abnormal muscle tone turns into lack of movement smoothness and intra-limb coordination (Lang & Beebe, 2007).

In the last decades, innovative robotic technologies have been developed in order to effectively help clinicians during the neurorehabilitation process. As "robotic technology" in this application domain it is intended any mechatronic device with a certain degree of intelligence that can physically intervene on the behavior of the patient optimizing and speeding up his/her sensorimotor recovery. The two key capabilities of these robots are: i) assessing the human sensorimotor function; ii) re-training the human brain in order to improve the patient quality of life. However, most of the studies in this field have been focused more on the development of the devices and less effort was made on maximizing their efficacy for promoting recovery.

As reported by Maggioni et al. (Maggioni *et al.*, 2016), providing a reliable assessment of the sensorimotor components is important in order to optimize the patient's chance of recovery. Despite this well-established evidence, these quantitative assessments by means of robotic devices are not continuously performed during clinical practice. Hence, the increased accuracy given by objective measurements of the performance is discarded in favor of objective clinical scales that are biased by the experience and the ability of the clinicians, leading to results that lack reliable measurement of the patient's impairment. Moreover, subtle sensory and motor abnormalities are hardly detected by clinical

measurements. In this framework, rehabilitation robotics is also able to improve the clinical evaluation, at least by placing the quantitative assessment side by side with the standard clinical evaluations.

At the same time, understanding how the brain controls movements and which are the mechanisms it applies to learn (or re-learn) skills is fundamental to plan an effective robot-based therapy, aimed at the promotion of the sensorimotor recovery. In this frame, the design of the most appropriate and effective control strategy (i.e. the most sophisticated assistance) plays a crucial role, and can be achieved by exploiting and properly applying the last findings in human neuroscience (Iandolo *et al.*, 2019).

In fact, the future aim is to apply the new findings to our rehabilitation device, Wristbot.

2.3 Device for wrist rehabilitation: Wristbot

During these three years, I contributed in the development of Wristbot. Wristbot is an end-effector robotic device designed for the wrist neurorehabilitation of patients with neurological or orthopedic disabilities (Figure 2. 1). It was developed in the Motor Learning, Assistive and Rehabilitation Robotics laboratory of the Italian Institute of Technology (IIT). The robot allows movements along the three wrist articulations, with a range of motion similar to a typical human subject: ±62° in flexion/extension, 45°/40° in radial/ulnar deviation, and ±60° for pronation/supination movements. It is provided with four brushless motors that allow guidance and assistance of wrist movements in the three above-mentioned planes, with a maximum torque of 1.53 Nm in flexion/extension, 1.63 Nm in radial/ulnar deviation, and 2.77 Nm in pronation/supination movements. In addition, these motors are chosen in such a way as to provide an accurate haptic rendering and compensate for the weight and inertia of the device, thus allowing free smooth movements. Angular rotations on the three axes are acquired by means of high-resolution incremental encoders with a maximum error of 0.17◦, thus making Wristbot an optimal tool to assess the rehabilitative process in an objective and precise way. Another peculiarity of the Wristbot is the possibility to provide assistive or perturbative forces that automatically adapt to the level of disability and performances of the patient. An intuitive graphical user interface (GUI) allows the therapist to choose the desired exercises and to set a wide range of parameters to continuously tailor the therapy to the patient's needs. As for the interaction with patients, they are requested to hold the handle of the Wristbot

to perform wrist movements and execute the task presented on a monitor. In fact, a virtual reality environment is integrated into the system in order to provide stimulating visual feedback and engaging interaction. The main advantages of the Wristbot are its programmability and multi-functionality, which allow for a highly personalized therapy. In addition, the quantitative functional assessment provided by the device constitutes a valuable tool to support clinicians in the choice of the optimal therapy.

For these reasons I used Wristbot in the study described in Chapter 5. In addition, I developed a set of exercises for assessment and training which are now in test phase in order to be included in the next future in clinical experimental protocols.

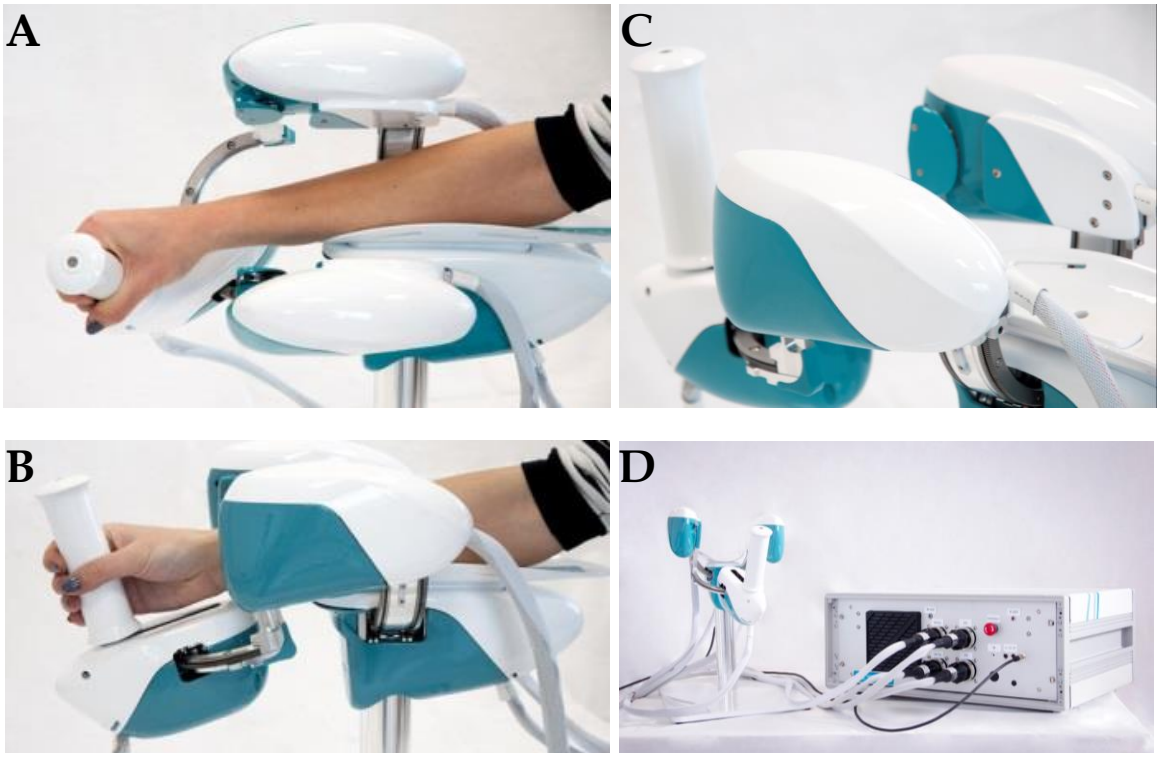

Figure 2. 1 Lateral view of Wristbot during combined movements in the flexion–extension and pronation–supination DOFs (A) and movements in the radial–ulnar deviation DOF (B); posterior–lateral view of the handle of Wristbot (C) and a frontal view of the device connected to the case, with the integrated PC and electronic control unit (D).

The first two chapters give an overview of the general context in which the studies presented in the following chapters fit. However, each chapter contains a more detailed section with the state of the art for the specific study.

Chapter 3

External disturbances

3.1 Effect of motor and sensory noise on upright standing

As mentioned in the introduction, since the standing human body can be simply modeled as a single inverted pendulum, the first studies are focused on the investigation of the mechanisms behind postural control.

3.1.1 *Introduction*

Balancing an inverted pendulum is a classic problem of unstable dynamics and control theory. An actual fact is that human body is a system with sensors and actuators and that maintaining upright posture is a typical example of a stabilized inverted pendulum system. Humans, in fact, maintain upright posture keeping the Center of Mass (CoM) of the body within the base of support, producing specific joint torques through muscles activations. The muscle activity modulates the biomechanical properties at joint level (stiffness and damping) in order to counteract to the toppling gravitational torque and to any other perturbation that tends to compromise upright standing. Many researchers tried to model the mechanisms and strategies that the brain adopts to generate the appropriate control signal mainly focusing only on the gravitational torque as perturbation (Asai *et al.*, 2009; Gawthrop *et al.*, 2011; Loram *et al.*, 2016). In this work, however, we want to focus on the effect of different noise sources in the postural stabilization process. In nature, as well as in control theory, a system is known as a *perturbed system* if it is deviated from its normal behavior. The energy sources that produce such deviation are usually known as perturbations and include any signal externally acting on the system, any internal variation in the identification of system parameters and/or any measurement

or actuation noise. Specifically, the possible mechanisms (Morasso *et al.*, 2014; Zenzeri *et al.*, 2014) that a *perturbed system* can use to achieve stability are the following ones:

- Stiffness strategy. Set a high stiffness to prevent small disturbances from being magnified (Winter *et al.*, 1998; Burdet *et al.*, 2001). In the case of postural stability, it reflects in co-contracting antagonistic muscles so that joint stiffness increases; however this mechanisms is ineffective due to a compliant series elastic element (tendon) in the ankle joint (Loram & Lakie, 2002*a*; Casadio *et al.*, 2005).
- Sensory-motor feedback strategy. Produce a control signal modulated in time and amplitude so that every perturbation is resisted forcefully enough and fast enough that it does not grow in size; this mechanisms depend upon neural transmission delays (Cabrera & Milton, 2002; Loram *et al.*, 2009*a*; Insperger & Milton, 2014).

In the present chapter, we investigate how different types of perturbations affect human postural control and its stability, exposing healthy participants to a highly destabilizing environment. The experiment try to show if there are performance difference based on the kind of perturbation applied to the system and if the mechanisms described above are applicable with different noise sources.

3.1.2 *Methods*

3.1.2.1 Ethical approval

The experiments reported in this study were approved by the Academic Ethics Committee of the Faculty of Science and Engineering, Manchester Metropolitan University (EthOS Ref 0567) and conform to the Declaration of Helsinki. Participants gave written, informed consent to the experiment which was performed in the Research Centre for Musculoskeletal Science & Sports Medicine at Manchester Metropolitan University.

3.1.2.2 Experimental setup

The experiment consisted in a simple postural balancing task. Participants stood with their feet on a stable footplate and were strapped rigidly to a one degree of freedom actuated device, named Whole Body Mover (WBM). The WBM (Figure 3. 1) is

composed of a vertical board rotating around a joint collinear with the ankles, connected to a direct drive linear actuator (XTA3810S, Servotube Actuator, Copley Motion, UK) at approximately 1m above the axis of rotation. An incremental position encoder is located in the linear actuator. The starting position of the WBM was set to 2° forward respect to the vertical line, to approximate physiological standing (Loram *et al.*, 2001) using an absolute position potentiometer mounted on the rotational axis. The task was implemented using Simulink, compiled using Real-Time Workshop and executed on a PC using Real-Time Windows Target within MATLAB (all from Math Works, Natick, MA, USA) with a control loop frequency of 1 kHz. Following each recording, all signals were saved at 100 Hz.

A control signal applied as torque to the virtual unstable system was generated by a myoelectric interface connected to the participant ankle muscles (Figure 3. 2). The interface was implemented by a multichannel surface electromyograph (sEMG) (Trigno, Delsys) with a sample frequency of 2 kHz and Ag/AgCl electrodes were used to measure the electrical activity of leg muscles Tibialis Anterior (TA) and calf muscles (intersection of Gastrocnemius Medialis and Soleus (G) of both right and left leg. Electrodes placement was accomplished according to SENIAMs (Surface ElectroMyoGraphy for the Non-Invasive Assessment of Muscles) recommendations (Hermens *et al.*, 1999). Once the electrodes were in place, the electrical activity in all muscles was recorded while muscles were at rest in order to remove noise due to spontaneous electrical activity, not corresponding to muscle work. Those dead-zone values were measured at the beginning of each experimental session. Throughout the task, sEMG signals were processed in real-time through a low-pass filter (cut-off frequency: 340 Hz) and then rectified. The specific control signal was generated by the sum of the muscular contributions of the two legs evaluated as the sEMG envelops signals difference between the two antagonist muscles (TA and G). The actuated position of the WBM was controlled to follow the output of the real time simulated unstable system using a proportional–integral–derivative (PID) controller. Using cross correlation to estimate the delay, during these tasks, the delay between simulated output and measured position of the WBM was 4±3ms (mean ± S.D.) from all 448 trials, which can be considered negligible respect to the physiological processes involved. If the WBM exceeded a range of motion of ±10° the WBM was deactivated and returned gently to the initial position of 2°, and the task continued automatically after a delay of 5s. This reset phase was termed “falling over”.

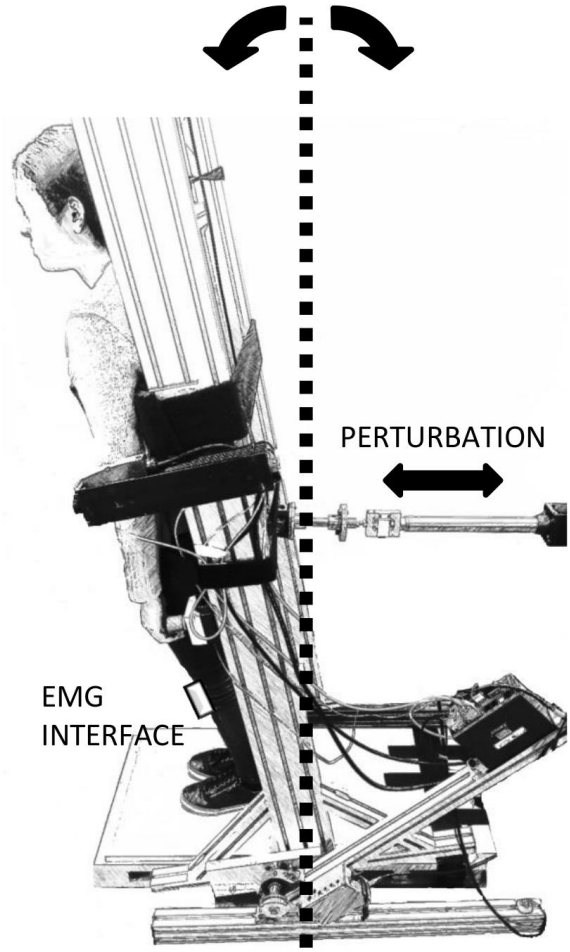

Figure 3. 1 Experimental setup. A typical subject connected to the Whole Body Mover. The subject controls the position of the rigid vertical bar through a control signal generated by a surface EMG interface and sent to a linear actuator that acts directly on the bar. The same actuator delivers also the perturbations during the task

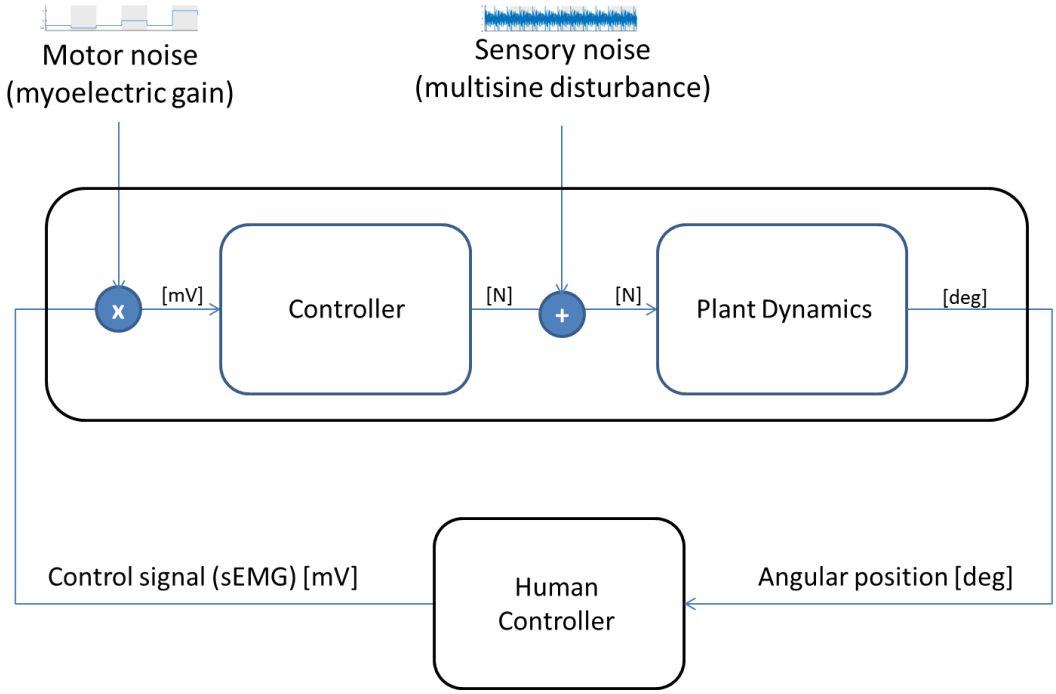

Figure 3. 2 Block diagram of the experimental setup. A control signal applied as torque to the virtual unstable system was generated by a myoelectric interface connected to the participant ankle muscles (Human Controller). The specific control signal was generated by the sum of the muscular contributions of the two legs evaluated as the sEMG envelops signals difference between the two antagonist muscles (Controller). The actuated position of the WBM was controlled to follow the output of the real time simulated unstable system (Plant Dynamics) provided to the participant as feedback.

3.1.2.3 Participants and protocol

Merely keeping the WBM within range was in fact a trivial task for participants and one which they learned in a matter of minutes. To ensure the task was challenging an input disturbance was applied and discrete changes to the gain of the myoelectric control signal were also applied.

The first perturbation provided is an additive one, external to the system, independent from the control signal and applied as an additional input to the plant, i.e. random rotations of the WBM board. For this reason we refer to it as Sensory Noise. Output and consequently output errors do not correlate linearly with the input error; in this case small perturbations are posited to have small effect on the output. Sensory Noise consisted in a multisine signal containing 100 frequency components equally spaced in the range 0.1-10 Hz and with 2 different tunable amplitudes: 1 Low Sensory Noise (LS) and 4 High Sensory Noise (HS).

The second perturbation causes abnormal muscle activation. In fact, to obtain the same motor output, muscle activity need to be modulated inversely to the applied gain; this means that a different number of motor units is recruited, depending on the magnitude of the perturbation itself. Moreover, any error in input to the control signal is also amplified if the perturbation is high. For these reasons we refer to it as *Motor Noise*. It consisted in a tunable gain with 2 different values: 1 Low *Motor Noise* (LM) and 4 High *Motor Noise* (HM).

In both cases the value 1 stands for the baseline condition while 4 for the extremely perturbed condition. Combining the two sources of perturbation, we obtained 4 different conditions (LMLS, LMHS, HMLS and HMHS).

The protocol consisted in a training and in an assessment phase.

Eight participants (1F + 7M, 36±9 years) were trained in all the 4 randomized conditions until they reached an acceptable postural stability level (overall mean success time > 55%) that exhibits in 28 trials. After training we assessed the postural stability in 4 trials, one for each condition. Each trial consisted in 120s of continuous exposition to the different perturbations.

3.1.2.4 Data analysis

In order to assess if and how postural stability is achieved in the different conditions, we computed the following outcome measures:

- Success Time (ST) [%]: percentage of the time while successfully balancing (i.e. without falling) with respect to the entire duration of the trial. This parameter permits to assess postural stability and to discriminate the difficulty of the task in the different conditions.
- Co-contraction Index (CI) [%]: percentage of the time while co-activating ankle antagonist muscles with respect to the duration of the trial when subjects succeed in stabilization. This parameter allows to assess the level of co-activation in terms of duration and to understand which strategies are adopted with the different perturbations.
- Effort Index (EI) [μV]: sum of the root mean square values computed on each muscle EMG filtered signal during the successful periods of the whole trial.

Regarding the statistical analysis we found out that data did not meet the assumption of normality. Therefore, non-parametric tests were chosen. In order to investigate the difference between conditions, we performed the Wilcoxon matched pairs signed-rank test. Significance level was set at 0.05. Population values are reported as median±interquartile range.

3.1.3 *Results*

The first expected result is that all participants easily accomplished the baseline condition, LMLS, (ST=100 %). However, left panel of Figure 3. 3 shows that the addition of *Motor Noise* and *Sensory Noise* resulted to have different effects on performance (LMHS: ST=100 %; HMLS: ST=69±30 %; HMHS: ST=61±26 %). Comparing the baseline condition with LMHS and with HMLS condition, we observe that *Sensory Noise* alone (LMHS) has no effect at all on performance, while *Motor Noise* alone (HMLS) affects performance in a significantly negative way (Z=2.366, p=0.018). Considering the extreme condition that combines the two types of high perturbations (HMHS), performance, even if it is lower, does not significantly differ from the HMLS. On the other hand it is significantly lower than LMHS (Z=2.201, p=0.028). This result suggests that this *Motor Noise* has a more degrading effect in terms of performance.

In order to understand what is the real effect of perturbations in terms of strategies and mechanisms adopted at muscular level, we report the analysis on the other two indicators CI and EI (Figure 3. 3, central and right panels). Dealing with *Motor Noise* only or *Sensory Noise* only forces subjects to adopt different control strategies. In fact, in the HMLS, CI is significantly lower than LMLS (HMLS: CI=1.58±4.96 %, LMLS: CI=5.68±9.93 %, Z=2.100, p=0.036), while in the LMHS it is significantly higher (CI=8.79±10.15 %, Z=2.521, p=0.012). Even if both the conditions HMLS and LMHS differ significantly from HMHS (Z=1.960, p=0.049 and Z=2.521, p=0.012), this extreme condition does not differ from the baseline revealing that the subjects are able to modulate the muscle activity effectively rejecting the disturbances.

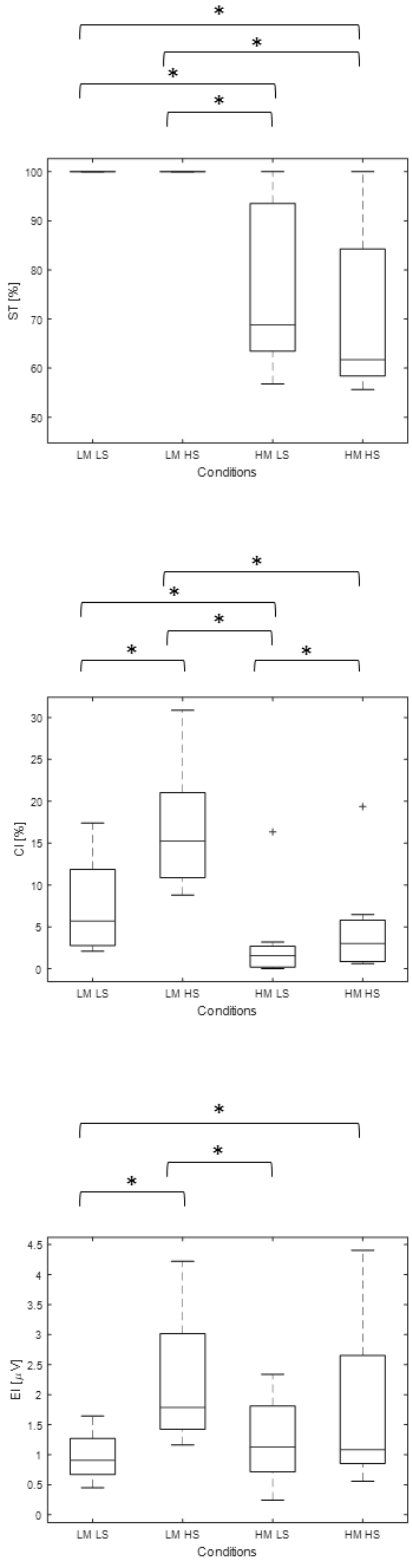

Figure 3. 3 Outcome measures: Success Time (ST [%]) on the top, Co-contraction Index (CI [%]) in the middle, Effort Index (EI [μV]) on the bottom. Box centers, edges, whiskers and crosses report population medians, interquartile limits, range and outliers respectively grouped by experimental conditions Statistically significant differences between conditions are reported (* : $p<0.05$).

In terms of muscular effort, participants spend higher effort in the LMHS condition than in the LMLS (LMHS: EI=1.78±1.59 μV, LMLS: EI=0.90±0.60 μV, Z=2.521, p=0.012). As for EI, the effect of the two sources of noises is different: the effort is higher with *Sensory Noise* then in the presence of *Motor Noise* (LMHS: EI=1.78±1.59 μV, HMLS: EI=1.13±2.69 μV, Z=2.521, p=0.012) and the participants are not able to decrease their muscular effort in all the cases.

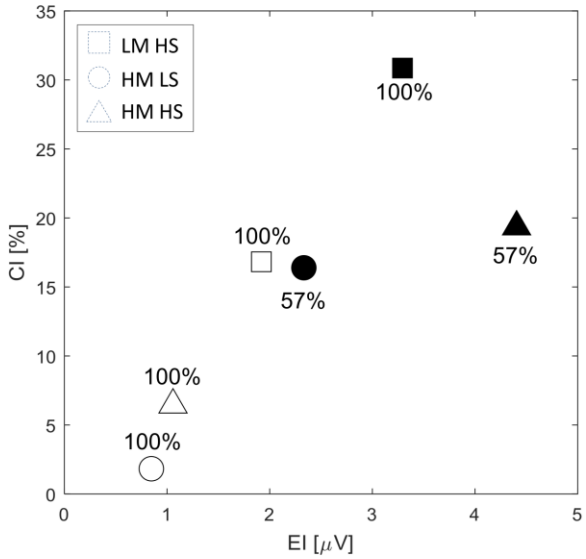

Figure 3. 4 Two representative participants behavior (Participant 1: white markers, Participant 2: black markers) in the following experimental conditions (Condition LMHS: square, Condition HMLS: circle, Condition HMHS: triangle). For each participant and each condition, we report: Co-contraction Index (CI [%]) on the x axis, Effort Index (EI [μV]) on the y axis and Success Time (ST [%]) as text.

Due to these population results we wanted to understand more in depth the differences between participants. Figure 3. 4 compares the best (Participant 1) and worst participants (Participant 2) in terms of mean performance in the perturbed conditions. We observe that in the LMHS condition, different levels of CI and EI allow to reach 100% of success. In fact, it is also the perturbed condition (Figure 3. 3, left panel) where all subjects succeed stabilizing the whole trial (the easiest perturbed condition to deal with for everyone). In the HMLS, Participant 2 shows both higher CI and higher EI. This finding illustrates the result shown by all participants, that it was not possible to succeed by co-contracting and stiffening the joints or producing high forces in this condition. The same can be observed in the HMHS condition, and this confirms once more the lower effect of *Sensory Noise* compared to *Motor Noise*.

3.1.4 *Discussion*

This work revealed that, in order to maintain balance in a highly destabilizing environment, humans can adopt different strategies in terms of muscular activations that were effective in different ways. One strategy was to increase the stiffness around the joint, producing torques high enough to compensate toppling torques and maintain equilibrium. The second strategy was to adapt the control signal, depending on the system output. *Motor* and *Sensory Noise* can drive the use of these strategies and the performance achieved.

In particular it is clear that *Motor Noise* does not allow adopting the 'cognitively easy' and 'energetically expensive' stiffening option, while subjects tend to co-activate when the *Sensory Noise* is the only perturbation applied. This can be due to the fact that *Motor Noise* can be associated to an abnormal muscle activation that interferes on our ability to generate the appropriate control signal especially in the case of high noise where less motor units needs to be recruited. The EI values in the HMLS condition demonstrate the inability for the participants to decrease the overall muscle activity. Moreover, performance assessment shows that, on average, it is harder to overcome *Motor Noise* by compliance, than *Sensory Noise* by co-activation. This is confirmed in the condition HMHS, where outcome measures are on average more similar to the HMLS condition than to the LMLS one.

Besides, looking at two different subjects (the best and the worst participant) in terms of ST, performance may depend also on the choice of the stabilization strategy. We show that it is possible to overcome also the *Motor Noise* if the internal system parameters are modulated in order to produce very low amplitude control signals but also very low errors. In this case co-activation is not so effective because even if a low amplitude signal is theoretically obtainable (since by design the control signal is the difference between antagonist muscles), producing high forces increases the endogenous motor noise.

There is a clinical need to reduce excessive muscle activation and co-contraction in a variety of motor disorders including spasticity, incomplete spinal cord injury, cerebral palsy and dystonia. Stabilization in presence of *Motor Noise* might be a suitable therapeutic approach. However, the main requirement to take advantage of such kind of error-enhancing method (Patton *et al.*, 2013; Liu *et al.*, 2018) may be an intact ability to

adapt. Therefore these findings could suggest new methods for postural stability rehabilitation exploiting the noise sources.

This work has been published as book chapter (Cherif *et al.*, 2019).

3.2 Motor control strategies and learning

The following section describes a study which is an extension of the previous one. In this case we investigated a possible relationship between the control strategy adopted by participants to counteract perturbations and their level of learning.

3.2.1 *Introduction*

Postural balance requires the whole body centre of mass (CoM) to be maintained within the base of support during both self-initiated and externally triggered disturbances of stability. In human postural sway, the dynamic relationship between the combined sagittal ankle joint moment and sagittal position of the CoM is similar to the control of an unstable, inverted pendulum (Winter *et al.*, 1998; Morasso *et al.*, 2019). Since the passive stiffness of the ankle joint is lower than the growth-rate of the gravitational toppling torque, an active feedback control mechanism is needed for upright standing (Loram & Lakie, 2002*a*; Casadio *et al.*, 2005). Human control of an external, unstable inverted pendulum using the postural lower leg muscles (calf, and tibialis anterior) provides a balance task which replicates a key component of postural standing balance (Loram *et al.*, 2001) .

In order to study the process of postural balance, participants were strapped to, and controlled an actuated system, with an unstable (inverted pendulum) time constant of a typical human body. In this experiment, the sensory feedback, the motor action and the ownership of self-movement ensure the task feels very similar to postural balance. The system was controlled by a torque determined by activations of the calf and tibialis muscles of the participants (Figure 3. 1). This linearized inverted pendulum system is represented by an equation of motion including two parts (1).

$$T = mgh\theta + I\ddot{\theta} \qquad (1)$$

The first part is a linear relationship between ankle moment T and pendulum angle θ, where *m* is the mass of the pendulum, *g* is the gravitational acceleration, *h* is the distance between the centre of mass and the joint and *I* the moment of inertia around the centre of mass. Deviation from the linear relationship (second part of the equation) represents the acceleration and also represents the torque error from the equilibrium torque required for the angle of the pendulum. When plotted as torque versus angle, the best-fit line indicates

the torque vs angle relationship of the inverted pendulum and torque differences/errors from this ideal line are related to acceleration (Loram & Lakie, 2002*b*). Postural balance requires the person to prevent falls which in turn requires the participant to maintain an appropriate torque for any angle and also to regulate the angle within limits of stability (corresponding to the base of support). To prevent falls there are many possible feedback mechanisms and strategies.

Previous studies showed that humans adopt a strategy from a spectrum of choices ranging from two extremes which we describe as minimising variance in position (stiffness control: SC) or minimising force error (force accuracy control: FAC) (Loram & Lakie, 2002*b*; Saha & Morasso, 2012; Di Giulio *et al.*, 2013; Zenzeri *et al.*, 2014). This spectrum of choice is fundamental within control theory. Within the optimal feedback control framework this choice is represented within the cost function as prioritising regulation of position or regulation of effort (Burdet & Milner, 1998; Todorov & Jordan, 2002).

For unstable tasks involving the upper limbs, (Saha & Morasso, 2012; Zenzeri *et al.*, 2014; Avila Mireles *et al.*, 2017) observed two extreme strategies. The first strategy (high-stiffness strategy) implies the production of a convergent, restoring force field, taking advantage of the elastic properties of the body/environment system. This can be a successful strategy but it has two main disadvantages: it works only if body stiffness is greater than the rate of growth of the divergent field and it is energetically expensive. The second strategy (low-stiffness strategy), instead, is based on explicit positional feedback from different sensory channels (e.g. proprioception and vision). These strategies have also been identified by (Loram *et al.*, 2001) who studied human control of an inverted pendulum.

Therefore, from previous literature we focus attention on two strategy extremes:

- Stiffness control strategy (SC), which consists in minimising position sway.
- Force accuracy control strategy (FAC), achieved minimising force error: a high weight given to sensory feedback, with minimal acceleration.

These extremes are illustrated in Figure 3. 5. Figure 3. 4A, represents a variation of forces unrelated with the relatively narrow range of positions. Figure 3. 4B shows a more accurate mapping of the force vs position and a wider range of positions.

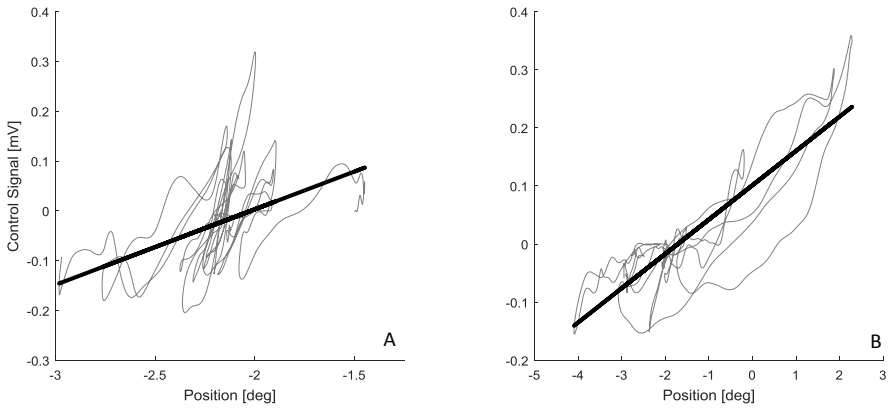

Figure 3. 5 Representative examples of the two control strategies. (A) Stiffness control strategy (SC). (B) Force accuracy control strategy (FAC). In example (A), the fluctuation on control signal (ankle torque) is quite large and does not follow the equilibrium control signal v position line very closely. In example (B) the control signal does follow the equilibrium value closely for range of positions and hence the correlation between control signal and position is higher than in example (A).

In postural control, the consequences of the choice within the spectrum of possibilities (SC to FAC) for learning and for fall prevention remain unknown. For postural control high variance in position (sway) has been viewed as a sign of poor balance control and increased fall risk (Le Clair & Riach, 1996; Piirtola & Era, 2006). Alternatively, according to the exploratory hypothesis postulated by (Riccio, GE; Newell, KM; Corcos, 1993) and supported by other scientists (Carpenter *et al.*, 2010; Rajachandrakumar *et al.*, 2018), postural sway is viewed not as pure noise in the postural control system, but as part of a perception-action strategy that allows humans to gain essential information about their interaction with the environment.

Minimisation of position variance (SC) per se, does not require ability to maintain appropriate torque for any angle. The ability to maintain an appropriate torque for any angle (FAC) requires greater control facility than the ability to minimise position variance, since FAC requires regulation of force in addition to regulation of position. Arguably, FAC requires implicit knowledge of the torque vs angle relationship of the inverted pendulum. Attaining FAC requires a learning process. Following the previous literature, we hypothesize (i) that minimising sway (SC) reduces exploration of system properties such as the force vs position relationship and is associated with poor learning and limited reduction in falls; and (ii) that minimising force error (FAC) maximizes accurate mapping of the force vs position and it is associated with faster learning and fewer falls.

Participants were strapped to and controlled an inverted pendulum system and the only instruction given was to avoid falls, i.e. maintain the pendulum within the limits of upright balance. Using fall rate as a measure of performance, participants were tested in one session (PRE), then trained in five successive sessions over several days, and then tested again post training (POST).

We devised metrics to quantify the extent to which the FAC strategy and also to which the SC strategy is followed. The FAC metric was the change in correlation of force with position between POST and PRE test sessions. The SC metric was the change in sway between PRE and POST test sessions.

To investigate hypothesis (i) we use regression to test whether the FAC metric is associated with change in performance (falls) and with change in a range of descriptive measures including acceleration, muscle effort and co-contraction.

To investigate hypothesis (ii) we use regression to test whether the SC metric is associated with change in performance (falls) and with change in a range of descriptive measures.

In summary, the aim of this study is to test two hypotheses: (i) FAC is associated with faster learning and fewer falls and (ii) SC is associated with no learning and no reduction in falls.

3.2.2 *Methods*

3.2.2.1 Ethical approval

The experiments reported in this study were approved by the Academic Ethics Committee of the Faculty of Science and Engineering, Manchester Metropolitan University (EthOS Ref 0567) and conform to the Declaration of Helsinki. Participants gave written, informed consent to the experiment which was performed in the Research Centre for Musculoskeletal Science & Sports Medicine at Manchester Metropolitan University.

3.2.2.2 Experimental setup

The experiment consisted in a postural balancing task. Participants stood with their feet on a stable footplate and were strapped rigidly to the same device (WBM) used in the study described in the previous section (see 3.1.2.2).

3.2.2.3 Participants and Protocol

Fifteen healthy participants (6 F + 9 M, 33±8 years) took part in the experiment (Table 3. 1). Participants were first prepared for sEMG recording and baseline thresholds were recorded as above. Participants were then strapped to the WBM and given a short familiarisation with the task of approximately 5 mins which was sufficient to feel comfortable with the task. For the balance task, participants were instructed to not 'fall over', which was explained as meaning to keep the WBM within the range of motion (± 10°).

PARTICIPANT	SEX	AGE(y)	WEIGHT(kg)	HEIGHT(cm)
P1	F	31	53	160
P2	F	26	63	171
P3	F	29	59	167
P4	M	54	67	178
P5	M	27	94	183
P6	M	31	92	186
P7	M	32	80	178
P8	M	47	72	173
P9	F	25	58	164
P10	M	39	60	160
P11	M	34	70	169
P12	F	27	54	164
P13	M	36	75	176
P14	F	36	53	160
P15	M	34	94	180

Table 3. 1 Participants details: sex, age, height and weight.

Merely keeping the WBM within range was in fact a trivial task for participants and one which they learned in a matter of minutes. As in the study described in the previous section, to ensure the task was challenging an input disturbance was applied and discrete changes to the gain of the myoelectric control signal were also applied.

- A multisine disturbance was added to the control signal and hence to the input of the plant dynamics. The multisine disturbance contained 100 frequency components equally spaced in the range 0.1-10 Hz. For each trial the phases were randomised and the crest factor (ratio of maximum deviation to SD) was limited to 3 making the signal unpredictable but periodic (Pintelon & Schoukens, 2001).
- The gain of myoelectric control signal was changed periodically during the task (each period lasted 20 s). This perturbation changes the force output applied to the system from the normal muscle activation. To maintain constant force output, during a change in myoelectric gain, a participant would have to adjust muscle activity inversely to the change in myoelectric gain.

Four multisine disturbance amplitudes (1, 2, 3, 4) and four myoelectric gain levels (0.5, 1, 2, 4) were applied (Figure 3. 6).

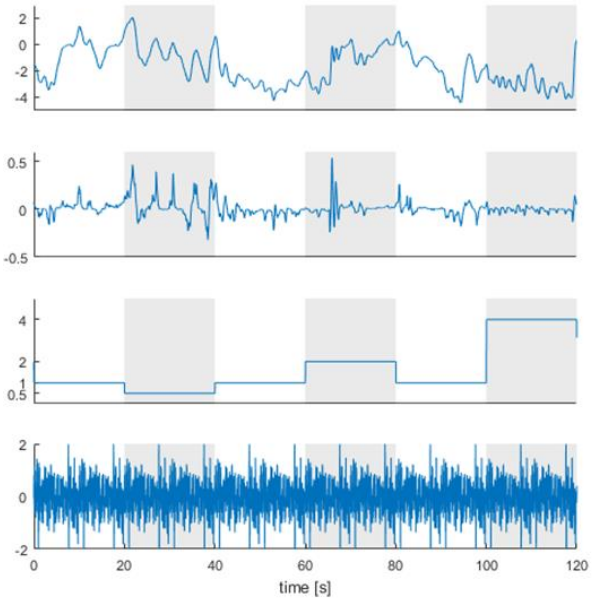

Figure 3. 6 Representative signals recorded during the experiment. Starting from the top, the figure shows the angular position [°], the control signal [mV], the gain applied to the control signal and the multisine disturbance [N]. Vertical bands indicate the trials with constant gain. Without any disturbance or challenge, the task feels trivial and to the participant as if they are "doing nothing". Adding a disturbance and changes in myoelectric gain forces the participant to engage in the task to prevent themselves from falling over.

Following familiarization, the experiment included 7 sessions. We refer to the first session of the training as PRE and to the last session (session 7) as POST. Each session consisted of 64 trials of 20s duration, including all disturbance amplitude and myoelectric gain levels randomized.

3.2.2.4 Data Analysis

The angular position, extracted from the encoder was smoothed using a sixth order Savitzky – Golay filter with a cut-off frequency of 10Hz, which was also used to estimate the subsequent time derivatives. The control signal and the filtered sEMG signals were normalized by the maximum value of the signal, computed considering trials of each participant during the whole experiment.

To address our hypothesis we designed the following measures:

- Success Time (*ST*) [%]: percentage of the time while successfully balancing (i.e. without falling) respect to the entire duration of the trial. This parameter represents the performance outcome of each participant during each training session.

The following measures describe the manner of performance:

- Linearity index (*L*): Pearson correlation coefficient computed between the control signal and the angular position. It is computed as a measure of accuracy in mapping force to position over a range of positions.
- Sway (*sway*) [deg]: angular range of variation explored in the antero-posterior direction. It was computed as two times the standard deviation of the angular position.
- Co-contraction index (*CC*) [%]: percentage of the time while co-activating ankle antagonist muscles respect to the duration of the trial when participants succeed in stabilization. We considered a muscle active when overcoming a threshold (30% of the maximum normalized sEMG signal). This parameter was evaluated separately for right and left leg and the mean value of the two sides was considered. The computed indicator allows assessing the level of co-activation in terms of duration, associated with stiffness control.

- Effort index (E) [mV]: sum of the root mean square values related to the sEMG signals of each muscle. This measure was computed to quantify the muscular effort exerted.
- Mean Acceleration (a) [deg/s^2]: Mean angular acceleration. It captures how much the control signal, on average, diverges from its linear dependence on the angle.

For each measure, we averaged the values of all 64 trials to represent the behaviour for each session.

To characterize learning, we computed the change (Δ) in each measure between the first (PRE) session and the last (POST) session.

$$\Delta X = X_{POST} - X_{PRE} \qquad (2)$$

As shown in Equation 2, change in measure (ΔX) was calculated as the difference between POST mean value and PRE mean value for each participant. Hence, a positive change means an increase of that measure across training. Conversely a negative change means a decrease.

To quantify the extent to which the FAC strategy is followed we calculate a FAC metric. The FAC metric is calculated as the change in correlation of force with position between POST and PRE test sessions (ΔL).

To quantify the extent to which the SC strategy is followed we calculate a SC metric. The SC metric was change in sway between PRE and POST test sessions (Δ$sway$).

Following the flowchart in Figure 3. 7, we tested our two hypothesis through the following steps: (i) we determined whether there was a spectrum of strategies (positive to negative) observing the distribution of FAC (ΔL) and SC (Δ$sway$) metrics, (ii) we used regression analysis to assess learning (change in measures) in relationship with FAC/SC metric and (iii) we used regression analysis to characterize performance (falls) related to FAC/SC metrics. The statistical significance threshold for regression analysis was set at P = 0.05.

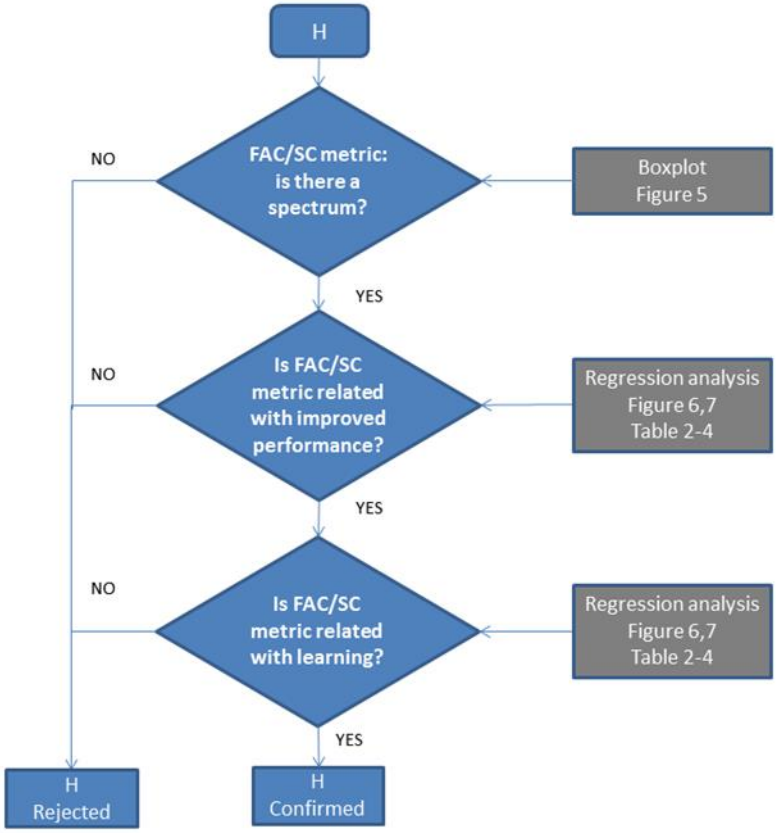

Figure 3. 7. Flowchart to test the two hypotheses (H). Using boxplots we observed the distribution of FAC/SC metrics. Using regression analysis, we tested for significant correlations between FAC/SC metric and number of falls (performance in the instructed task). Using regression analysis, we test for significant correlations between FAC/SC metric and manner of performance (learning as indicated by the other measures).

3.2.3 *Results*

3.2.3.1 Distribution of strategies

This sample of participants shows a spectrum of positive and negative values of both the force accuracy strategy (FAC metric Δ*L)* and the stiffness control strategy (SC metric, Δ*sway*). The inter quartile ranges (IQR) cross zero (Δ*L*: IQR=0.1153; Δ*sway*: IQR=0.9752) and the median change is close to zero (Δ*L*=0.006; Δ*sway*=-0.135 deg) for the FAC and SC strategy respectively (Figure 3. 8). These distributions ensure we can examine the relationship between increasing or decreasing FAC metric and SC metric on performance (falls).

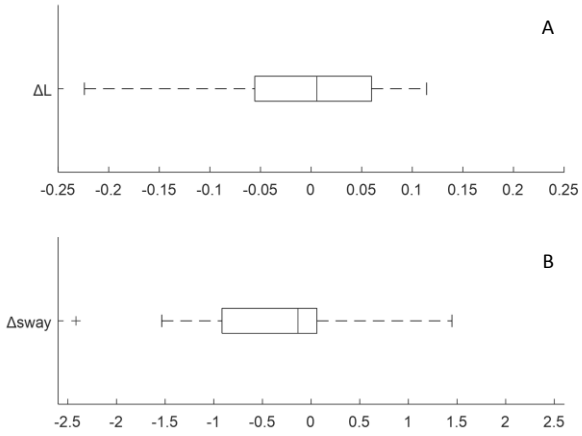

Figure 3. 8 Distribution of strategy metrics of the participants: (A) FAC metric (B) SC metric. In each box plot the central mark indicates the median, and the left and right edges of the box indicate the 25th and 75th percentiles, respectively. The whiskers extend to the most extreme data points not considered outliers. The outliers are plotted individually using the '+' symbol. For each metric, there was a range of participants including those changed positively and those who changed negatively.

3.2.3.2 Effect of force accuracy control (FAC) and stiffness control (SC) strategy on performance (falls)

The hypothesis to be verified is whether the strategy is associated with a change in performance, i.e. the instructed outcome which is to prevent falls.

For the participants of this study, the force accuracy strategy (FAC) was associated with a reduction in falls. Specifically, as a result of training, between PRE and POST test sessions, a change in percentage of success time (Δ*ST)* is correlated positively with a change in linearity index (Δ*L), (*R=0.67, P=0.006, Table 3. 2, Figure 3. 9E), reflecting that an improvement in force accuracy is associated with reduced falls.

Moreover, the stiffness control strategy (SC) was not associated with any change in falls. There is no significant correlation between change in sway (Δ*sway)* and change in percentage of success time (Δ*ST),* (R=0.008, P=0.978, Table 3. 2, Figure 3. 10E), i.e. increase in sway is not associated with a reduction in falls.

Finally, force accuracy and stiffness control metrics were not correlated with the performance measure (*ST*) calculated in the PRE test session (Δ*L*: R=-0.032, P=0.909; Δ*sway*: R=0.282, P=0.308) (Table 3. 3). After training, force accuracy metric was

positively correlated with the performance measure (*ST*) calculated in the POST test session (R=0.612, P=0.015), whereas stiffness control metric did not correlate with POST *ST* (R=0.219, P=0.432) (Table 3. 4).

Hence our first hypothesis is supported. Positive change in FAC metric is associated with improved performance. The second hypothesis is contradicted. Neither positive change in SC metric is associated with improved performance, nor is negative change in SC metric associated with poor performance.

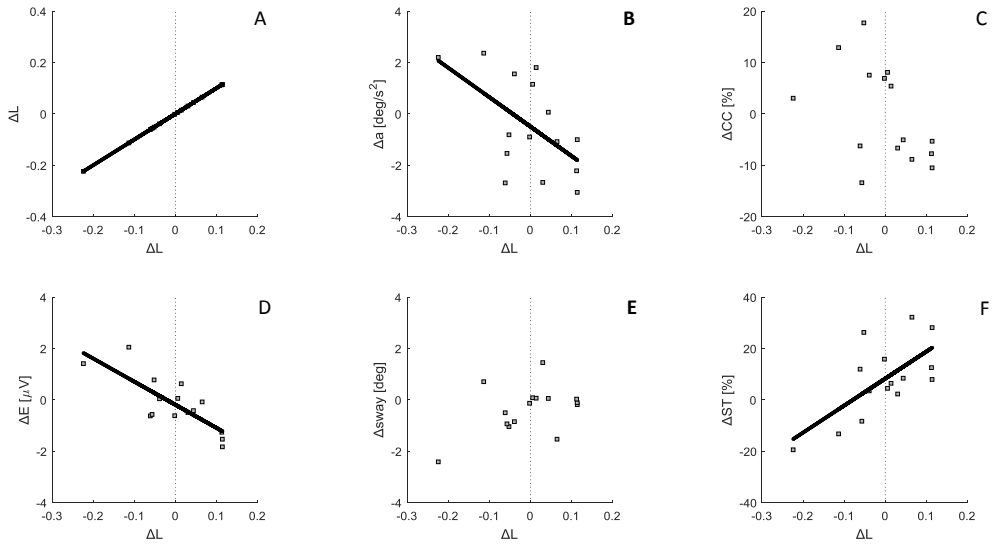

Figure 3. 9 Linear regressions of FAC metric with: (A) FAC metric, (B) change in acceleration, (C) change in co-contraction, (D) change in effort, (E) SC metric (F) change in success time percentage. Each subplot represents data points (grey squares) and the regression line, when correlation is significant. The vertical dotted line corresponds to change in metric equal to zero.

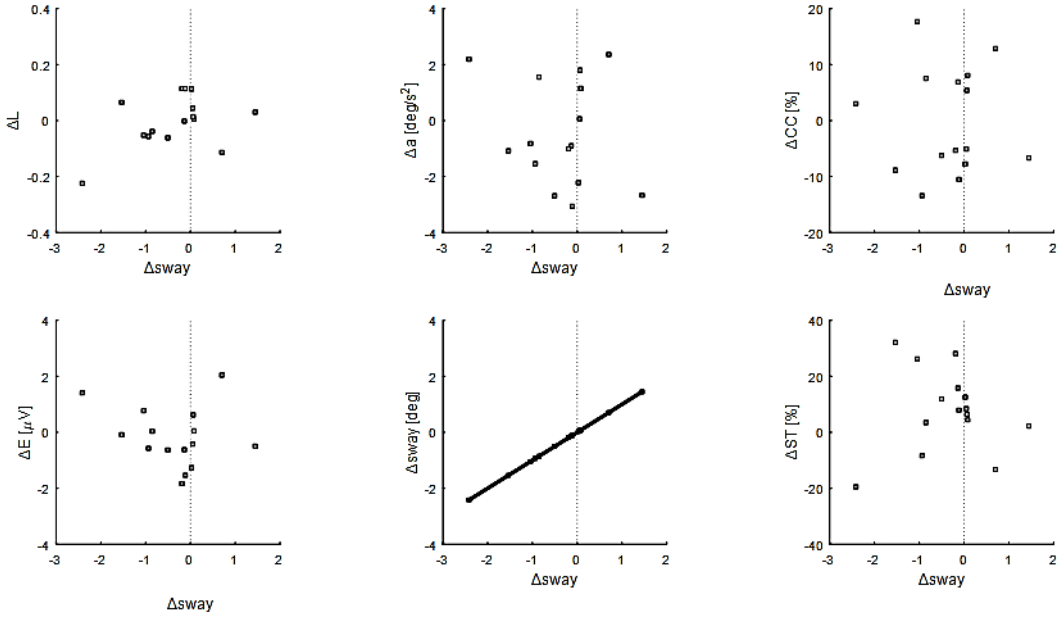

Figure 3. 10 Linear regressions of SC metric with: (A) FAC metric, (B) change in acceleration, (C) change in co-contraction, (D) change in effort, (E) SC metric (F) change in success time percentage. Each subplot represents data points (grey squares) and the regression line, when correlation is significant. The vertical dotted line corresponds to change in metric equal to zero.

3.2.3.3 Effect of force accuracy control (FAC) and stiffness control (SC) on the manner of performance (effort, acceleration)

While instructed performance is measured by falls, the further aspect of the hypothesis to be verified is whether the strategy is associated with a change in *manner* of performance. The force accuracy strategy (FAC) was associated with a reduction in effort and in acceleration. As a result of learning, between PRE and POST test sessions, change in effort (Δ*E)* and change in acceleration (Δ*a*) are correlated negatively with a change in the linearity index (Δ*L*), (Δ*E*: R=-0.7903, P=0.0005*;* Δ*a*: R=-0.567; P=0.027) (Table 3. 2, Figure 3. 9), i.e. an improvement in force accuracy is associated with reduced effort and reduced acceleration.

Moreover, the stiffness control strategy (SC) was not associated with any change in the manner of performance. There is no significant correlation between change in sway (Δ*sway*) and change in effort (Δ*E*: R=0.208, P=0.45) or change in acceleration (Δ*a*: R=-0.214, P=0.444) (Table 3. 2, Figure 3. 10), i.e. a change in sway is not associated with a change in effort and acceleration.

Finally, force accuracy and stiffness control metrics were not correlated with any of the descriptive measures nor the performance measure calculated in the PRE test session (Table 3. 3). After training, force accuracy metric was positively correlated with POST *L* (R=0.582, P=0.023) and negatively correlated with POST *E* (R=-0.655; P=0.008) calculated in the POST test session, whereas stiffness control metric did not correlate with any measure (Table 3. 4).

Hence our first hypothesis is confirmed: Force accuracy control strategy is associated with learning to improve performance and reduce force error, minimizing acceleration and effort. Our second hypothesis is rejected: Stiffness control strategy is not associated with change in performance or change in manner of performance.

	Δ*L*	**Δ*sway***
Δ*L*	R=1; P=0	R=0.445; P=0.097
Δ*a*	R=-0.567; P=0.027	R=-0.214; P=0.444
Δ*CC*	R=-0.472; P=0.076	R=-0.021; P=0.941
Δ*E*	R=-0.7903; P=0.0005	R=0.208; P=0.45
Δ*sway*	R=0.445; P=0.097	R=1; P=0
Δ*ST*	R=0.67; P=0.006	R=0.008; P=0.978

Table 3. 2 Regression analysis of FAC and SC metric with: FAC metric, change in acceleration, change in co-contraction, change in effort, SC metric and change in success time percentage. All R and P values are reported.

	Δ*L*	**Δ*sway***
PRE *L*	R=-0.614; P=0.015	R=-0.299; P=0.279
PRE *a*	R=0.14;P=0.618	R=0.091; P=0.746
PRE *CC*	R=0.375;P=0.169	R=0.112; P=0.692
PRE *E*	R=0.424;P=0.115	R=-0.118; P=0.674
PRE *sway*	R=-0.386;P=0.156	R=-0.705; P=0.003
PRE *ST*	R=-0.032; P=0.909	R=0.282; P=0.308

Table 3. 3 Regression analysis of FAC and SC metric: FAC metric, acceleration, co-contraction, effort, SC metric and success time percentage relative to the PRE session. All R and P values are reported.

	ΔL	***Δsway***
POST *L*	R=0.582; P=0.023	R=0.232; P=0.406
POST *a*	R=-0.447; P=0.094	R=-0.14; P=0.618
POST *CC*	R=-0.161; P=0.567	R=0.068; P=0.809
POST *E*	R=-0.655; P=0.008	R=-0.31; P=0.261
POST *sway*	R=0.177;P=0.527	R=0.584; P=0.022
POST *ST*	R=0.612;P=0.015	R=0.219;P=0.432

Table 3. 4 Regression analysis of FAC and SC metric: FAC metric, acceleration, co-contraction, effort, SC metric and success time percentage relative to the POST session. All R and P values are reported.

In conclusion, our first hypothesis that Stiffness Control is associated with learning and better performance was rejected.

Our second hypothesis that Force Accuracy Control is associated with faster learning and better performance was confirmed.

3.2.4 *Discussion*

This study used a challenging postural task, to investigate the relationship between the control strategy adopted to maintain balance and the level of learning and robustness to falls.

Our hypotheses were (i) that minimising force error (FAC) maximizes accurate mapping of the force vs position relationship and it is associated with faster learning and fewer falls; and (ii) that minimising sway (SC) reduces exploration of system properties such as the force vs position relationship and is associated with poor learning and limited reduction in falls. We devised measures descriptive of the strategies and tested those for correlation with measure of performance and manner of performance. The results confirm the predicted associations, however, the interpreting the relevance of the preceding theory requires some discussion.

Results confirm that as a group, participants maintained balance using a spectrum of control strategies (Figure 3. 8). We show that prioritizing regulation of force (FAC) was correlated with better learning and better performance (falls reduction) (Figure 3. 9), whereas regulation of position (SC) was not (Figure 3. 10). Specifically, increased correlation between force and position (representing an improvement in force accuracy,

$\Delta L>0$), was associated with improvement in performance (*ST*), and decreased correlation between force and position, representing a deterioration of force accuracy ($\Delta L<0$), was associated with poorer performance (Figure 3. 9E). By contrast, minimising sway (SC) was not associated with change in any measures except sway and was not associated with reduction in falls. Sway was unrelated to performance (falls) and manner of performance (effort, co-contraction, acceleration) (Figure 3. 9, Table 3. 2,Table 3. 3).

The SC and FAC metrics were uncorrelated, removing possible evidence of association between exploration of position and ability to maintain an appropriate torque for the position of the inverted pendulum. A correlation between reduction in sway and decreased performance, or manner of performance, would have supported the hypothesis that sway allows acquisition of information important for learning (Riccio, GE; Newell, KM; Corcos, 1993). However, the absence of such a correlation does not refute the exploration hypothesis. We have also to consider that the FAC metric denotes ability to correlate force with position over a range of positions of an unstable system. FAC is thus equivalent to combining low force error (low acceleration) with wide range of positions. Hence the exploration hypothesis remains neither supported nor refuted.

Since force minimization (FAC) is linearly related to fall rate, whereas position minimization (SC) is not, the variable FAC is identified as more important than position for performance (falls) and manner of performance (effort, acceleration). Increased FAC represents a combination of reduced acceleration and increased sway, including also reduced acceleration and constant sway, or unchanged acceleration and increased sway. The importance of FAC is in line with a computational study (Insperger *et al.*, 2013) showing that once the position, velocity and acceleration (which is proportional to force error) are estimated in an optimal way, the proportional– derivative–acceleration (PDA) controller provides better stability properties than the corresponding proportional–derivative (PD) controller.

However, given physiological delays, a PDA controller has to predict the actual state based on the delayed position, velocity and acceleration. Prediction accuracy is relevant to performance. Accuracy in the implicit perception of the torque vs angle relationship of the inverted pendulum is crucial to the relationship between motor commands (force) and motion, enabling the central nervous system to adapt the dynamics of the body to the environment. The observed correlation of increasing force accuracy control (FAC) with decreasing effort (Figure 3. 9D), combined with no correlations with sway minimization

(SC) (Figure 3. 10, Table 3. 3), supports the hypothesis that learning is related to force accuracy. Participants who improved force accuracy improved their performance and reduced their effort. This relationship is consistent with previous works showing how control becomes more economical as the dynamics of the task are learned (Milner & Cloutier, 1993; Thoroughman & Shadmehr, 1999; Emken *et al.*, 2007; Finley *et al.*, 2013).

Correspondingly, the change in acceleration correlated negatively only with FAC metric; i.e. force accuracy and learning are associated with minimization of acceleration more than minimisation of sway (Figure 3. 9B, Figure 3. 10B). Experimental and modelling studies on quiet standing suggest that the goal of the central nervous system is not to keep the centre of mass at a constant position, but rather to minimize its acceleration (Aramaki *et al.*, 2001; Morasso *et al.*, 2019).

Concerning muscles co-contraction, we expected to find *CC* positively correlated with the SC metric, supposing that minimization of position variance (stiffness control) is achieved by co-contraction of the antagonist muscles similarly to upper limb. However, co-contraction did not correlate with any of the strategy metrics (Table 3. 2, Table 3. 3 and Table 3. 4). The lack of association (CC vs SC) is reasonable because in natural standing, ankle stiffness is not enhanced by co-contraction due to the low series stiffness of the tendons crossing the ankle joint (Loram & Lakie, 2002*a*; Casadio *et al.*, 2005). Likewise in this experiment co-contraction generated no passive change to the computer controlled dynamics of the inverted pendulum.

It remains unclear why participants adopt one strategy rather than another. During the PRE session, all participants started from similar conditions, since neither FAC nor SC showed any correlation with any measures of performance (Table 3. 3). Furthermore, we found no correlation between any anthropometric features (height, mass) or age and the strategy adopted.

In conclusion, this study showed that the adoption of a force accuracy control strategy led the participants to better performance, better energetic efficiency and better learning, independently on their control strategy on position. From an optimal motor control perspective, the strategy is represented by the choice of the cost function to minimize (Scott, 2012): our data suggest that prioritising regulation of force leads to better learning. If we interpret our results from an intermittent control perspective (Gawthrop *et al.*, 2014*b*), we can speculate that learning to use the FAC strategy leads to ‘more

intermittent' active control. This change related to learning may be seen as a change in the trigger parameters (e.g. increase of the thresholds on the states responsible for switching on the active control).

Since our FAC metric predicts reduced falls and more economical balance, we propose this measure as a potential clinical indicator and also as a potential measure for feedback to guide training to improve balance. A number of studies conducted on athletes and elderly people suggest that decreased muscles activation and lower joint stiffness levels prevent muscle fatigue, falls and injuries (Butler *et al.*, 2003; Benjuya *et al.*, 2004). Our evidence is limited to 15 participants, but the results support further investigation of use of this metric to train people to change their strategy and avoid potential falls or injuries in everyday life situations. This metric, and possibly also this experimental regime, might prove beneficial for several populations - ranging from young athletes to elderly people with impaired balance, but also Parkinson's disease patients or stroke survivors.

This work has been submitted and is now under review (A. Cherif, I. Loram, J. Zenzeri. "Human balance of an inverted pendulum: force accuracy rather than high stiffness is associated with greater learning and reduced falls". Under review for Scientific Reports).

3.3 Intermittency in balance control

Results of the previous study were interpreted in both an optimal control and an intermittent control perspective, since the nature of postural control is an open question. The following study puts light on the possible mechanisms behind postural control, focusing on understanding if they are linear or non-linear.

3.3.1 *Introduction*

Regulation by negative feedback is fundamental to engineering and biological processes, including control of movement, systemic physiological variables (blood pressure, temperature) and cellular processes including gene expression. Whereas biological regulation is usually explained using continuous feedback models from classical and modern engineering control theory, an alternative engineering control paradigm, intermittent control (Gawthrop *et al.*, 2011, 2014*b*), has also been suggested for biological control systems (Craik, 1947; Vince, 1948; Neilson & Neilson, 2005; Bye & Neilson, 2008).

A continuous controller is a state feedback model, completely linear time invariant (LTI). The principles separating intermittent from continuous control can be (i) a clock trigger (discrete sampling), e.g. a minimum delay (open loop delay) must have elapsed since the previous event to initiate an action and/or (ii) an event trigger, e.g. the prediction error exceeding a threshold triggers a response. These principles make intermittent control not LTI.

Evidences of these principles in motor control have been repeatedly observed.

There is some experimental evidence that human control systems are event driven (Navas & Stark, 1968; Loram *et al.*, 2012) and event-driven control was used to explain postural control as intermittent predictive open loop/feedforward control which uses discrete or event triggered sampling to update the controller (Craik, 1947; Gawthrop *et al.*, 2014*a*).

Another possible explanation is provided by intermittent state switching controllers (Bottaro *et al.*, 2005; Asai *et al.*, 2009). These models are intermittent controllers characterized by a switching function defined in the phase plane: control bursts are generated when the current state vector (position and velocity) exits an area of uncertainty around the reference point in the phase plane.

In clock or event triggered sampling, refractoriness has been defined as the inability to modify an already initiated control response for a certain amount of time and it was explained through the Single Channel Hypothesis. This hypothesis postulates that certain stages in the process of sensory analysis (SA), response planning/selection (RP/S) and response execution (RE) cannot overlap (Craik, 1947; Gawthrop *et al.*, 2011; van de Kamp *et al.*, 2013*b*). In other words, when two unpredictable stimuli are presented closely spaced in time, the response to the first stimulus will, at some point, interfere with the response to the second stimulus. A minimum refractory duration is linked to time taken for some process to recover. However, refractory duration can be adapted by adjusting decision thresholds. Such a role would be evident when making decisions involving a high degree of response conflict (Frank, 2006).

(van de Kamp *et al.*, 2013*b*) provided evidence of refractoriness in visuo-manual control in healthy subjects. However, balance control is a different system from manual control.

In fact the neural systems responsible for postural control are separate from the neural substrates that underpin control of the hand (Malina *et al.*, 2004).

In addition, experimental evidence has been presented (van der Kooij & de Vlugt, 2007) in which the authors advocate that postural responses to external stimuli are dominated by continuous feedback and cannot be explained by intermittent control. However (Gawthrop *et al.*, 2011) showed how an intermittent controller can appear as a continuous controller. They presented simulation results to show that fixed sample interval intermittent control can masquerade as continuous control. This is relevant to event-driven control: an intermittent controller with fixed sampling interval is recast as an event-driven controller.

Since the nature of intermittency in human motor control remains an open question, in this study we investigate whether postural control is linear or non-linear and, in case of non-linearity, we try to provide an explanation for the nature of non-linearity. We investigate presence or absence of responses to any stimuli, the time since previous stimulus/response, the state and the interaction of state with stimulus (indicating prediction or surprise)**.**

3.3.2 *Methods*

3.3.2.1 Ethical approval

The experiments reported in this study were approved by the Academic Ethics Committee of the Faculty of Science and Engineering, Manchester Metropolitan University (EthOS Ref 0567) and conform to the Declaration of Helsinki. Participants gave written, informed consent to the experiment which was performed in the Research Centre for Musculoskeletal Science & Sports Medicine at Manchester Metropolitan University.

3.3.2.2 Experimental setup

The experiment consisted in a postural balancing task. Participants stood with their feet on a stable footplate and were strapped rigidly to the same device used in the previous two studies (see 3.1.2.2) (Figure 3. 1).

3.3.2.3 Participants and Protocol

Twenty three healthy participants (7 F + 16 M, 35±11 years) took part in the experiment. Participants were first prepared for sEMG recording and baseline thresholds were recorded as above. Participants were then strapped to the WBM and given a short familiarisation with the task of approximately 5 mins which was sufficient to feel comfortable with the task.

In the current study, participants controlled the dynamics of a marginally stable load (van de Kamp *et al.*, 2013*b*). Participants were told that every now and then, the WBM would gently push them forwards or backwards and were instructed to not 'fall over', which was explained as meaning to keep the WBM within the range of motion (± 10°).

To minimize the predictability of the pushes, the sequences of impulse stimuli were designed in the following way. Spatial unpredictability of the double step stimuli was achieved by varying the direction of the impulses (forward-forward, forward-backward, backward-forward, backward-backward, see Figure 3. 11). Forward-forward and backward-backward combinations are defined as unidirectional (uni) double stimuli; forward-backward, backward-forward are named bidirectional (bi) double stimuli.

Temporally, stimulus predictability was eliminated by varying the inter stimuli interval (ISI) through 8 levels: 0.15, 0.25, 0.35, 0.55, 0.8, 1.4, 2.5, 4 s. The eight different double stimuli were presented four times (one for each combination of directions) in a randomized order, for a total of 32 double stimuli in each trial. Each participant performed 5 trials.

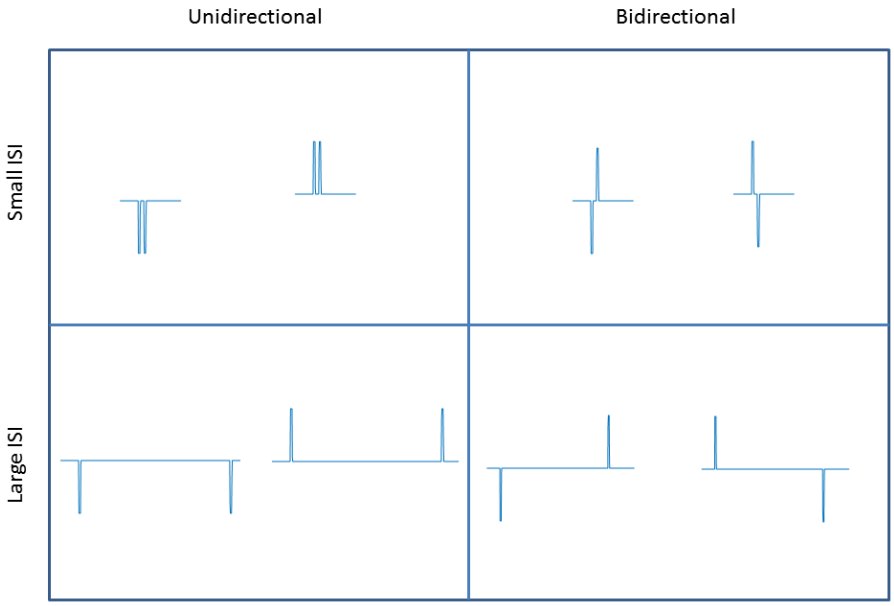

Figure 3. 11 Representative set of the impulses double stimuli used in the experimental protocol. Top panels show double stimuli separated by a small inter stimuli interval (ISI=0.15s). Bottom panels show double stimuli separated by a large inter stimuli interval (ISI=4s). Left and right panels differ for the direction of the consecutive stimuli: on the left there are examples of unidirectional double stimuli (uni), on the right the second stimulus has reversed direction respect to the first (bi).

3.3.2.4 Data analysis

Following (Loram *et al.*, 2012), we used a multi-step process to estimate the Response Time delay (RT) for each first and second stimulus (i.e. RT1 and RT2) by modeling the closed loop relationship between the stimuli (pulses sequence) signal and the control signal as a low order, zero delay, autoregressive external input (ARX) process.

First, the ARX model's order (4th) was set such that the number of coefficients was sufficient to capture the participants' responses. We reconstructed the impulses sequence by sequentially and individually adjusting the instant of each impulse not to increase the fit but to estimate onset times of each response to each stimulus and test whether these is a systematic pattern to those onset times. This was done in a time-invariant and in a non-time-invariant way.

Time-invariant optimization means that a best ARX fit is achieved by reconstructing the impulses sequence using equal adjustments of the instant of all impulses (basically determining the time delay of the ARX model). The non-time-invariant optimization method allowed different adjustments of the instant of the first and second impulses and can be referred to as an 'adjusted ARX model'. If the description can be improved by optimizing the delay to each impulse, this procedure will provide a distribution of delayed responses to each first and second step (RT1 and RT2). The non-time-invariant optimization allowed also non response cases: stimuli for which the response delay was over 1 s were considered as missing response cases.

The system states (position and velocity) were obtained by the recorded encoder position using a sixth order Savitzky – Golay filter with a cut-off frequency of 10Hz. To investigate the reason behind missing responses and the possibility of an event triggered mechanism, we observed the states right before (30 ms) the onset of the stimuli. In addition, we consider the interaction of direction of the stimuli with the velocity state (Velocity*Stim computed as signed stimulus amplitude multiplied by signed velocity state, 30 ms prior to stimulus onset).

Analysis of the delays with respect to ISI can test for refractoriness.

Analysis of the missing responses can test for event triggered control policies.

Without requiring any model based assumptions, the following tests provide evidence which can discriminate against continuous control and quantify the extent of refractoriness in this task:

- Is the system linear or non-linear?

Linearity between stimuli and responses would be supported by a better fitting of the original ARX than the same order adjusted version or by no systematic effects in distribution of onset times.

In case of non- linearity,

- Is RT2 greater than RT1?

A hypothesis of no refractoriness would predict equal delays. Refractoriness would increase RT2 but not alter RT1.

- Is there an interaction between the factors: Step Number (first and second) and ISI (levels 1 through 8)?

A hypothesis of refractoriness would predict an interaction between ISI and Step Number. Refractoriness would alter RT2 for small ISI.

- Is RT1 independent of ISI?

A refractory hypothesis would predict that RT1 is independent of ISI.

- What is the ISI up to which RT2 is significantly greater than RT1?

Testing within each level of ISI for differences between RT1 and RT2 will reveal the ISI up to which there is interference between RT2 and RT1 and quantifies the duration of refractoriness.

- Is there always a response or are there any missing responses to stimuli?

In case of missing responses,

- Is the presence or absence of response state-dependent? Does it depend on position, velocity or acceleration prior to stimulus onset?

Testing this dependency may reveal event-triggered control policy, especially for the first impulse which is not affected by any interference.

The first measures of interest were the distributions of RT1 and RT2. A repeated measures ANOVA design was used to test for the effects of Stimulus Number (first and second), ISI (level 1 through 8) and interactions.

Then, repeated measures ANOVA design was used to investigate also possible relationship between state (prior to stimuli onset) and Response presence. We tested for the effect of Stimulus Number (first and second), ISI (level 1 through 8), response (present and missing) and their interactions.

The average of the Greenhouse–Geisser and Huyhn-Feldt corrections of degrees of freedom was used based upon the estimates of sphericity. Post-hoc ANOVAs were run to evaluate significant main and interaction effects.

3.3.3 *Results*

Constructing the adjusted set-points resulted in a better (ARX) description of the data: this is evident when we look at the response amplitude and even more when we look at the actual timing of the responses (Figure 3. 12).

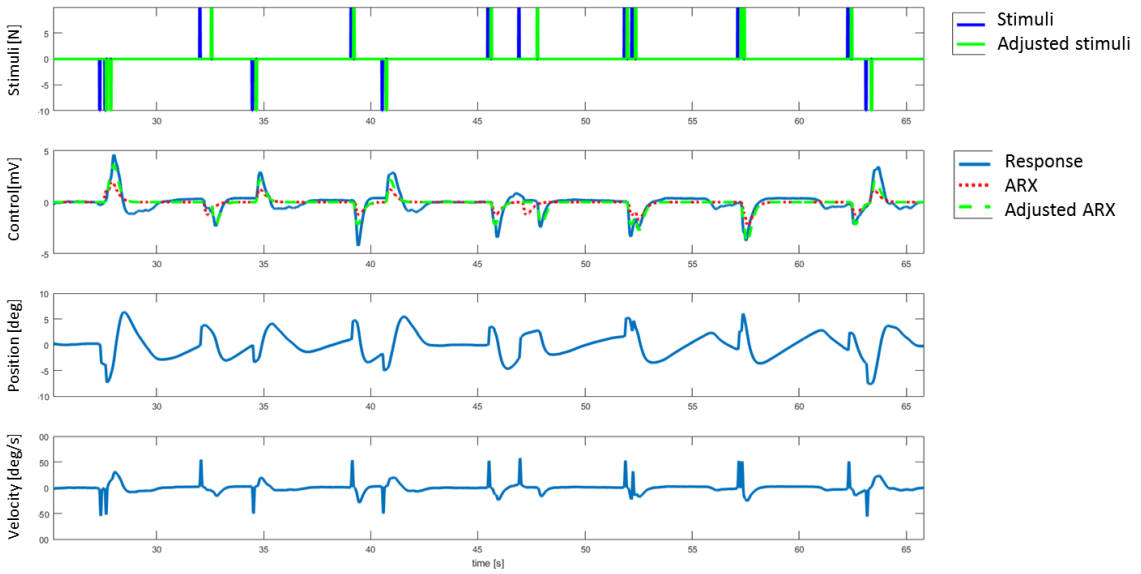

Figure 3. 12 Reconstruction of the set-point (top panel) and of the responses (bottom panel). Top panel show in blue the original impulses stimuli delivered in the experiment and in green the optimized reconstructed stimuli. In the second panel, the dotted line (red) shows the time-invariant optimized ARX fit corresponding to the original double stimuli. The dashed line (green) shows the best fitting ARX model corresponding to the non-time-invariant optimized impulses sequence. The third panel shows the position of the system over time. The bottom panel shows the velocity of the system over time.

The analysis revealed that allowing variable delays and missing responses improved data description. Figure 3. 13 illustrates two representative examples of responses to double stimuli. Left panel shows an example where the participant responds to both stimuli (blue solid lines). Right panel shows an example where no response is a better description than a response within the physiological range of time delays. Looking at the example in the left panel with a small ISI, we observe that the response to the second impulse is interfered by the response to the first impulse. This interference is characterized by an elongation of the second response time compared to the first response time.

These results support the hypothesis of non-linearity of the processes behind balance control. To further investigate the nature of this non-linearity, we analyzed the effect of the number of the stimulus on the response times. Figure 3. 13 shows the distributions of response times to first and second stimuli. It is clear that RT2 distribution has a lower peak, which is also slightly shifted towards greater values. The remaining RT2 values are spread on higher values, as shown by a more relevant tail of the distribution.

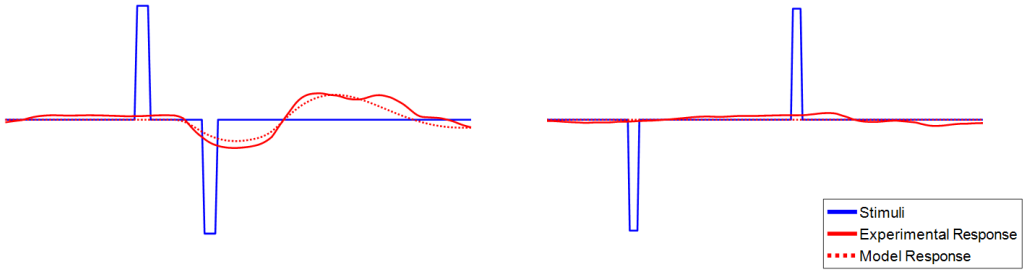

Figure 3. 13 Representative non- linear responses over time (red solid lines). Left panel shows an example where the participant responds to both stimuli (blue solid lines). Right panel shows an example where the participant does not respond to any stimuli. The dotted red line shows the best fitting ARX model corresponding to the non-time-invariant optimized impulse sequence.

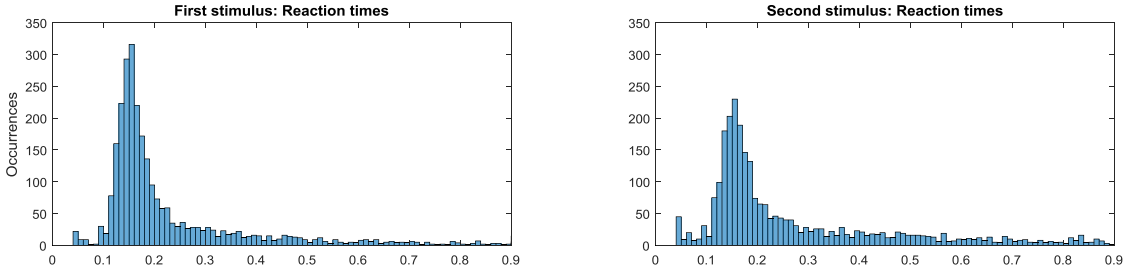

Figure 3. 14 The distributions of response times to first (RT1, left panel) and second stimuli (RT2, right panel). Top panels show the distributions including all stimuli pairs. The x axis represents RT [s], the y axis represents the occurrences for each value.

To test for refractoriness, we need to look at the behavior for the different ISIs. Figure 3. 15 shows that the distribution of RT1 is very similar between ISIs whereas the distribution of RT2 changes between ISIs. In particular the distribution of RT2 for large ISIs is comparable to the distributions of RT1, whereas the distribution for small ISIs tends to flatten and spread towards higher values.

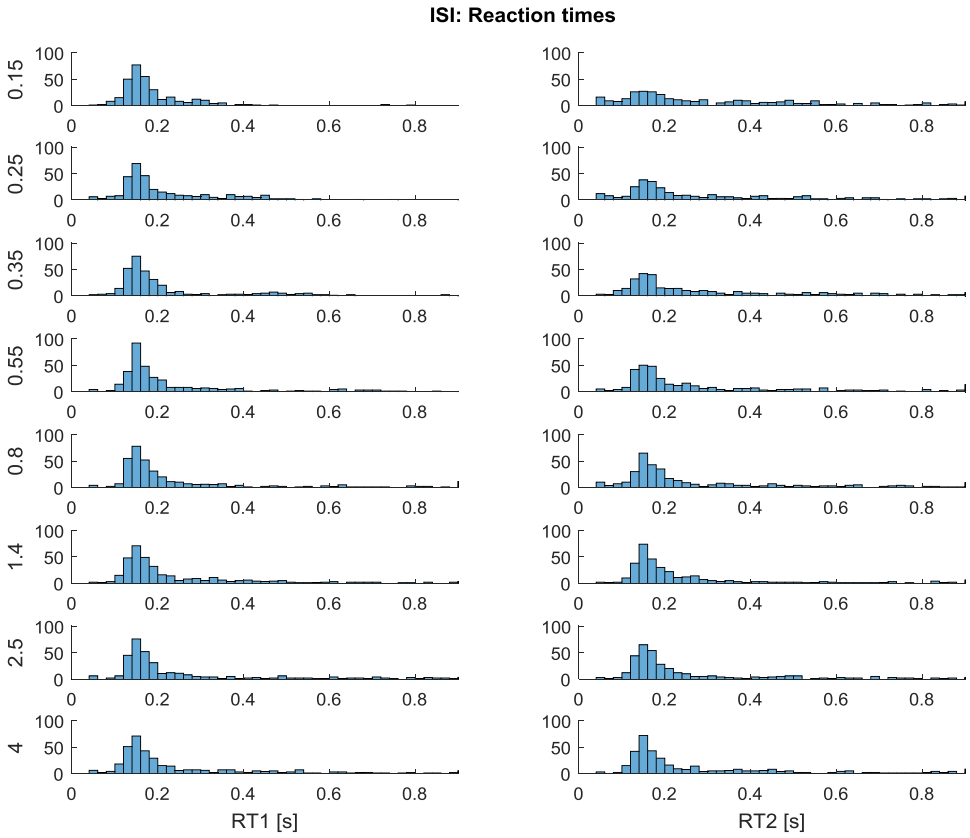

Figure 3. 15 The distributions of response times to first (RT1, left panels) and second stimuli (RT2, right panels) divided by the 8 ISIs (0.15, 0.25, 0.35, 0.55, 0.8, 1.4, 2.5, 4 s). The x axis represents RT [s], the y axis represents the occurrences for each value. Top panels show responses to double stimuli with the smallest ISI (0.15 s). Moving towards the bottom panels, the ISI grows reaching the maximum value (4 s).

To test these results we performed statistical analysis. We obtained a mean value for each participant for each ISI and we averaged them to test the general behavior (Figure 3. 16). Statistical test confirms that RT2 is significantly greater than RT1 (mean±S.D: RT1=0.24± 0.06s; RT2=0.30±0.06s; $F(1, 22) = 101$, $p<0.001$). In addition, there is an ISI effect ($F(7, 154) = 3.06$, $p = 0.01$) and an interaction effect ($F(7, 154) = 9.55$, $p<0.001$): the difference between RT1 and RT2 is significant for small ISIs up to 0.55 ($p<0.001$). Interestingly, ISI has an effect also on RT1 ($F(7, 154) = 6.96$, $p <0.001$).

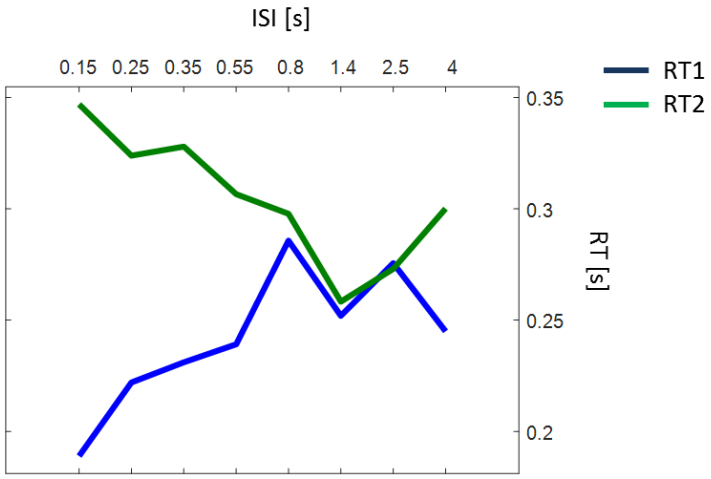

Figure 3. 16 The inter-participant means (22 participants in each condition) in RT1 (blue line) and in RT2 (green line).

Results confirm that the response to the second impulse is interfered by the response to the first impulse, when the responses occur.

However, data revealed that participants do not always respond to stimuli and the adjusted ARX was able to identify also when the response was missing (Figure 3. 13).

The percentage of missing responses identified by the adjusted ARX is around 20% in all conditions.

To investigate the reason for missing responses and investigate the possibility of an event triggered mechanism, we observed position, velocity and the interaction of stimulus direction with velocity right before (30 ms) the onset of the stimuli. Then we performed statistical analysis on: displacement from vertical (absolute value of position), speed (absolute value of velocity) and the interaction of stimulus direction with velocity right before (30 ms) the onset of the stimuli.

Displacement before stimulus 1 is significantly different from position state before stimulus 2 ($F(1, 22) = 15.1$, $p = 0.000808$). This is due to the fact that before the delivery of the second stimuli, the position state is perturbed due to the first stimuli (see Figure 3. 17), especially when the two stimuli are close in time. However there is no main effect of the Response factor: position is the same before either response or missing responses cases ($F(1, 22) = 0.00405$, $p = 0.95$). Interaction effect ($F(1, 22) = 5.08$, $p = 0.0346$).

Figure 3. 18 shows that speed is higher before the second stimulus of the couple is delivered. This is again evidence that the state is perturbed by the first stimulus, when the second occurs. Similarly to position, for the velocity state, there is a main effect of the

stimulus order (F(1, 22) = 97.8, p = 1.48e-09) and no effect of presence of response (F(1, 22) = 2.76, p = 0.111) with no interaction effect (F(1, 22) = 0.972, p = 0.335).

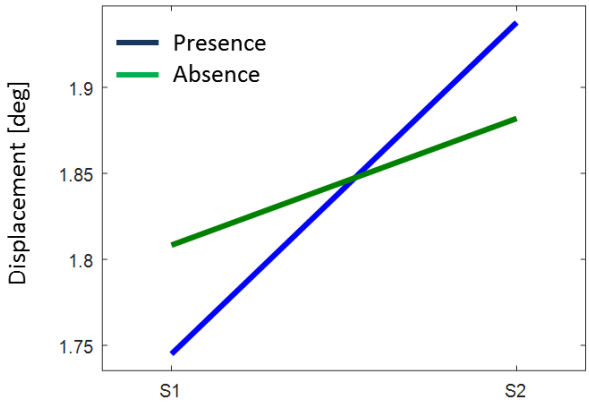

Figure 3. 17 Mean displacement (absolute value of position state) sampled 30 ms prior to the onset of the stimuli. Lines show in blue the position state before a response, in green the position state before a missing response.

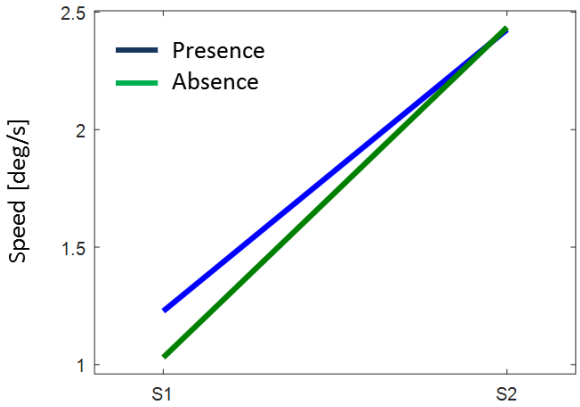

Figure 3. 18 Mean speed (absolute value of velocity state) sampled 30 ms prior to the onset of the stimuli. Lines show in blue the position state before a response, in green the position state before a missing response.

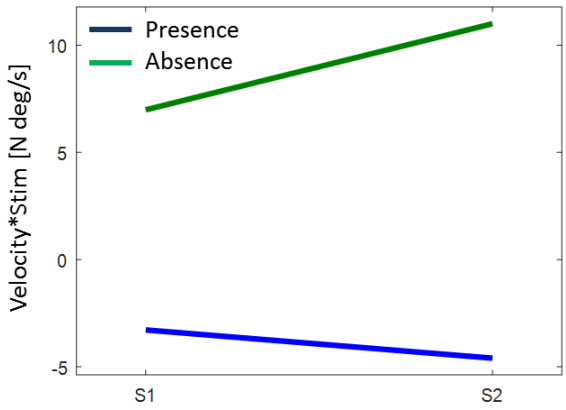

Figure 3. 19 Mean Velocity*Stim (representing the interaction of stimulus direction with velocity state) sampled 30 ms prior to the onset of the stimuli. Lines show in blue the position state before a response, in green the position state before a missing response

These results, in particular the ones for the first stimulus which is not affected by any interference, suggest that response was not position dependent or velocity dependent.

To analyze the interaction of stimulus direction with velocity state we used Velocity*Stim value sampled 30 ms prior to the onset of the stimuli. This metric allows understanding if the stimuli perturbation is in the same direction (Velocity*Stim>0) or in the opposite direction (Velocity*Stim<0) to the system motion prior to the occurrence of the stimuli. Figure 3. 19 shows a main effect of the Response factor ($F(1, 22) = 52.7$, $p = 2.83e\text{-}07$): Velocity*Stim is positive before a response whereas it is negative before a missing response. The same phenomenon is observed for both first and second stimuli (no Order effect: $F(1, 22) = 0.779$, $p = 0.387$; no interaction effect $F(1, 22) = 2.98$, $p = 0.0981$). This means that the presence of the response depends upon the interaction of stimulus direction with state. There are two possible explanations for this: prediction error threshold is not exceeded so easily when stimulus is in same direction as movement or participants are refractory since they have already responded to movement.

3.3.4 *Discussion*

In this study, we provide evidence for systematic non-linearities in postural control, which are the key feature discriminating intermittent from continuous control.

Specifically we provide evidence for refractoriness and state-dependent inhibition of responses.

Since perturbations can elicit both stereotypical motor reflexes and voluntary control processes we examined the values of time delays in context with neurophysiological delay. Short-latency reflex (SLR) occur with a delay of 20-50 ms whereas voluntary reaction occurs with a delay greater than 100 ms. Between them, there is long latency reflex (LLR) which occurs earlier (50-100ms) than standard metrics of voluntary reaction time yet can sometimes be voluntarily modified by a subject, but they can be only gated or modulated in amplitude (Pruszynski & Scott, 2012). In our experiment, the magnitude of RTs identified is associated to voluntary control.

Our results showed that delays to the second stimuli were on average longer than delays to the first stimuli (Figure 3. 14). This finding leads to the rejection of a hypothesis of zero refractoriness that predicts equal ranges and equal averages in RT.

Our results showed the interaction between Stim Number and ISI that was predicted by the alternative hypothesis of refractoriness. Breaking down this interaction showed that delays to the second stimuli increased with decreasing ISI levels. Since the refractory duration is defined as the temporal separation of stimuli beyond which there is no interference, we evaluated the inter-stimuli interval (ISI) up to which the time to respond to the second step (RT2) is elongated relative to the time to respond to the first step (RT1). Our data show that the critical ISI has to be greater than 0.55s and below 0.8 seconds, which is the ISI for which RT2 and RT1 become comparable (Figure 3. 15 and Figure 3. 16).

Moreover ISI affects also RT1: RT1 decreases as ISI decreases. This is consistent with intermittent control where sensory information is sampled more frequently than the stimuli that we deliver, i.e. approaching a time repeating (clock-driven) intermittent control rather than event-driven intermittent control (Loram *et al.*, 2012). This would occur because the prediction error increases, requiring sampling, even without the disturbance of the stimuli.

The second feature of non-linearity found in our data is the presence of missing responses. Participants did not respond to 20% of the stimuli delivered. This percentage remains unchanged for each ISI level and for both Stim1 and Stim2. This means this is a general phenomenon, unrelated with the interference between stimuli.

Therefore we investigated the possibility of event-triggered control. Results showed no correlation between presence of response and position state by itself or velocity state by itself. However, taking into account the direction of motion of the system prior to stimuli

and the direction of the stimuli, we found that inhibition of response depends upon the interaction of stimulus direction with velocity state. Specifically when the perturbation is delivered in the same direction of motion, there is a higher probability of missing responses than when the perturbation is against the direction of motion. One possible explanation is that prediction error is important: a stimulus in the current direction does not exceed prediction error threshold, and does not evoke a response whereas an opposing perturbation may cause a greater prediction error and consequently evoke a response. Moreover, Velocity*Stim is higher when velocity is higher. Results show that No response is more likely when Velocity*Stim is lower, whereas a response is more likely when velocity is higher and thus the person is more likely to be refractory when the stimulus comes. This result is in line with event-triggered intermittent control mechanism.

It is important to mention one possible limitation of the method which sometimes classifies the weaker responses as missing responses. This is because the method allows only 0% (No response) or 100% amplitude (Response). Further analysis will be performed, going in the direction of a more dynamical system, e.g. including in the model variation of responses amplitude with a time dependency. However, an actual fact is that missing (or weak) responses were more likely observed when the direction of the stimuli was opposite to current sway motion.

In summary, the mechanisms involved in human balance are non-linear in nature and intermittency applies to it.

This work is in preparation for Journal of Physiology (A. Cherif, J .Zenzeri, I. Loram. "Intermittency in human balance". In preparation for Journal of Physiology.)

Chapter 4

Self-generated disturbances

4.1 Influence of an additional joint on motor control

The previous chapter took into account standing as single inverted pendulum destabilized by external perturbations.

Here we address what happens if the central nervous system controls balance but with an additional joint (the hip). An additional thing to coordinate could be a disturbing factor. For this reason, we investigated whether the double inverted pendulum is a worthy complication of standing models than the single one and consequently if a hip strategy is worthy.

4.1.1 *Introduction*

Bipedal upright standing on a stable surface is an ability acquired early in life and performed in a fully automatic manner without any degree of attentional effort. Apparently, it seems hardly a worth topic in the study of balance and postural control, except for the clinical setting, given the simplicity of an experimental investigation typically based on force platform measurement of involuntary sway movements in the sagittal plane. The implicit assumption underlying the clinical interest of body sway is that the projection of the body center-of-mass on the standing surface (CoM) is the regulated variable of the postural control system, which can be indirectly accessed by measuring the position of the center-of-pressure (CoP). A number of performance measures of maintenance of this posture, based on the CoP-CoM pair, have been developed which are used in clinical decision making (Visser *et al.*, 2008) in relation with a number of pathological conditions, such as the following ones: cerebellar ataxia (Diener *et al.*, 1984; Baloh *et al.*, 1998; Bakker *et al.*, 2006), vestibular dysfunctions (Black *et al.*,

1988; Allum *et al.*, 2001; Alvarez-Otero & Perez-Fernandez, 2017), peripheral neuropathy due to diabetes (Di Nardo *et al.*, 1999; Reid *et al.*, 2002; Bittar *et al.*, 2016), Alzheimer's disease (Chong *et al.*, 1999; Lee *et al.*, 2017), multiple sclerosis (Williams *et al.*, 1997; Hebert & Manago, 2017), Parkinson's disease (Błaszczyk *et al.*, 2007; Rossi-Izquierdo *et al.*, 2014), traumatic brain injury (Buster *et al.*, 2016; Gandelman-Marton *et al.*, 2016), stroke (Ondo *et al.*, 2000; van Asseldonk *et al.*, 2006) and identification of malingerers for forensic medicine (Uimonen *et al.*, 1995).

The underlying biomechanical model is a Single Inverted Pendulum (SIP), pivoted around the ankle. In this framework, sway movements are interpreted as back and forth oscillations of the SIP under the action of opposing forces, namely the destabilizing force of gravity, counteracted by the stabilizing effect of ankle muscles. However, the mechanisms and control principles involved were and are not evident and are still topics of scientific dispute. In this framework, an influential proposal is the muscle stiffness control model by Winter et al. (Winters *et al.*, 1988) which may be considered as a member of the family of control models related to the Equilibrium Point Hypothesis (EPH) (Feldman, 1966; Bizzi *et al.*, 1982; Feldman & Levin, 1995). The attractive feature of Winter's model, common to all the members of the EPH family, is that it offers a simple control scheme for regulation of posture: it exploits the mechanical properties of muscles by providing almost instantaneous corrective response to disturbances, thus reducing the operating demands on the Central Nervous System (CNS). The crucial element of the model, in the case of upright standing, is the stiffness value of the ankle joint, in comparison with the rate of growth of the toppling torque due to gravity which thus identifies a critical value of stiffness. As a matter of fact, different direct methods for evaluating the ankle stiffness (Loram & Lakie, 2002*a*; Casadio *et al.*, 2005) demonstrated that ankle stiffness is clearly under-critical. A similar conclusion was reached by van Soest et al. (Soest *et al.*, 2003) on the basis of a detailed neuromuscular model: they found that even at maximal co-contraction levels of the ankle muscles the joint stiffness is insufficient to achieve a locally stable system. This result was further supported by specific measurements of the stiffness of the Achilles tendon (Fletcher *et al.*, 2013) that exhibited a compliance level incompatible with the stiffness control hypothesis, taking into account that this important tendon is serially connected to the ankle plantar flexor muscles. It is also worth mentioning that the inefficiency of attempting to modulate joint

stiffness via co-contraction of antagonist muscles is peculiar of the ankle joint, thus highlighting the specificity of the control mechanisms of the bipedal standing posture.

As a consequence of the insufficient physiological level of the ankle stiffness, it became clear that it was necessary to supplement such passive compensation mechanism of gravity-driven instability with suitable active control strategies. Many approaches have been investigated for solving this problem and the most simple solution adopted by a number of researchers was a conventional, linear, continuous-time feedback controller, based on proportional and derivative feedback (continuous *PD* control model) (Peterka, 2000; van der Kooij *et al.*, 2001; Mergner *et al.*, 2002; Kiemel *et al.*, 2002; Masani, 2003; Creath *et al.*, 2005). The cybernetic problem here is that such feedback information is delivered to the spinal and supra-spinal control centers through multiple sensory channels (proprioceptive, cerebellar, and visual) with a significant delay, well exceeding 0.2 s. In such conditions the *PD* control parameters must be tuned carefully by taking into account two contrasting constraints: i) the constraint of static stability, that dictates a minimum value of the *P* parameter as a function of the gravity toppling influence, and ii) the constraint of dynamic stability, that imposes an upper bound for the *PD* parameters, stronger and stronger as the delay increases.

In order to improve the robustness of the *PD* control paradigm, an intermittent version was proposed (Bottaro *et al.*, 2008; Asai *et al.*, 2009, 2013), characterized by a simple switching mechanism defined in the phase plane of the SIP (q vs. $\dot{q}$, where q is the ankle rotation angle). As a matter of fact, there is ample evidence suggesting the discontinuous nature of the feedback control action in upright standing. Consider, for example, the analysis of posturographic patterns (Collins & De Luca, 1993; Morasso & Schieppati, 1999; Morasso & Sanguineti, 2002), EMG signals (Gatev *et al.*, 1999; Loram & Lakie, 2002*a*; Asai *et al.*, 2013), and the non-uniform character of sway path (Matheson & Lee, 1970). From the computational point of view, the power of the intermittent control strategy for stabilizing the SIP system is that it exploits an implicit "affordance", provided by the intrinsic dynamics of such tasks, namely the fact that the uncontrolled SIP is characterized by a saddle-like instability, including a stable and unstable manifold in the phase plane: when the driving action is switched off, the state vector is attracted to the equilibrium configuration, if the vector is closer to the stable than to the unstable manifold, whereas it is repulsed away in the opposite case. This "affordance" suggested to adopt an alternation strategy between an off-phase, in the former case, and an on-

phase, in the latter case, as reported in previous studies (Bottaro *et al.*, 2008; Asai *et al.*, 2009, 2013). Remarkably, this strategy can succeed to achieve bounded stability, driving the sway patterns towards a limit cycle, even if the dynamics of the on-phase is unstable when applied continuously, thus increasing in a substantial way the size of the stability area in the space of control parameters in comparison with a conventional continuous control paradigm (Asai *et al.*, 2009, 2013). Moreover, it is worth noting a crucial difference between the continuous and intermittent paradigms: in the former case, the target of the controller is the unstable upright condition, whereas, in the latter case, the target is the whole stable manifold, with the simple decision paradigm to switch off the control action if the state vector is sufficiently close to it.

On the other hand, the SIP model has been challenged by several recent studies clearly showing that movement around the hip joint are not negligible (Aramaki *et al.*, 2001; Creath *et al.*, 2005; Zhang *et al.*, 2007): in particular, the range of variation of the angular displacement, velocity, and acceleration of the hip were demonstrated to be significantly greater than those of the ankle, with a systematic increase of the ankle-hip difference from angular variations to the corresponding first and second derivative. As a consequence, it has been suggested that the SIP model should be substituted by a multi-link paradigm, at least a Double Inverted Pendulum (DIP) model, involving the coordinated control of ankle and hip joints. Ankle-hip joint coordination patterns have been analyzed both in the time and frequency domain. In the former case it was found that the acceleration profiles are strongly characterized by anti-phase patterns; the same holds, to a smaller degree, also for the velocity profiles, whereas the rotational profiles exhibit an overall mild in-phase correlation (Aramaki *et al.*, 2001). Moreover, in the frequency domain, the rotational profiles of the two joints appear to be characterized by co-existing coordination patterns (in-phase and anti-phase, respectively) after a suitable frequency analysis (Creath *et al.*, 2005; Zhang *et al.*, 2007): the leg and trunk segments of the body move in-phase at low frequency (below 0.5 Hz) but they switch to anti-phase coordination at high frequency (above approximately 0.9 Hz).

Having accepted the fact that the SIP model misses part of the observable behavior, it remains an open question the origin of the coordination between the two body segments of the DIP model, in terms of fundamental mechanisms and control principles involved. We believe that this question can be met in an efficient manner by extending the SIP model rather than rejecting it. The idea is to associate a single degree of freedom Virtual

Inverted Pendulum (VIP) to the actual DIP. The VIP is an inverted pendulum that connects the ankle joint to the overall CoM of the body: the oscillations of this virtual pendulum, namely the rotations of the virtual ankle, are functions of the real rotation patterns of the two joints of the DIP model, i.e. ankle and hip. Although this inverted pendulum does not exist physically, its oscillations are directly perceivable by standing subjects through the CoP, namely by means of a combination of tactile and proprioceptive sensors of the feet. In this manner, it is possible to regulate the stabilization of the ankle joint with a control mechanism which is quite similar to the one already studied for the SIP model, namely an intermittent feedback controller complementing the intrinsic stiffness of the ankle muscles. As regards the hip joint we suggest a stiffness strategy similar to the one originally proposed by Winter et al. (Winter *et al.*, 1998). This strategy for the hip joint is feasible because there is not the limitation of the Achilles tendon in the ankle joint; moreover, the critical stiffness value is strongly smaller for the hip than for the ankle case for purely biomechanical reasons, thus requiring a very small amount of co-contraction of the hip muscles for achieving a working level of hip stiffness. Specifically, for an inverted pendulum the gravity-driven toppling torque is $\tau_g = \mathrm{mgh}\sin(\mathrm{q}) \approx \mathrm{mgh}\,\mathrm{q}$ and thus the critical value of stiffness is $K_{crit} = \mathrm{mgh}$ where m is the mass of the pendulum and h is the distance between the hinge of the pendulum and the CoM. Thus, the critical stiffness of the whole body hinged around the ankle is much greater than the critical stiffness of the upper body, hinged around the hip. The biological plausibility of this strategy is also consistent with the coherence analysis of muscle activity during quiet stance (Saffer *et al.*, 2008) which shows a lack of correlation between the oscillations of the trunk and the activity of the muscles, which exert direct control over it.

Summing up, we propose a hybrid control of the VIP/DIP model: intermittent active control of the ankle (via the VIP part of the model) and passive stiffness control of the hip (via the DIP part). The simulations demonstrate that the proposed model is compatible with the complex inter-joint coordination patterns summarized above, without any need of explicit high-level coordination mechanisms. Moreover, SIP and VIP sway patterns appear to be quite similar and thus we are confident to claim that in spite of the fact that hip rotation is far from being negligible and indeed has larger amplitude than ankle oscillations, its role is marginal, as regards the active stabilization of upright posture around the ankle, which is the main source of instability and thus the main target of active

CNS control. In this sense, we suggest that the core of the fundamental control mechanism of the upright posture is still captured by a variation of the SIP.

4.1.2 *Methods*

4.1.2.1 DIP/VIP model

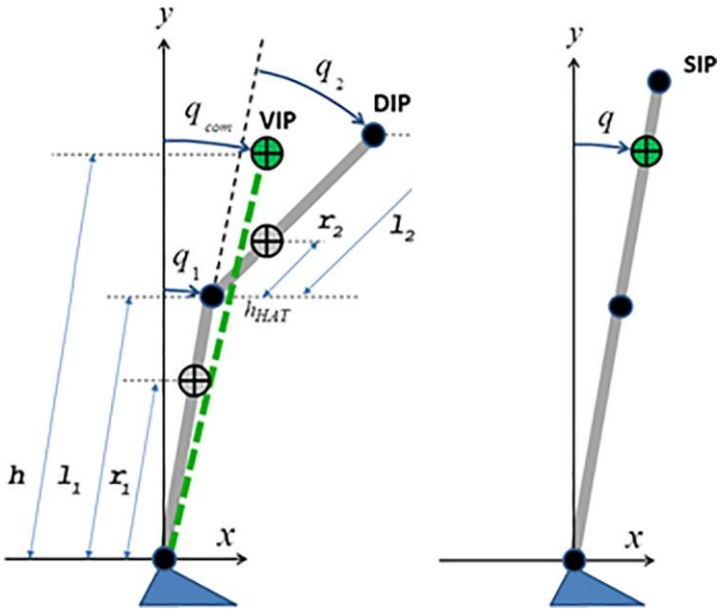

Figure 4. 1 Biomechanical models. The DIP/VIP model (left panel) and the corresponding SIP model (right panel).

The DIP model has two links that are related, respectively, to the legs (total mass m_1, leg-length l_1, distance of the barycenter from the ankle axis r_1, and moment of inertia around the barycenter I_1) and to the upper body (HAT: Head-Arm-Trunk) characterized by the corresponding parameters ($m_2,\ l_2, r_2, I_2$). The two degrees of freedom are the ankle rotation angle (q_1) and the hip angle (q_2).

The VIP model has a single degree of freedom (q_{com}) and consists of a single virtual inverted pendulum that links the ankle to the global CoM of the DIP model; its mass equals the total mass of the DIP ($m = m_1 + m_2$) and *h* denotes the corresponding length.

The DIP model fully characterizes the biomechanics of the standing body and the associated VIP model is instrumental for active control based on the intermittent

paradigm. The dynamic equations of the DIP model can be obtained by using the Lagrangian approach that yields the following non-linear ODE:

$$\boldsymbol{M}(q)\,\ddot{q} + \boldsymbol{C}(q,\dot{q})\,\dot{q} + \boldsymbol{G}(q) = \boldsymbol{\tau} \tag{1}$$

For simplicity we use the following synthetic notation: $s_1 = \sin q_1$, $s_2 = \sin q_2$, $s_{12} = \sin(q_1 + q_2)$, $c_{12} = \cos(q_1 + q_2)$.

$\boldsymbol{M}(q)$ is the inertia matrix that varies as a function of the hip rotation angle according to the following formula:

$$\begin{cases} M_{11} = a + 2b\,c_2 \\ M_{12} = M_{21} = d + b\,c_2 \\ M_{22} = d \end{cases}$$

$$\begin{cases} a = I_1 + I_2 + m_1 {r_1}^2 + m_2\left({l_1}^2 + {r_2}^2\right) \\ b = m_2\,l_1\,r_2 \\ d = I_2 + m_2\,{r_2}^2 \end{cases} \tag{2}$$

$\boldsymbol{C}(q,\dot{q})\dot{q}$ represents the Coriolis and centrifugal generalized forces:

$$\begin{cases} C_{11} = -b\,s_2\,\dot{q}_2 \\ C_{12} = -b\,s_2\,(\dot{q}_1 + \dot{q}_2) \\ C_{21} = b\,s_2\,\dot{q}_2 \\ C_{22} = 0 \end{cases} \tag{3}$$

$\boldsymbol{G}(q)$ is related to the gravity dependent torques (g is the gravity acceleration):

$$G(q) = -g\begin{bmatrix} (m_1\,r_1 + m_2\,l_1)\,s_1 + m_2\,r_2\,s_{12} \\ m_2\,r_2\,s_{12} \end{bmatrix} \tag{4}$$

$\boldsymbol{\tau}$ is the total control torque that has the purpose to compensate the intrinsic instability of the upright posture and includes three contributions, determined by different control mechanisms: a bias torque $\boldsymbol{\tau}_B$, a stiffness torque $\boldsymbol{\tau}_S$, and an intermittent control torque $\boldsymbol{\tau}_I$:

$$\boldsymbol{\tau} = \boldsymbol{\tau}_B + \boldsymbol{\tau}_S + \boldsymbol{\tau}_I \tag{5}$$

A noise signal was added to the total control torque, with a comparable power and a frequency band limited to 10 Hz.

4.1.2.2 The feed-forward bias torque $\boldsymbol{\tau}_B$

It compensates for the toppling torque due to gravity in the reference posture $q_{ref} = [q_{1ref},\ q_{2ref}]$ and it is applied to both joints.

$$\boldsymbol{\tau}_B = -g\begin{bmatrix} (m_1\,r_1 + m_2\,l_1)\sin q_{1ref} + m_2\,r_2\,\sin(q_{1ref} + q_{2ref})) \\ m_2\,r_2\sin(q_{1ref} + q_{2ref})) \end{bmatrix} \tag{6}$$

4.1.2.3 The stiffness torque $\boldsymbol{\tau}_S$

It expresses the elastic properties of ankle and hip muscles and it is attributed to both joints, relative to the same reference posture:

$$\boldsymbol{\tau}_S = -\begin{bmatrix} K_a\left(q_1 - q_{1ref}\right) + B_a\,\dot{q}_1 \\ K_h\left(q_2 - q_{2ref}\right) + B_h\,\dot{q}_2 \end{bmatrix} \tag{7}$$

where K_a is the ankle stiffness (with the corresponding damping factor B_a) and K_h is the hip stiffness (with the corresponding damping factor B_h). The ankle stiffness is smaller than the critical value determined by the rate of growth of the gravity-dependent toppling torque of the whole body, in agreement with the measurements of the ankle stiffness (Loram & Lakie, 2002*a*; Casadio *et al.*, 2005); in contrast, the hip stiffness is hypothesized to be greater than the critical value corresponding to the upper body, according to the working hypothesis of the hybrid VIP/DIP model:

$$\begin{cases} K_a < \left(m_1 + m_2\right) g\, h \\ K_h > m_2\, g\, r_2 \end{cases} \tag{8}$$

4.1.2.4 The intermittent feedback control torque $\boldsymbol{\tau}_I$: stabilization of the VIP model

This control torque is applied only to the ankle joint as a function of the VIP angle and angular velocity (q_{com}, $\dot{q}_{com}$). The VIP angle is reconstructed on-line from the two angles of the DIP system:

$$\begin{cases} x_{com} = m_1\, r_1\, s_1 + m_2\, (l_1 + r_2)\, s_{12} \\ y_{com} = m_1\, r_1\, c_1 + m_2\, (l_1 + r_2)\, c_{12} \end{cases} \quad \Rightarrow \quad q_{com} = tan^{-1}\left(\frac{x_{com}}{y_{com}}\right) \tag{9}$$

The intermittent control strategy was originally conceived, as already commented in the introductory section, for stabilizing the SIP system by extending the conventional PD feedback controller in order to reduce the risk of instability due to the delay of the feedback signals. The basic idea was to exploit the implicit "affordance" of saddle-like instability, namely the presence of a stable and unstable manifold in the phase plane, thus suggesting the following heuristics: to switch off the feedback control action when the state vector is closer to the stable manifold than to the unstable one and to reactivate it in the opposite case. The robustness of this control paradigm is due to the fact that, even if the active control is unstable when permanently applied, the combination of actively controlled orbit segments with orbit segments driven by intrinsic dynamics may end up in

bounded oscillatory patterns. It is worth emphasizing that the target of active control in the conventional continuous *PD* paradigm is the upright unstable equilibrium configuration whereas in the intermittent paradigm it is the whole stable manifold, thus extending significantly the range of values of the *PD* parameters that can support bounded stability (Asai *et al.*, 2009).

The working hypothesis investigated in this work was to apply it to the VIP model instead of the SIP model and then verify with the DIP model simulation if such hybrid mechanism could achieve the double goal of dynamic stabilization of the standing body and reproduction of the experimentally obtained ankle-hip coordination patterns.

More specifically, having defined $\Delta q_\delta = (q_{com}^{ref} - q_{com}(t-\delta t))$ as the delayed angular error of the global CoM of the DIP model, with the corresponding angular speed error $\Delta \dot{q}_\delta$, the intermittent control action is defined in the phase plane of the VIP model as follows:

$$\tau_I = \begin{bmatrix} C \\ 0 \end{bmatrix}, \text{ with } \begin{cases} C = P \cdot \Delta q_\delta + D \cdot \Delta \dot{q}_\delta & \text{if } \Delta q_\delta \cdot (\Delta \dot{q}_\delta - \alpha \cdot \Delta q_\delta) > 0 \\ C = 0 & \text{otherwise} \end{cases} \quad (10)$$

Here $[P, D]$ are the proportional and derivative parameters, respectively, of the *PD* intermittent controller, which is activated in the first and third quadrant of the VIP phase plane, with an additional small slice determined by the parameter α. For this parameter we used the value 0.4, in agreement with the analysis in (Asai *et al.*, 2009).

4.1.2.5 Parameters of the DIP/VIP model

The anthropometric parameters, which were derived from the whole-body model described in (Morasso *et al.*, 2015), are listed in Table 4. 1:

Leg				HAT (Head-Arm-Trunk)			
$\boldsymbol{l_1}$[m]	r_1[m]	m_1[kg]	I_1[kg m²]	l_2[m]	r_2[m]	m_2[kg]	I_2[kg m²]
0.9	0.58	28	9.21	0.88	0.32	53	5.35

Table 4. 1 Anthropometric parameters of the DIP model

The critical levels of stiffness of the two joints, namely the stiffness values that match the coefficients of the gravity toppling torques, are given by the two following expressions:

$$\begin{cases} K_a^{crit} = (m_1 + m_2) g\, h \\ K_h^{crit} = m_2\, g\, r_2 \end{cases} \quad (12)$$

The ankle stiffness of the DIP model, that is known to be under-critical, was set to 60% of the critical level, as suggested by direct measurements of ankle stiffness (Casadio *et al.*, 2005). For the hip stiffness we used over-critical values in order to validate the feasibility of the hypothesis about the hybrid stabilization strategy: active at the ankle (intermittent delayed feedback) and passive at the hip (via the intrinsic visco-elastic properties of hip muscles); the default value for most simulation was twice the critical hip stiffness. The corresponding damping coefficients (B_a and B_h) are not critical. The chosen value for the ankle comes from empirical measurements (Casadio *et al.*, 2005); for the hip we chose a value in order to have a damping coefficient equal to 0.7. The robustness of the hybrid stabilization strategy was also tested by varying the hip stiffness, for which direct empirical estimates are not available, in a large range. The employed values of the visco-elastic parameters are listed in Table 4. 2.

Ankle		Hip	
$\boldsymbol{K_a}$[Nm/rad]	B_a[Nms/rad]	K_h[Nm/rad]	B_h[Nms/rad]
494	30	331	30

Table 4. 2 Visco-Elastic Parameters of the DIP Model

The *PD* parameters of the intermittent controller were selected heuristically after having identified the intervals of stability.

According to literature on sensorimotor integration in human postural control (Mergner *et al.*, 2002; Peterka, 2002) and cart inverted pendulum paradigm (Milton *et al.*, 2016), the feedback delay of the intermittent *PD* controller was varied in the range of 0.20-0.25 s. In most simulations reported in the results the most challenging value (0.25 s) was used. The simulation were carried out with Matlab (MathWorks), using the forward Euler method with a time step of 0.001 s. Figure 4. 2 (upper panel) illustrates the overall block diagram of the hybrid DIP/VIP control model.

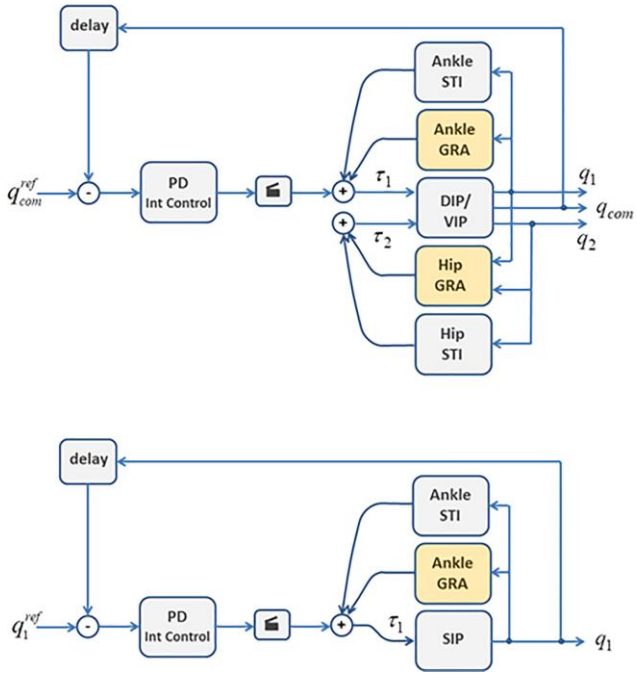

Figure 4. 2 Control models. Upper panel: the hybrid DIP/VIP control model. q1: ankle rotation angle; q2: hip rotation angle; qcom: VIP rotation angle. τ1: total ankle torque; τ2: total hip torque. GRA: Gravity torque model. STI: Stiffness torque model. The DIP/VIP block corresponds of the overall dynamics of the DIP/VIP model. Lower panel: the simplified SIP model.

4.1.2.6 SIP model

Figure 4. 1 (right panel) illustrates the SIP model. The anthropometric parameters are the same of the DIP/VIP model. Also the model equations are quite similar to the DIP/VIP model. The model has a single degree of freedom, the ankle rotation angle, whereas the hip angle is kept constant (equal to 0). The control parameters are the same, taking into account that equation 10, namely the computation of the intermittent feedback control torque, is applied directly to the ankle joint. Figure 4. 2 (lower panel) illustrates the block diagram of the equivalent SIP model.

4.1.3 *Results*

In order to validate the proposed hybrid postural controller we needed to address two main issues: *robustness* in terms of stability and *plausibility* in terms of inter-joint coordination. As regards the former issue we verified, by means of multiple simulations, the range of values of the *P* and *D* parameters which yielded bounded stability.

The initial condition of the simulations was characterized by a tilt angle of the ankle joint of 2 deg and a null angular velocity (plus a null angle of the hip joint for the DIP/VIP

model). The reference angles of both joints were set to zero. The adopted stability criterion was that after an initial short transient (typically 5-10 seconds) and for a suitable observation time (at least 180 s) the orbits in the phase plane of both VIP and DIP/VIP models ($q_{com}\ vs.\ \dot{q}_{com}$) did not exceed the initial tilt. Table 4. 3 shows the range of values of the control parameters, for both types of models, which support a stable sway motion.

	P/mgh	D [Nms]
SIP	0.5 – 0.9	0 - 430
DIP/VIP	0.3 – 0.9	0 - 470

Table 4. 3 Range of Stability of the Intermittent Controller.

The value of *P* is expressed as a fraction of the critical stiffness value for the SIP model (*m* denotes the total mass of the standing body and *h* the distance of the CoM from the ankle). The data reported in the table document that the intermittent control model is rather robust (for both models) because it allows a large range of variation. However, the DIP/VIP model is slightly better because it allows a larger range of variation. For most simulations reported, the following values were used:

$$\begin{cases} P\ /(mgh) = 0.6 \\ D = 70 \text{ Nms} \end{cases} \tag{13}$$

The robustness of the intermittent feedback mechanism in complementing the intrinsic muscle stiffness is consistent with the study by van Soest et al. (Soest *et al.*, 2003), which concluded that the combination of muscle properties and time-delayed spindle feedback is insufficient to obtain a system with reasonable local stability.

Figure 4. 3 shows an example of sway movements (ankle and hip rotations) generated by the DIP/VIP hybrid model with the values above of the *PD* parameters and the other parameters listed in the model section. It appears that the oscillatory patterns of the two joints have a similar amplitude, emphasizing that the motion of the hip joint cannot be neglected, in agreement with what observed by many researchers (Aramaki *et al.*, 2001; Creath *et al.*, 2005; Zhang *et al.*, 2007; Sasagawa *et al.*, 2009, 2014; Suzuki *et al.*, 2015). Figure 4. 4 shows the opposing torques acting on the ankle joint: the toppling torque due to gravity and the stabilizing control torque that combines the muscle/tendon stiffness effect and the crucial intermittent control action.

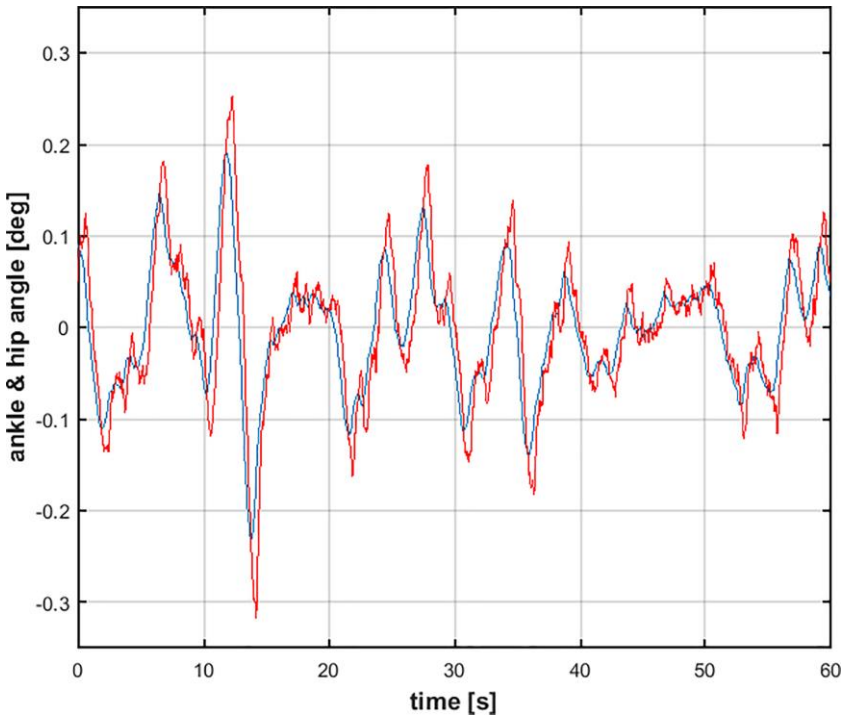

Figure 4. 3 Sway movements generated by the simulation of the DIP/VIP hybrid model. Blue trace: ankle joint rotation; Red trace: hip joint rotation

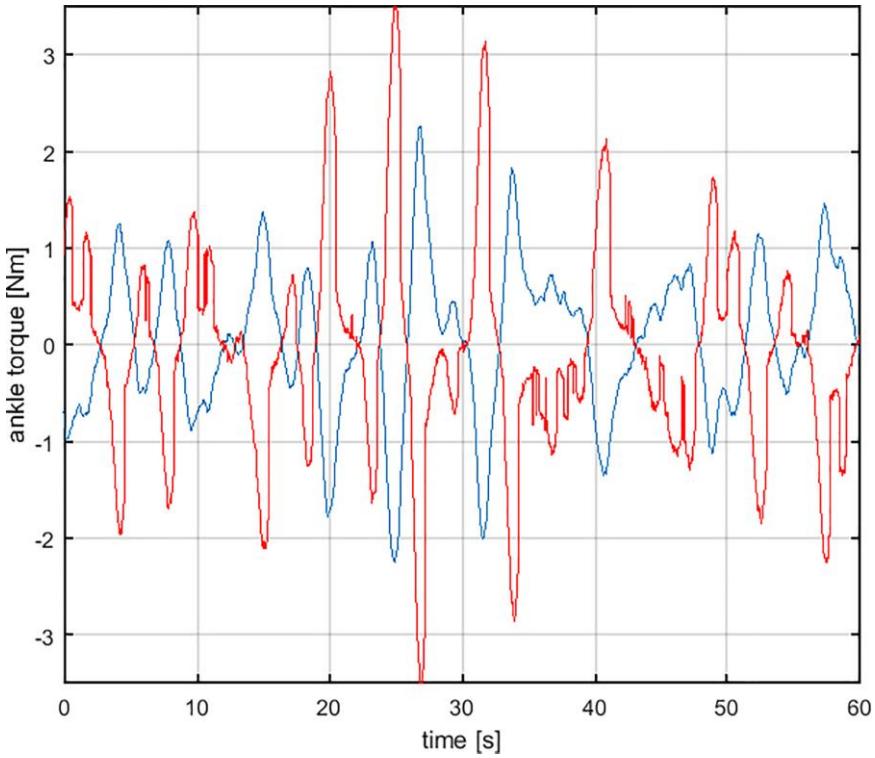

Figure 4. 4 Stabilizing ankle torque generated by the simulation of the DIP/VIP hybrid control model. The DIP/VIP model (red trace) includes the stiffness component (passive, intrinsic, zero-delay feedback) and the intermittent control torque (active, delayed feedback). The counteracting ankle toppling torque due to gravity is displayed by the blue trace.

Although the previous analysis of the simulation results seems to emphasize the inadequacy of the SIP model to explain the massive contribution of the hip to overall sway movements, the comparison of the sway orbits in the phase plane of the SIP model and the VIP component of the DIP/VIP hybrid model (Figure 4. 5) seems to tell a different story. The antiphase coordination of ankle and hip motion, first described by (Aramaki *et al.*, 2001), tends indeed to minimize the acceleration of the global CoM (Suzuki *et al.*, 2015) and thus the VIP oscillations of the DIP/VIP end up mimicking the oscillations of the old-fashioned single-DoF SIP model.

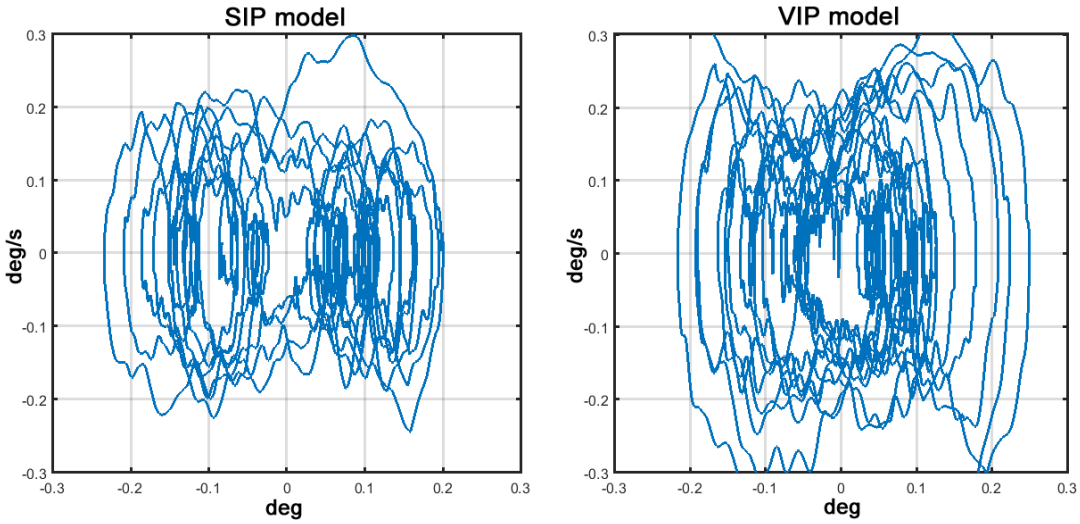

Figure 4. 5 Sway orbits in the phase plane ($\boldsymbol{q_{com}}$ $\boldsymbol{vs.}$ $\boldsymbol{\dot{q}_{com}}$). Left Panel: oscillations of the SIP model. Right panel: oscillations of the VIP part of the hybrid DIP/VIP model. Both orbits correspond to a 60 s sway

In order to better understand such similarity of VIP-SIP oscillations, we may consider the range of variation (RoV) of different variables during an observation window of 180 s, having defined as "range" the interval containing 90% of the samples stored during the observation time. Table 4. 4 shows the RoVs for angular rotations, angular speeds and angular accelerations of the two models (DIP/VIP vs. SIP).

	DIP ankle	DIP hip	VIP	SIP
Angular rotation [deg]	± 0.11	± 0.13	± 0.13	± 0.20
Angular speed [deg/s]	± 0.17	± 0.34	± 0.20	± 0.19
Angular acceleration [deg/s²]	± 2.7	± 10.2	± 0.94	± 0.94

Table 4. 4 Range of Variation

The observation of the table reveals that in the case of the DIP model the RoV of the hip is systematically larger than the ankle: very small difference for the angular rotation, larger (twice) for angular speed, and very large (three times) for the angular acceleration. Such data are comparable with what was found empirically by observing the spontaneous sway of standing subjects (Aramaki *et al.*, 2001; Sasagawa *et al.*, 2009). Moreover, the theoretical study by (Kuo & Zajac, 1993) about multi-joint movement strategies based on biomechanical constraints indicates that the set of biomechanically feasible accelerations greatly favors a combination of ankle and hip movement in the ratio 1:3, in agreement with our simulations.

The RoV of the ankle motion in the SIP and VIP models is quite similar up to the first time derivative. In contrast, in the case of acceleration it is quite a different story: the angular acceleration of the ankle in the SIP model is much smaller than the acceleration of either joints of the DIP model and it is indeed almost coincident with the acceleration of the virtual VIP joint. Both our simulation results and the experimental results by (Aramaki *et al.*, 2001) suggest that the main effect of the hip-ankle coordination is not to keep the CoM at a constant position, but rather to minimize its acceleration. In summary, such consistent ankle-hip coordination makes the behavior of the VIP component of the hybrid DIP/VIP model almost indistinguishable from the old fashioned SIP model.

A third element of evaluation of the simulation results is more specifically related to the type of inter-joint coordination characteristic of the DIP model (Sasagawa *et al.*, 2014). This relationship can be visualized by plotting ankle vs. hip motions separately for angular rotations, angular velocities, and angular accelerations, respectively (see Figure 4. 1). The figure shows that angular rotations are positively correlated (the slope of the regression line is 1.02), whereas the trajectories of the angular velocity and angular acceleration exhibit a compensatory, anti-phase relationship (stronger for acceleration than for velocity): the slope of the regression line is -3.60 for velocity and -3.61 for acceleration. The results coming from our simulations are quite compatible with the experimental data of (Aramaki *et al.*, 2001) for the experiments performed with closed eyes. In particular, the regression lines calculated from their experimental data have the following slopes: 1.32 (angular rotations), -3.40 (angular velocities), -3.12 (angular accelerations).

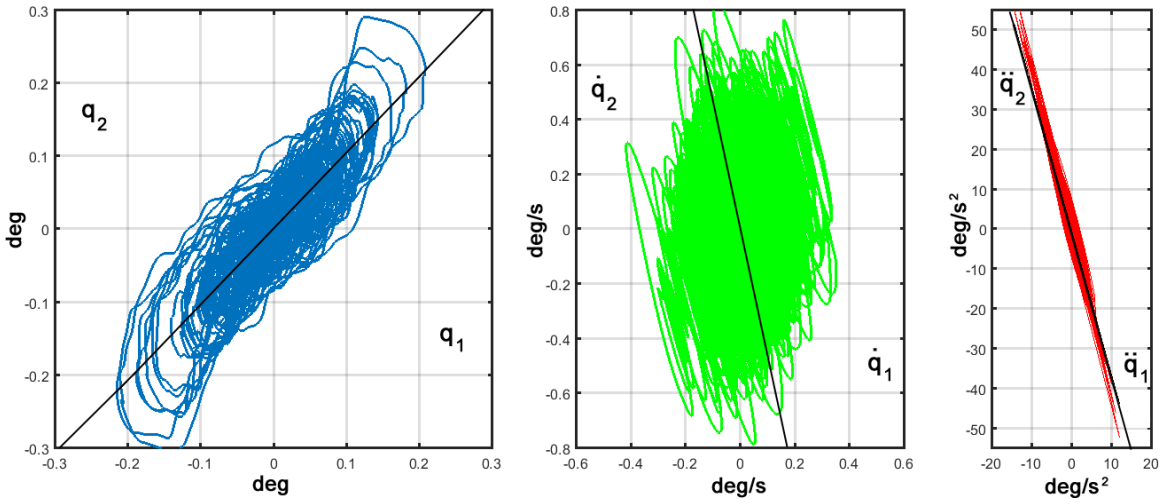

Figure 4. 6 Coordination of Ankle ($\boldsymbol{q_1}$) and Hip ($\boldsymbol{q_2}$) oscillations from the simulation of the DIP/VIP hybrid model. The quantities showed are the angular rotations (left panel), the angular velocities (central panel) and the angular accelerations (right panel). The plotted traces correspond to a 60 s sway.

As a matter of fact, coexistence of both in-phase and anti-phase coordination patterns between the upper and lower body have been found in investigations which perturb upright stance as well in the analysis of quiet stance (Zhang *et al.*, 2007): compare, for example, Fig 5 of (Aramaki et al., 2001), obtained from healthy subjects where knee and head-neck-trunk movements were restricted by suitable splints, with Figure 4. 6 of our simulation. The coordination patterns of our simulations between states of the ankle and the hip fit well with the ones shown for representative experimental data in (Aramaki et al., 2001). In particular, there is evidence of in-phase coordination for the low frequency components of hip and ankle rotations (up to 0.5 Hz) and anti-phase coordination for high frequency components (beyond 0.9 Hz). We verified to which extent this kind of correlation is compatible with the hybrid nature of the DIP/VIP model, without any specific arrangement in this direction in the formulation of the model. In order to carry out this analysis, the oscillatory patterns of the ankle and hip rotations generated by the model were low-pass and high-pass filtered by means of 4th order Butterworth filters (with cutoff frequencies of 0.5 Hz and 0.9 Hz, respectively): remarkably we found a correlation coefficient equal to 0.7365 (in-phase coordination) for the low-frequency components and equal to -0.3996 (anti-phase coordination) for the high-frequency components, in agreement with the experimental data (Aramaki *et al.*, 2001; Peterka, 2002; Zhang *et al.*, 2007; Sasagawa *et al.*, 2014).

The hybrid DIP/VIP model is based on the combination of an explicit control mechanism (the intermittent controller) and an implicit mechanism based on the visco-elasticity of the hip muscle. As regards the latter mechanism, no direct measurement of hip stiffness is available, to our knowledge, and thus we do not have specific evidence about the fact that physiological values of this variable are indeed above the critical level for providing stiffness stabilization of the hip joint: $K_h^{crit} = m_2\, g\, r_2$ where m_2 is the HAT-mass and r_2 is the distance of the HAT-CoM from the hip joint. However, in the case of the hip joint the muscles are not connected to the upper body through very compliant tendons, as the Achilles tendon of the ankle joint. This fact, indeed, strongly limits the possibility of increasing the joint stiffness via co-contraction of antagonistic muscles in the ankle joint, as demonstrated by Loram et al (Loram *et al.*, 2009*a*). Moreover, there are three significant issues in favor of the stiffness stabilization hypothesis of the hip joint:

i) the larger size of the hip muscles, in comparison with the ankle muscles, suggests a bigger value of the natural hip stiffness than the ankle stiffness, even without particular levels of co-contraction of antagonist hip muscles; ii) the critical value of the hip stiffness is much smaller than the ankle stiffness for purely biomechanical reasons (e.g. 165 Nm/rad vs. 823 Nm/rad with the anthropometric parameters used for the simulations of this study); iii) the coherence analysis of muscle activity during quiet stance (Saffer *et al.*, 2008) shows a lack of correlation between the oscillations of the trunk and the activations of the muscles, which exert direct control over it.

All these issues strongly support the physiological plausibility of a stiffness strategy for the hip in contrast with an active strategy for the ankle. The credibility of this hypothesis was also tested by evaluating the sensitivity of the hybrid control paradigm for a large range of variation of the hip stiffness above the critical level. First of all, we found that stability can be achieved for values of the hip stiffness at least 20% over the critical level. For values 20 times greater than the critical level the DIP/VIP model is practically coincident with the SIP model. As shown in the Table 5, when the ratio between the hip stiffness and the corresponding critical value is varied between 1.2 (the limit value for stability) and 20 (the value beyond which the DIP model behaves like a SIP) the slope of the regression line of the hip vs. ankle acceleration graph is moderately increased, while keeping the negative sign, i.e. maintaining the anti-phase relationship. Near the instability condition (hip stiffness only 20% higher than the critical value) the RoV of the three rotation angles ($q_1,\ q_2,\ q_{com}$) is more than doubled, as expected for the influence of

instability. For higher values of the hip stiffness, the RoV of q_1 and q_{com} remain approximately constant, the former a little bit larger than the latter; in contrast, the RoV of the hip rotation q_2 decreases as a consequence of the increase of hip stiffness, thus approaching a dynamical regime similar to the VIP model. It is quite surprising, on the other hand, that the slope of the regression line in the acceleration graph remains approximately constant, emphasizing the robustness of the hybrid control scheme for a very large variation of the hip stiffness. Moreover, the simulation results reported above provide an indirect estimate of the physiological level of hip stiffness adopted by standing subjects in absence of task specifications beyond the implicit one, namely "stand comfortably quiet". The experimental data obtained in such condition (Aramaki *et al.*, 2001; Saffer *et al.*, 2008; Sasagawa *et al.*, 2009, 2014; Suzuki *et al.*, 2015) agree on the fact that the amplitude of the hip rotation is systematically larger than the ankle rotation. Since in our simulations this occurs if the hip stiffness is no greater than twice the critical stiffness, we feel confident to suggest that this kind of value may be a reasonable trade-off between stability and minimization of effort. Of course, this does not exclude that subjects may choose higher values of co-contraction for specific environmental conditions.

$\frac{Hip\ stiffness}{Critical\ stiffness}$	1.2	1.6	2	5	10	20
slope of regression line $\ddot{q}_1\ vs.\ \ddot{q}_2$	-3.4	-3.6	-3.6	-3.8	-3.9	-4.0
RoV q_{com} [deg]	± 0.295	± 0.144	± 0.126	± 0.114	± 0.129	± 0.120
RoV q_1 [deg]	± 0.235	± 0.112	± 0.104	± 0.106	± 0.126	± 0.120
RoV q_2 [deg]	± 0.590	± 0.195	± 0.126	± 0.036	± 0.019	± 0.009

Table 4. 5 Influence of the hip stiffness

4.1.4 *Discussion*

It has been suggested (Sasagawa *et al.*, 2014) that the ankle-hip coordination during postural sway motion may be explained as an explicit attempt by the CNS to minimize the amplitude of the resultant angular acceleration of the CoM by applying a multi-joint optimal control paradigm. In particular, it is hypothesized that the ankle and hip torques are modulated in a temporally anti-phase manner to one another in each of the two joints

in order to induce appropriate acceleration profiles. In this way, it is suggested that, by taking advantage of the inter-joint interaction, the CNS prevents the net torques from producing large amplitudes of the resultant angular accelerations. Implicit in this approach is that the old-fashioned SIP model is an over-simplification of a much more sophisticated postural control mechanism. However, we believe that this is not the only possible explanation of the observed coordinated patterns. The alternative explanation is that minimization of the CoM acceleration and the associated inter-joint coordination are not explicitly coded but are the implicit biomechanical consequences of the dynamical interaction between the actively stabilized lower body and the stiffness stabilized upper body, namely the hybrid VIP/DIP control model. The simulations performed in this study demonstrate that this simple model can explain inter-joint coordination without an explicit intervention of the CNS: thus the brain can address a single DoF stabilization problem quite similar to the one considered in the investigation of the old-fashioned SIP model. The difference is that the same intermittent control paradigm must be applied to a Virtual version of the SIP model, namely the VIP model that shares with the bi-axial DIP model the estimated position of the CoM. In addition to the empirical support to this explanation coming from the analysis of the simulation results related to the kinematics of coordinated sway patterns, an additional line of evidence is provided by the analysis of muscle activity during quiet stance carried out by (Saffer *et al.*, 2008): they did not find any correlation between movements of the trunk and the activity of the muscles which exert direct control over it, whereas this correlation exists between ankle muscles and ankle oscillations. Thus the active intervention of the CNS seems to be limited to the ankle joint via the leg muscles (as implied by the SIP model) and the viscous elastic properties of the hip muscles determined by their tonic activity seem to be sufficient to stabilize the trunk, while inducing a characteristic hip-ankle coordination as a side effect of the overall dynamics.

There is also a paradoxical effect of the proposed extension of the SIP model to the VIP/DIP model. Our previous studies, which were focused on the intermittent control of the standing posture (Morasso & Schieppati, 1999; Morasso & Sanguineti, 2002; Jacono *et al.*, 2004; Bottaro *et al.*, 2008; Asai *et al.*, 2009), were prompted by a criticism of the proposed stiffness control paradigm of balance in quiet standing (Winter *et al.*, 1998), in the framework of a SIP model. The paradox consists of the fact that having accepted the biaxial nature of sway movements we offer support for a crucial role of stiffness control

of balance. However the paradox is only apparent because we also suggest that the old-fashioned SIP model should be substituted by a more realistic DIP/VIP model with a hybrid control paradigm: active, intermittent control of the ankle joint and passive stiffness control of the hip joint. With such preliminary clarifications in mind we think that the old-fashioned SIP model is far from dead and indeed we agree with Gage et al. (Gage *et al.*, 2004) who argue in favor of the "kinematic and kinetic validity of the inverted pendulum in quiet standing". The SIP model is clearly a simplification of the more realistic DIP model but it is not an over-simplification because it captures the essential part of the DIP dynamics, provided that we accept a hybrid control paradigm.

On the other hand, we should clarify that the validity of the VIP model, associated with the hybrid control paradigm, is restricted to experimental conditions that allow the quick and sizeable production of ankle torque capable to transmit effective motion to the whole-body. This implies, in particular, that the support surface is rigid and of large area. Moreover, it seems natural to associate such requirements to the distinction between ankle and hip strategies for postural oscillations in the sagittal plane, that was formulated years ago by (Nashner & McCollum, 1985): they hypothesized that the ankle strategy stabilized the CoM by moving the whole body as a single-segment inverted pendulum by production of torque at the ankle; the hip strategy, in contrast, was supposed to move the body as a double-segment inverted pendulum with counter phase motion at the ankle and hip. They also suggested that the hip strategy should be observed in situations that limit the production of ankle torque, such as standing on a compliant surface, a behavior that was soon verified in reality (Horak & Nashner, 1986). However, we wish to point out that there is a strong difference between the ankle-hip coordination observed in such situation and the coordinated patterns considered in this study that assume a hard support surface: in the former case the range of motion of the CoP is strongly limited, whereas in the latter case it can exploit the whole length of the foot. Moreover, there is a reversal of the ratio between the amplitude of the oscillations of the CoP and CoM in the two oscillatory paradigms (it is greater than one in the ankle strategy and smaller than one in the hip strategy) as well as an inversion of the roles of the two variables (the CoP is the control variable and the CoM is the controlled variable in the ankle strategy, whereas the opposite characterizes the hip strategy). In order to complete this view about the great importance for the standing body of the contact with the ground, we should also take into account the recent study by (Wright et al., 2012) who clarified that rather than serving as

a rigid base of support, the foot is compliant and sensitive to minute deformations, thus contributing to the stabilization of upright standing with the great sensitivity of a kind of incorporated force platform.

Summing up, the proposed modeling and control framework is directly applicable to the behavior of healthy subjects standing on a rigid surface, whose behavior is usually described in terms of the ankle strategy. On the other hand, one may speculate to which extent and in which sense this framework could be extended to interpret clinical and/or pathological conditions, as in the case of elderly people (Panzer et al., 1995; Kato et al., 2014), people with low back pain (Mok et al., 2004), patients affected by somatosensory or vestibular loss (Horak et al., 1990), as well as general pathological conditions (multiple sclerosis, Parkinson's disease, etc. (Termoz et al., 2008; Huisinga et al., 2018): clinical and/or pathological conditions that are frequently characterized by an enhanced presence of the hip strategy. As a matter of fact, the interaction of the two strategies and the mechanisms that may explain the shift from one strategy to the other were addressed in a previous theoretical work (Suzuki *et al.*, 2012) that applied intermittent control policies to the ankle and/or hip joints in a double inverted pendulum model. In particular, four types of model components were defined (off-off, on-off, off-on, on-on in relation with the ankle/hip pair of joints) where "on" means that the intermittent controller is active for the corresponding joint and "off" means that the active controller is switched off and the joint is partially stabilized only by passive resistance. The study showed that temporally coordinated active torque patterns, referred to as intermittent ankle, hip, and mixed strategies, can emerge by modulating the parameters of the active and passive model components. The modeling/control paradigm proposed in this paper may be considered a specific case of that theoretical study, related to the "on-off" model component, namely the organization of the postural stabilization system in which active (intermittent) control is limited to the ankle whereas the hip is stabilized in a passive manner by the viscous-elastic properties of the hip muscles. The innovation, with respect to the general approach of (Suzuki et al., 2012), is that the ankle controller takes into account the oscillation of the VIP, not of the leg per se. The underlying assumption is related to the fact that the brain has a reliable, although delayed, access to the state of the VIP as well as to the relative position of CoP and CoM over time. It is plausible that for a healthy subject standing on a rigid surface this kind of information is readily available, to a great extent via the sensing capabilities of the foot (Wright et al., 2012). Modifications

of the environmental conditions (increased compliance or decreased size of the support surface) as well as sensorimotor impairments may affect the reliability of the VIP bodily image thus forcing the brain to carry out a massive recruitment of body masses, as in the hip strategy, in order to equilibrate directly the CoM with respect to the CoP. In these cases another interesting point would be to explore the linearized inverted pendulum and flywheel model where the rotation of the flywheel segment around the CoM corresponds to the hip strategy and the varying leg length accounts for the motion in the knee joint.
In our opinion this is a promising research target, to be addressed with a combination of theoretical, modeling, and experimental studies.

This work has been published as journal article (Morasso *et al.*, 2019).

4.2 Influence of an additional task on motor control

The simulation study described in the previous section shows that the consideration of our body as double inverted pendulum does not require active control and coordination of both ankle and hip. The central nervous system can ignore the hip and control only the center of mass.

Hence, we made the situation even more complex for the brain. In the following section another double balancing task situation is investigated. Our main question was: Does the CNS need to actively control two concurrent balancing tasks? Does an additional balancing task interfere with postural control?

4.2.1 *Introduction*

Balancing tasks are ubiquitous in our life: in apparently trivial activities, like upright standing; in extreme sport gestures, like tight-rope walking; in children's play, like stabilizing a stick on the fingertip; in skilled dance gestures, like arabesque, etc. Accordingly, equilibrium maintenance or recovering equilibrium after a transient loss is one of the main functions of the sensory-motor system, including a number of intricate interactions with the cognitive system, in the framework of embodied cognition (Morasso *et al.*, 2015). Moreover, preserving mind-body equilibrium is a deep philosophical concept, in particular for the eastern Taoism-derived philosophy, as well as a psychophysical goal for achieving wellness. In most cases it is an active, voluntary process, although it may incorporate reflex/unconscious components. Remarkably, the fact that the variety of balancing tasks may involve quite different body parts, muscle groups, and sensory modalities, while the resulting outcome is quite similar, namely bounded oscillations around a nominal but never achieved equilibrium state, is strongly suggestive of a common dynamic mechanism, somehow abstracted from the specific sensory-motor implementation and supported by coordinated activity of the central nervous system (CNS).

Consider, for example, the phenomenon of 'light touch' that characterizes postural body sway during quiet upright standing (Jeka & Lackner, 1994; Clapp & Wing, 1999): the

tactile information originated from a very light contact of different parts of the body with an environmental referent (Rogers *et al.*, 2001) is capable to reduce significantly the standard sway amplitude. The plausible explanation of these phenomena is that the use of multiple sources of sensory feedback improves the accuracy of estimating the oscillatory patterns of the CoM, thus allowing faster and more accurate compensatory balance adjustments. In particular, light touch or synchronized vibrotactile stimulation can be considered artificial sensory feedbacks that provide additional sensory channels, synergistic with the standard physiological channels (proprioceptive, visual, and vestibular): this suggests an underlying multi-sensory data fusion process aimed at feeding the optimal estimate of the controlled variable (the CoM oscillation) to a suitable feedback controller. The crucial point is that the different sensory channels provide only indirect information of the controlled variable and thus adding a new channel (e.g. introducing light touch) or eliminating another (e.g. closing the eyes) has an immediate effect on balance.

Shifting now from the sensory to the motor aspect of balancing skills, we may point out that different mechanisms are potentially available and may be combined in different ways in different contexts. One mechanism available for regular upright standing is 'passive', namely ankle stiffness, in relation with body sway in the sagittal plane. Although the mechanical properties of ankle muscles do counteract the destabilizing effect of gravity, they are insufficient by themselves to compensate the rate of growth of the toppling torque (Morasso & Sanguineti, 2002; Loram & Lakie, 2002*a*; Casadio *et al.*, 2005) in this specific case and thus require additional active contributions. Moreover, in other balancing paradigms the stiffness mechanism is physically ineffective: for example, in upright standing on a very narrow support basis, like a tight-rope, the activation of ankle muscles will not produce any torque for compensating the medio-lateral oscillations of the body; similarly, in the manual stabilization of a stick on the fingertip no stabilizing torque can be produced on the virtual stick-finger joint. The missing control action must be provided by an active feedback mechanism driven by the more or less accurate estimate of the oscillations that need to be balanced: different possible alternatives of such feedback control actions have been investigated. The basic choice is continuous-time (Peterka, 2000; van der Kooij *et al.*, 2001; Mergner *et al.*, 2002; Kiemel *et al.*, 2002; Masani, 2003) vs. discontinuous-time or intermittent control action (Cabrera & Milton, 2002; Loram & Lakie, 2002*b*; Saffer *et al.*, 2008; Bottaro *et al.*, 2008; Milton *et al.*, 2009;

Asai *et al.*, 2009; Tanabe *et al.*, 2017), with or without an observer and a predictor in the control structure. The main challenge, for the family of balancing tasks we are considering, is the strong delay of the feedback information about the ongoing sway, of the order of 200 ms, and the fact that this delay is comparable to the potential falling time constant of the oscillating body. Moreover, such feedback is noisy and of very small amplitude, since the involved sensory channels operate near the perceptual thresholds. Therefore, it seems unlikely that the continuous/discontinuous-time feedback controller can incorporate a reliable predictor and/or a reliable estimate of high-order time derivatives of the error signals (e.g. acceleration).

The intermittency of the control actions is supported by various empirical observations: in visuo-manual tracking tasks, by the periodic change in phase relationship between target and hand (Inoue & Sakaguchi, 2014; Sakaguchi *et al.*, 2015); in balancing a cart inverted pendulum (CIP) (Cabrera & Milton, 2002), by the kinematics of the stick; in upright standing, by the observation that the EMG activity of the muscle controlling movements for balance stabilization is not continuous but intermittent and pulsatile (Loram & Lakie, 2002*b*; Saffer *et al.*, 2008; Tanabe *et al.*, 2017), and by the bimodal distribution of sway angles around the nominal equilibrium state (Bottaro *et al.*, 2008). Moreover, the reported fluctuations are highly suggestive of 'chattering', the dynamic signature of switch-type discontinuous controllers, suggesting a bounded stability regime, attracted by a limit cycle rather than an asymptotic equilibrium point, disturbed by noise.

In general, the mechanism that switches on and off the feedback control action may be clock-driven or event-driven, although the former solution seems quite unrealistic and unable to adapt to different contexts in the case of balancing tasks. The event-driven solution implies a threshold that can operate in two different manners: i) it is applied to an error signal, implementing a simple switch-like controller in which corrective movements are made only when the vertical displacement angle exceeds a certain threshold (Milton *et al.*, 2009); ii) it operates in the state space, taking advantage of the *affordance* provided by the saddle-type instability that characterizes the dynamics of an inverted pendulum (see Figure 4. 7).

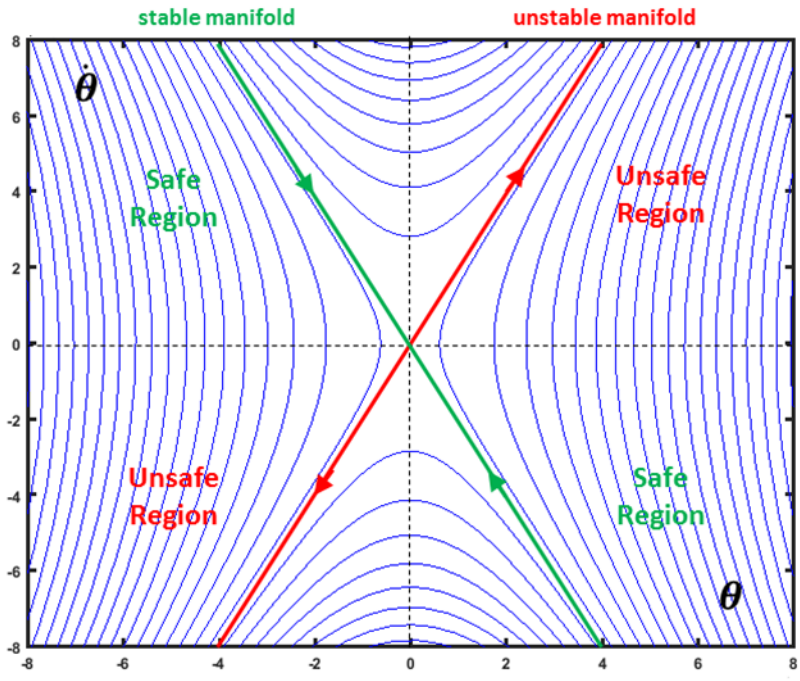

Figure 4. 7 Phase-plane representation of the saddle-like instability, enhancing the dynamic affordance and the rationale of the state-space intermittent control paradigm.

With this type of instability, the phase plane (θ vs. $\dot{\theta}$) can be divided into four regions: two fully-unstable or *bad* regions and two meta-stable or *safe* regions (see Figure 4. 7). If the state vector enters one of the *unsafe* regions it will monotonically diverge from the equilibrium state, attracted by the unstable manifold, until fall; in the other case, the state vector will temporarily approach the equilibrium state, under the action of the stable manifold: this is the affordance provided by the saddle-type instability for a state-space intermittent feedback controller. In particular, as long as the state vector remains inside a *safe* region (off-phase), the controller may turn-off any control action, letting the pendulum evolve at its natural pace, whereas it should switch-on the feedback control action as soon as the state vector enters one of the *unsafe* regions (on-phase). What is important is that, during the on-phase, the purpose of the control action is not to attract the state vector towards the nominal equilibrium state but to allow the state vector to approach or cross the stable manifold, thus turning off the control when this event is detected. The bounded stability that can be achieved with this intermittent feedback approach is quite robust because it can work also with delayed information of the state vector, producing a limit cycle as an alternation of segments of hyperbolic orbits (off-phases) and spiral orbits (on-phases).

In previous studies, it was demonstrated that the state-space intermittent feedback stabilization paradigm can explain in a detailed manner the oscillatory patterns of two very different balancing tasks: quiet upright standing (Bottaro *et al.*, 2008; Asai *et al.*, 2009) and stabilization of a CIP (Milton *et al.*, 2016; Yoshikawa *et al.*, 2016). These tasks differ in a number of ways: the former one has been perfected phylogenetically and ontogenetically during neurodevelopment, whereas the latter is an example of an unstable task that requires learning and adaptation to the degree of difficulty, related to the length of the pendulum and thus to the corresponding falling time constant. These tasks are also characterized by a different number of degrees of freedom, different muscle groups, a different role of muscle stiffness, and a different involvement of sensory modalities. Last but not least, this control paradigm can also explain the multi-joint coordination that underlies the apparent over-simplification of the single inverted pendulum model of quiet standing (Morasso *et al.*, 2019), focusing on the oscillation of the *virtual inverted pendulum* that links the ankle to the changing CoM. Moreover, neurodevelopment, for the stabilization of upright standing, or learning, for the stabilization of the CIP, both require a careful tuning of the sensory-motor parameters of the internal model that continuously monitors the evolution of the state, by optimally fusing the appropriate sensory channels. Summing up, although the intermittent control paradigm is the same, the implementation details are quite different and thus it seems unlikely these tasks are served by the same internal control model, suggesting instead that two instantiations of the same state-space intermittent control policy are implemented by the central nervous system as a pair of abstract internal control modules. In a sense, this may be considered an extension of the *principle of motor equivalence* (Lashley, 1930; Bernstein N, 1966) and opens the question about the mechanisms used by the brain for dealing at the same time with a pair of unstable tasks, characterized by similar dynamics but very different sensory-motor machinery. In particular, it is natural to formulate the following question: in a dual stabilization task, that requires the coordination of the two skills, the corresponding state-space intermittent feedback controllers requires an additional control level or can automatically compensate the interaction determined by the biomechanics of the body and the physics of the CIP?

Thus the purpose of this study is to attempt to answer this question by extending the state-space intermittent feedback framework to the investigation of a dual balancing task. Although it is clear that dual vs. single task effects have been extensively investigated,

most studies involved motor-cognitive tasks with a single balancing component, in a variety of situations, e.g. in young adults (Kiss *et al.*, 2018), in elderly (Sertel *et al.*, 2017), or in patients (Ghai *et al.*, 2017). Moreover, the attention was focused more on the quantification of the interaction effects rather than the underlying motor coordination and control problem. In this study we investigated the dual task of maintaining upright balance while stabilizing with the hands an inverted pendulum device. Figure 4. 8 shows the experimental paradigm: a young, healthy subject stands on a force platform and is required to keep her feet fixed during the stabilization of a CIP-like device that consists of a wooden bar (40 cm long, 2 cm diameter) kept firmly with the two hands. In the middle of the bar there is a ball-bearing connected to a wooden inverted pendulum (100 cm long). The subject is requested to balance the inverted pendulum, keeping the feet fixed on the ground and moving the two hands back and forth symmetrically. The motion of the subject and of the CIP-like device was measured by means of a motion capture system and the ground reaction force by a force platform. The combined oscillations of the body and CIP were also compared with the simulation results of a pair of state-space intermittent controllers applied to the biomechanical model of the body-CIP system sketched in Figure 4. 9.

Figure 4. 8 Experimental set-up. Markers for motion captures are attached to the body and to the CIP-like device; the subject stands on a force platform; surface electrodes record the electrical activity of different muscles of the legs/trunk/arms, however the analysis of their activation patterns were not included in this study.

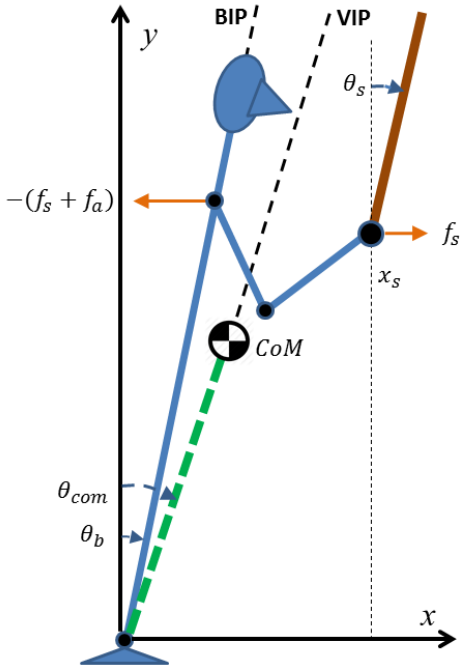

Figure 4. 9 Scheme of the dual balancing task. BIP: Body Inverted Pendulum; VIP: Virtual Inverted Pendulum. In the single balancing task there is no CIP-like device and the two arms are kept extended on the two sides of the body: in this case BIP and VIP coincide as well as the two angles θ_b and θ_{com}.

4.2.2 *Methods*

4.2.2.1 Subjects

Fourteen healthy young subjects with no known neurological impairments took part to the experiments (Table 4. 6). None of them had previous extensive experience of stick balancing. The research conforms to the ethical standards laid down in the 1964 Declaration of Helsinki, which protects research subjects, and was approved by the local ethical committee of Liguria Region (n. 222REG2015). The experiments were carried out at the Motor Learning, Assistive and Rehabilitation Robotics Lab of the Istituto Italiano di Tecnologia (Genoa, Italy).

Subject	Sex (M/F)	Age (y)	Weight (kg)	Height (cm)	HE (deg)	MLE (deg)	LBR (s)
1	F	27	60	170	1.04	1.94	230
2	M	33	84	178	0.10	2.59	42
3	F	27	63	159	2.75	8.91	49
4	F	25	60	158	1.61	1.60	32
5	M	27	78	178	0.45	2.48	72
6	M	30	70	178	1.96	4.45	40
7	M	25	67	177	0.06	2.92	115
8	M	27	85	181	0.24	2.93	56
9	M	27	75	177	0.42	1.33	75
10	F	24	55	164	1.64	0.78	36
11	M	26	72	179	2.47	3.89	40
12	M	28	72	178	3.68	19.52	65
13	M	25	62	170	0.42	2.15	36
14	F	26	48	166	2.50	1.22	36

Table 4. 6 Anthropometric and overall performance parameters. HE (Horizontal Error) and MLE (Medio-Lateral Error) refer to the accuracy in keeping the CIP-like device aligned with the horizontal and medio-lateral axes of the body, respectively, expressed as mean error. LBR is the Longest Balance Run achieved by each subject.

4.2.2.2 Experimental protocol

As a baseline, the subjects were initially asked to stay quietly upright, with parallel feet separated by about 20 cm, the arms extended on the sides of the body, the eyes open required to fixate a point on a white wall at eye-height, on top of a force platform (AMTI, Watertown, Mass, USA) that recorded the different components of the ground reaction force and the CoP displacements in antero-posterior (AP) and medio-lateral (ML) directions. Sway movements of the body were recorded for 120 seconds, excluding the initial 20 seconds from the analysis. This is the basic, single balancing task.

In the dual task the subjects stood with the feet in the same position, the elbows flexed at about 90 deg, holding the CIP-like device, consisting of a cylindrical wooden bar to be kept horizontal and aligned in the ML direction with the two hands. In the middle of the bar was mounted a ball bearing connected to a 1 m wooden stick that could rotate freely in the sagittal plane. The total weight of the CIP-like device is 0.375 kg. The task in this case was learning to balance the stick, namely avoiding the fall by keeping it approximately upright, while maintaining the feet fixed in the initial position, for the

longest possible time interval. In order to achieve this goal the subjects learnt to move the CIP-like device back and forth, where the control variable is the force transmitted to the device as a function of the state of the stick (the tilt angle and the corresponding angular velocity). On this purpose all the subjects spontaneously chose to keep their eyes fixed on the oscillating stick, in order to estimate its variable state. Although all the subjects had some experience in their childhood of balancing long sticks on the hand, none of them was a professional or amateur balancer. Therefore they needed a suitable training until they mastered the task for at least 30 seconds continuously over consecutive trials. The training time was different for the different subjects, typically about 30 minutes.

Kinematic data of the body inverted pendulum and of the CIP-like device were collected using an optoelectronic system (VICON, Oxford Metrics, Oxford, UK); markers were placed on ankles, knees, hips, shoulders, elbows, wrists and forehead of the participants and on the CIP-like device (two markers on the two extremities of the hand-held bar and one marker on the tip of the stick).

The electrical activation of different muscles of the legs/trunk/arms was also recorded by means of surface electrodes, although it was not specifically used for the present study. It could provide preliminary evidence for future extended studies.

4.2.3 *Results*

4.2.3.1 Experiments

The experiments involved fourteen healthy young subjects after a short training of stick balancing. Consider that there is dynamic interaction between the two tasks. The purpose of the arm movements is to apply a force $f_s(t)$ via the hand to the CIP-like device, capable to induce an acceleration profile of the stick $\ddot{x}_s(t)$ appropriate for balancing the pendulum. This force, with a minus sign, is reflected at the shoulder together with the force $f_a(t)$, necessary for accelerating the mass of the arm while it is carrying the hand, back and forth, with the mentioned acceleration profile. Thus, $-(f_s(t) + f_a(t))$ is a self-generated disturbance to the upright stance stabilization induced by the CIP stabilization process. The preliminary question we needed to answer was then the following one: to which extent such dynamic interaction modifies the posturographic spatio-temporal features that characterize quiet standing? Figure 4. 10 shows typical patterns related to

one subject indicating that the anticipated dynamic interactions modify only in a rather minor way the posturographic descriptors (see Table 4. 7), while keeping the same structure: i) the angular sway size (expressed by the standard deviation of θ_{com}) is markedly increased, ii) the phase portrait is slightly shifted in the direction of the CIP, as indicated by the small change of the mean value of θ_{com} from the single to the dual balancing task, but keeps its structure, 3) the power spectral density graph is basically unchanged: panel E of Figure 4. 9 shows that the bi-logarithmic plot is simply shifted upward, because the sway amplitude is increased, but is roughly approximated by a straight line with the same negative slope in the low-frequency range, in agreement with the power law scaling regime described by Collins & De Luca (Collins & De Luca, 1993). They found that temporal patterns of postural sway, i.e. the time course of the CoP (Center of Pressure), for healthy adults exhibit power-law-like behavior in the low-frequency regime, namely increments of the CoP path behave as those of a random walk with negative correlation, corresponding to movements approaching the upright posture. Table 4. 7 reports, for all the subjects, the amplitude of sway (expressed as standard deviation of θ_{com}) in the single and dual task, respectively, as well as the amount of the shift of the median value of the sway angle: on average, the amplitude is increased from 0.23 deg in the single task to 1.18 deg in the dual task, with a forward shift of 0.9 deg.

Figure 4. 11 shows typical combined CIP/body balancing patterns, during the dual task, in the time and frequency domains and Table 4. 8 reports characteristic parameters of the different subjects. As regards the CIP-like device, generally speaking, as one may expect, such patterns are similar to those recorded in studies where the CIP was stabilized by a sitting subject (Milton *et al.,* 2016; Yoshikawa *et al.,* 2016). The range of motion of the stick, measured by the standard deviation of the θ_s angle, is close to 2 deg; the spectrum of such oscillations has a well-marked peak, below 1 Hz (0.39 Hz on average); the range of hand motion, measured by the standard deviation of x_s, is about 10 cm. However, what is more interesting is the interaction/coordination between the two balancing motions. In particular, there is no correlation between the oscillation of the body θ_{com} and the oscillation of the stick θ_s, whereas there is a positive correlation between the hand forward/backward motion x_s and the body angle θ_{com} (0.87 on average) and a negative correlation between x_s and θ_s (-0.58 on average). While the latter anti-correlation may be attributed to a pure mechanical effect, expressing the bounded stability of the stick

inverted pendulum, the former one suggests an indirect synergy between the two intermittent stabilization processes, aimed at the extension of the range of movement of the hand motion that is required for improving the chance of stabilizing the stick while keeping the feet fixed in the starting position.

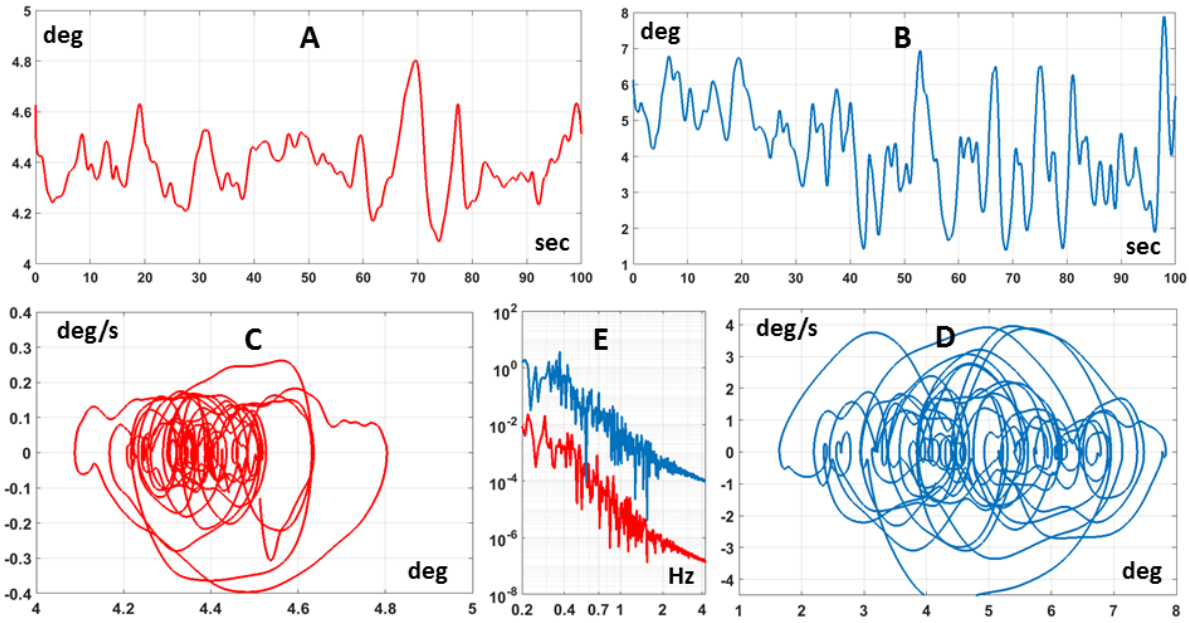

Figure 4. 10 Experimental results. Influence of CIP balancing movements on the posturographic features of body sway, characteristic of quiet standing. Each panel shows typical patterns related to subject 7. Panel A: angular sway sequence θ_{com} of the body inverted pendulum in the single balancing task; Panel B: θ_{com} in the dual balancing task; Panel C: Phase Portrait (θ_{com} $vs.$ $\dot{\theta}_{com}$) in the single task; Panel D: Phase Portrait in the dual task; Panel E: Power Spectral Density of the two angular sway sequences, in rad^2/Hz.

We label indirect the synergistic effect in the sense that it may not be coded in a specific modification of the controller; in contrast, it may express the consequence of the interaction between the two stabilization processes. The acceleration profile of the quick back and forth arm movements learned by the subjects for keeping the stick from falling are, at the same time, a disturbance for the standing body stabilization process and the purposive actions generated by the stick stabilization process. As we will show in the following section, this hypothesis is supported by the simulation studies, further emphasizing the robustness as well as the flexibility of the state-space intermittent feedback control paradigm.

Subject	Single balancing task	Dual balancing task	
	STD θ_{com} (deg)	STD θ_{com} (deg)	$\Delta\theta_{com}$ (deg)
1	0,37	1,27	0,20
2	0,20	0,72	1,37
3	0,23	0,74	0,07
4	0,32	1,61	0,56
5	0,17	1,17	1,31
6	0,22	1,20	1,57
7	0,12	1,48	0,42
8	0,30	0,98	0,90
9	0,34	0,92	0,32
10	0,46	1,11	0,11
11	0,23	1,58	2,47
12	0,22	1,20	2,01
13	0,20	1,52	1,13
14	0,25	0,96	0,20
Median	**0,23**	**1,18**	**0,90**
Model	**0,25**	**1,31**	**1,42**

Table 4. 7 Comparison between the single and the dual balancing tasks. STD: Standard Deviation; θ_{com}: tilt angle from the vertical of the body inverted pendulum; $\Delta\theta_{com}$: shift, from the single to the dual task, of the mean value of θ_{com}

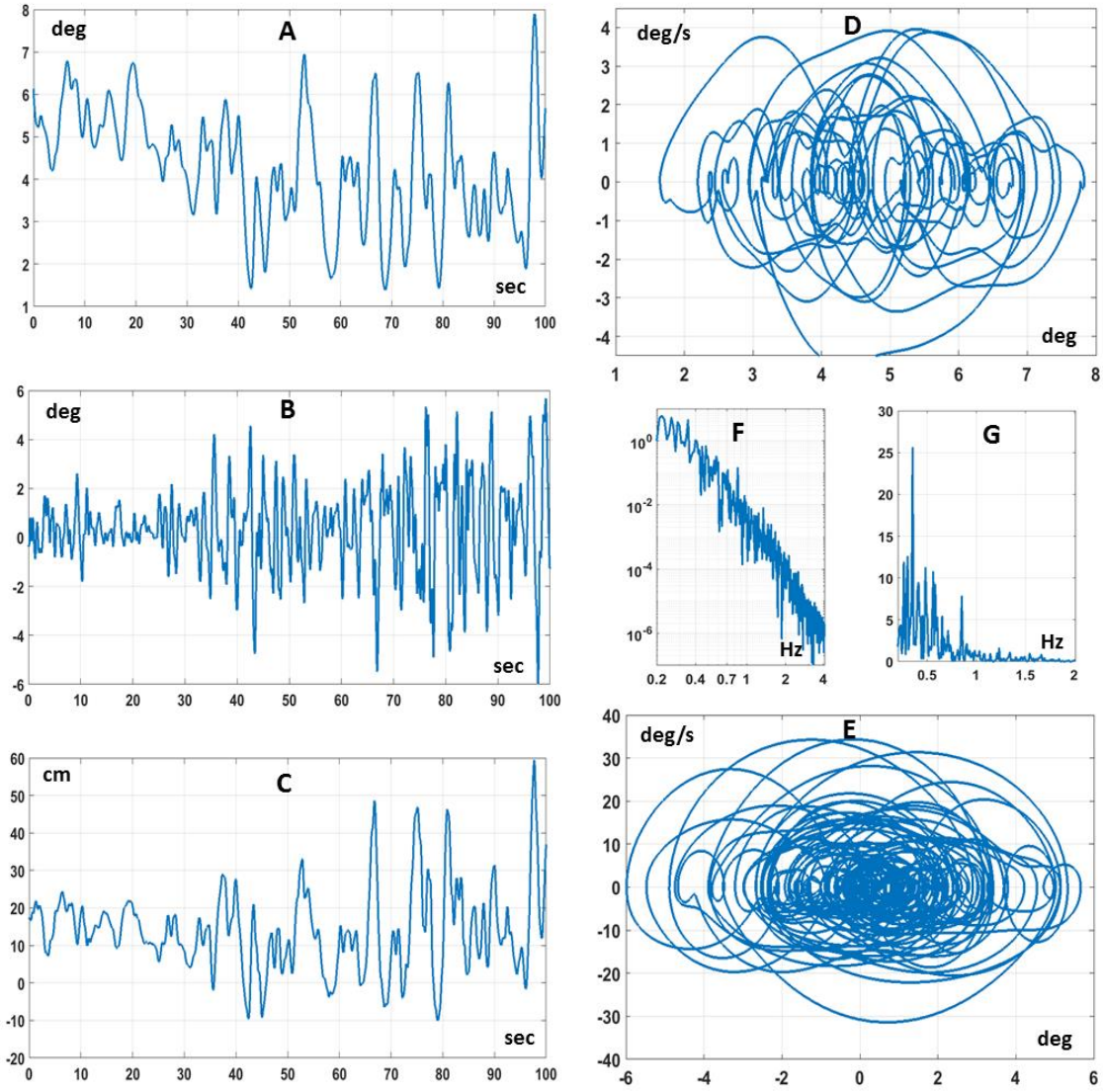

Figure 4. 11. Experimental results. Typical spatio-temporal patterns recorded in the dual balancing task (subject 7). Panel A: sequence of sway angles θ_{com} of the body inverted pendulum; Panel B: sequence of CIP stick angles θ_s; Panel C: sequence of CIP motion x_s; Panel D: Phase Portrait of the body motion ($\theta_{com}\ vs.\ \dot{\theta}_{com}$); Panel E: Phase Portrait of the CIP motion ($\theta_s\ vs.\ \dot{\theta}_s$); Panel F: Power Spectral Density of the body angles θ_{com}; Panel G: Power Spectral Density of the stick angles θ_s.

Subject	STD θ_s (deg)	Freq-peak θ_s (Hz)	STD x_s (cm)	Corrcoeff x_s $vs.$ θ_s	Corrcoeff x_s $vs.$ θ_{com}
1	2.86	0.35	13.69	-0.67	0.74
2	1.32	0.39	11.83	-0.25	0.18
3	2.65	0.41	11.43	-0.75	0.76
4	1.93	0.39	13.85	-0.65	0.90
5	2.53	0.41	12.12	-0.66	0.91
6	1.00	0.43	9.46	-0.30	0.92
7	1.54	0.37	6.49	-0.11	0.90
8	1.59	0.35	8.86	-0.67	0.87
9	1.86	0.39	10.71	-0.61	0.81
10	0.81	0.34	8.46	-0.38	0.23
11	1.65	0.31	14.37	-0.54	0.95
12	1.51	0.34	8.31	-0.71	0.76
13	0.84	0.56	7.89	-0.44	0.93
14	1.44	0.51	8.89	-0.56	0.87
Median	**1.57**	**0.39**	**10.09**	**-0.58**	**0.87**
Model	**1.52**	**0.41**	**15.03**	**-0.61**	**0.76**

Table 4. 8 Characteristic indicators of the dual balancing task. STD: Standard Deviation; θ_s: tilt angle of the stick from the vertical; x_s: back and forth motion of the CIP-like device; Freq-peak: frequency peak of the FFT of θ_s; Corrcoeff: Correlation Coefficient.

4.2.3.2 Simulations

The dynamical model of the CIP-like device has two degrees of freedom (θ_s & x_s) but is an under-actuated system because the only control variable available (the force $f_s(t)$ applied by the hand to the CIP) is unable to regulate simultaneously the state of the two controlled variables. However, the goal of the control process is more limited: it consists of keeping one variable (θ_s) in a *small* neighborhood of equilibrium, while allowing the other variable (x_s) to oscillate semi-freely in a *large* range compatible with arm-length. The model, that can be derived by the Lagrange equations and has been already employed in a previous work[25], is expressed by the following equation:

$$\begin{bmatrix}\ddot{\theta}_s\\ \ddot{x}_s\end{bmatrix}=\begin{bmatrix}A_{11}(\theta_s) & A_{12}(\theta_s)\\ A_{21}(\theta_s) & A_{22}(\theta_s)\end{bmatrix}\begin{bmatrix}\sin\vartheta_s\\ f_s\end{bmatrix} \quad 1$$

$$\begin{cases} A_{11}=\dfrac{1.5}{L\left(M_s+m_s(1-0.75\ \cos^2\theta_s)\right)}\left((M_s+m_s)g-0.5\,m_sL_s\,\dot{\theta}_s{}^2\cos\theta_s\right)\\ A_{12}=\dfrac{-1.5\cos\theta_s}{L_s\,(M_s+m_s(1-0.75\ \cos^2\theta_s))}\\ A_{21}=\dfrac{1}{M_s+m_s(1-0.75\ \cos^2\theta_s)}\left(0.5\,m_s\,L_s\,\dot{\theta}_s{}^2-0.75\,m_s\,g\cos\theta_s\right)\\ A_{22}=\dfrac{1}{M_s+m_s(1-0.75\ \cos^2\theta_s)}\end{cases}$$

L_s is the length of the stick, m_s is its mass, $M_s$is the mass of the held bar, and g the gravity acceleration. The state-space (i.e. $\theta_s\ vs.\dot{\theta}_s$) intermittent control law for the real time computation of $f_s(t)$ is expressed by the following equation, respectively for the on-phases and off-phases:

<u>On-phase</u>

Activation condition: $\theta_s(t-\delta)\ \left[\dot{\theta}_s(t-\delta)\ +\alpha\,\theta_s(t-\delta)\right]<0$

Control Action: $f_s(t)=P_s\,\theta_s(t-\delta)+D_s\,\dot{\theta}_s(t-\delta)+P_x\,x_s(t-\delta)+D_x\,\dot{x}_s(t-\delta)$ 2

<u>Off-phase</u>

Dis-activation condition: $\theta_s(t-\delta)\ \left[\dot{\theta}_s(t-\delta)\ +\alpha\,\theta_s(t-\delta)\right]\geq 0$

Control Action: $f_s(t)=0$

δ is the feedback delay (0.18 s in the simulation experiments); α is the slope of the switching function in the phase plane; $P_s,\ D_s\ , P_x, D_x$ are the controller gain parameters: the function of the first two is to constrain the stick oscillations near a limit cycle in the phase plane around the vertical, thus avoiding the fall, while the function of the other two elements of the control action is simply to limit the CIP motion to a physiological range, compatible with the arm length. The two groups of gains must be tuned considering a trade-off between stick motion and hand motion: increasing the hand gains will reduce the range of hand motion but increase the range of stick motion, with a greater risk of fall; in contrast, reducing the hand gains will also reduce the stick risk of fall but may force the hand beyond arm reachable positions. In the simulation experiments the control force was affected by a white noise: its power could be increased in the simulations to the same value of the control force before driving the system to instability.

The dynamical model of the body inverted pendulum has one degree of freedom (θ_b) and is expressed by the following equation:

$$\ddot{\theta}_b = \boldsymbol{I_b}^{-1}\left(T_{grav} - T_{stif} - T_{int} + T_s + T_a\right) \quad 3$$

I_b is the moment of inertia of the body around the ankle.

$T_{grav} = m_b\, g\, L_b \sin\theta_b = K_g \sin\theta_b$ is the gravity destabilizing torque (m_b is the body mass and L_b is the distance of the body CoM from the ankle).

$T_{stif} = K_a\, \theta_b + B_a \dot{\theta}_b$ is the torque due to the viscous-elastic properties of the ankle muscles (K_a is the stiffness and B_a is the corresponding viscous coefficient: in accordance to experimental evaluations[7,8] $K_a < K_g$);

T_{int} is the state-space intermittent control law that supplements the insufficient stabilizing effect of T_{stiff} for counteraction T_{grav};

$T_s = -f_s\, L_s \cos\theta_b$ is the disturbing torque for the body stabilization due to the control force transmitted to the CIP device (L_s is the distance of the shoulder from the ankle);

$T_a = -f_a\, L_s \cos\theta_b$ is the associated disturbance torque due to the acceleration of the arm mass.

In particular, the state-space intermittent control action, which is formally quite similar to equation 2, is described by the following equation:

<u>On-phase</u>

Activation condition: $\theta_b(t-\delta)\ \left[\dot{\theta}_b(t-\delta) + \alpha\, \theta_b(t-\delta)\right] < 0$

Control Action: $T_{int}(t) = P_b\, \theta_b(t-\delta) + D_b\, \dot{\theta}_b(t-\delta)$

4

<u>Off-phase</u>

Dis-activation condition: $\theta_b(t-\delta)\ \left[\dot{\theta}_b(t-\delta) + \alpha\, \theta_b(t-\delta)\right] \geq 0$

Control Action: $T_{int}(t) = 0$

P_b, D_b are the controller gain parameters: their function is to constrain the oscillation of the body inverted pendulum near a limit cycle in the phase plane; α is the slope of the switching function in the phase plane.

The state-space intermittent control models described by equations 1,2,3,4 were simulated for both the single and dual balancing tasks. In the former case the two characteristic angles of the body inverted pendulum (θ_b and θ_{com}) coincide, whereas diverge in the latter. Figure 4. 12 shows a typical simulation result of the dual balancing

task. Table 4. 7 and Table 4. 8 compare the simulation with the experimental results for both types of tasks.

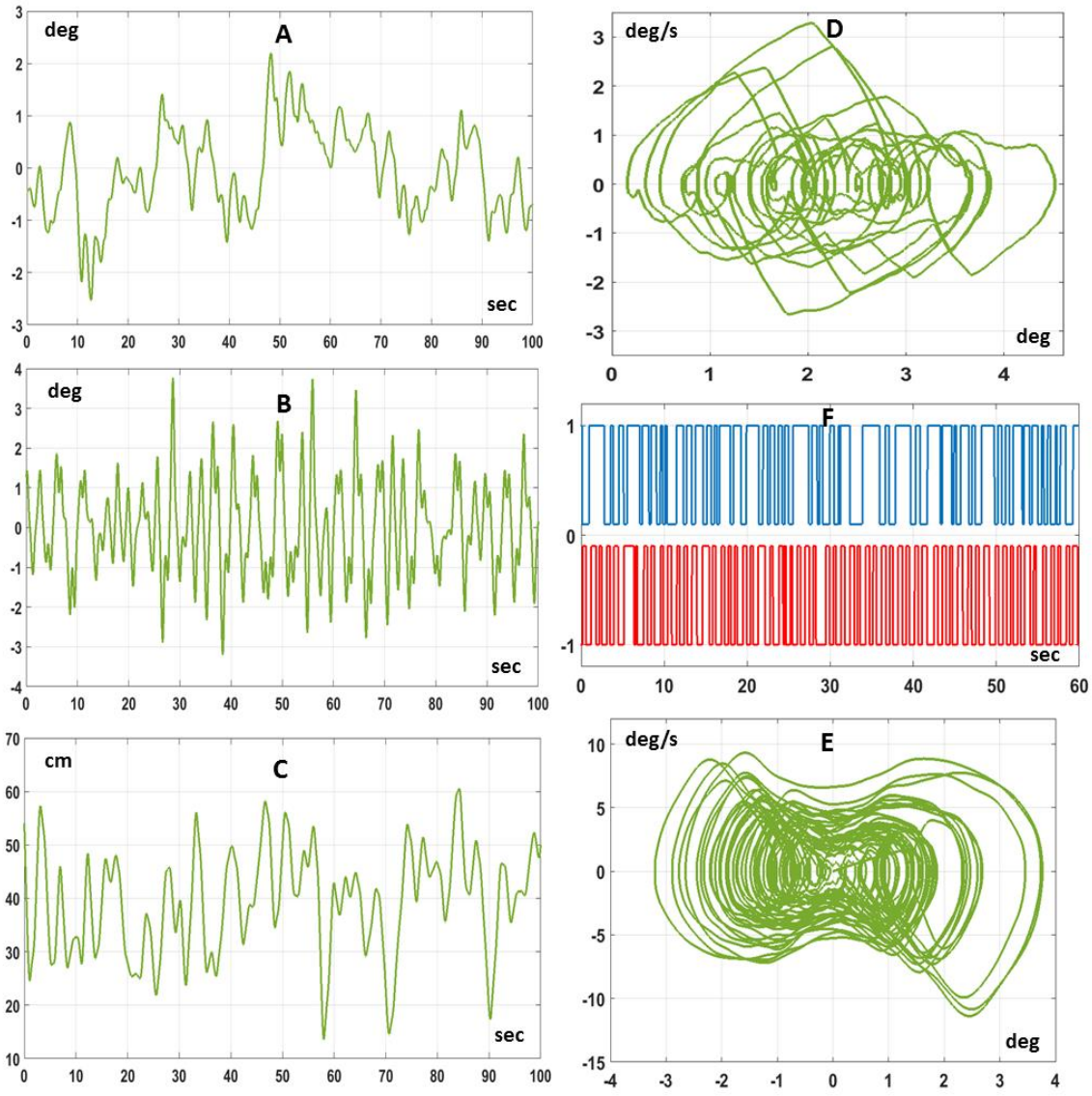

Figure 4. 12 Simulation results of the dual intermittent control model. Panel A: sequence of sway angles θ_{com} of the body inverted pendulum; Panel B: sequence of CIP stick angles θ_s; Panel C: sequence of CIP motion x_s; Panel D: Phase Portrait of the body motion (θ_{com} $vs.$ $\dot{\theta}_{com}$); Panel E: Phase Portrait of the CIP motion (θ_s $vs.$ $\dot{\theta}_s$); Panel F: On-off patterns of the state-space intermittent controllers: blue trace for the body controller (0: inactive, 1: active); red trace for the CIP controller (0: inactive, -1: active).

The robustness of state-space intermittent control paradigm of the body is supported by the experimental results on the amplitude of sway which can accommodate the rather massive self-generated disturbance. The simulation experiments allowed us to evaluate that such disturbance, resulting from the acceleration of the arm and the CIP device, is close to 90% of the total torque acting on the ankle (with a standard deviation of about

3.7 Nm) during the dual balancing task. Of course such disturbance is mostly determined by the arm movements because the weight of the arm is much greater than the CIP device.

Overall, the working hypothesis of testing the capability of the two independent state-space intermittent controllers to successfully stabilize the dual balancing task without any specific modification of the control actions is confirmed. The spatio-temporal features of the experimental and simulation behaviours are quite similar. In particular, the positive correlation between the hand motion and the body sway as well as the anti-correlation between the hand motion and the stick oscillation are found in both cases. Moreover, the Power Spectral Density (PSD) of the body sway angle in both balancing tasks exhibits the same power law scaling regime in the low frequency range (up to 2-3 Hz) for all the subjects as well as the model simulations. This is consistent with the analysis of universal and individual characteristics of postural sway during quiet standing[33] that has shown that the power-law behavior at the low-frequency regime is a universal indicator of the control law whereas the high-frequency regime is sensitive to the anthropometric/biomechanical parameters.

We also analyzed the activation/inactivation sequences generated by the pair of state-space intermittent feedback controllers in the dual balancing task. Figure 4. 12 (panel E) shows a typical pair of sequences of on-off activations of both intermittent controllers. It appears clearly that the average switching rate of the body intermittent controller is lower than that the CIP controller one: 0.68 Hz vs. 1.03 Hz. In both cases, the duration of the on-phases is somehow longer than the off-phases: with a mean duration of the on-phase of 880 ms (on-phase) vs. 585 ms (off-phase) for the body controller and 537 ms (on-phase) vs. 436 ms (off-phase) for the CIP controller. Moreover the on/off switching times do not appear to be correlated. Thus, the behavioral coordination and coherence that characterizes the dual balancing task, observed in the experiments and reproduced in the simulations, seems to be consistent with two internal control models, with similar design but independent control actions, that interact through the biomechanics of the body and the mechanics of the external environment.

4.2.4 *Discussion*

It has been suggested (Sakaguchi *et al.*, 2015) that intermittent control is the natural and rational solution devised by the human brain for answering the fundamental question of motor neuroscience: how the human body may succeed to perform a *fast* motor task in a real-time fashion with the *slow* sensory-motor system. This is somehow in contrast with the common wisdom that the brain stabilizes unstable body dynamics using impedance control, by regulating co-activation levels of antagonist muscles (Hogan, 1984). In this framework, the strategy of the CNS would be to learn the optimal impedance for compensating the destabilizing effect of gravity, by selecting the appropriate groups of antagonist muscles and optimally tuning co-activation levels in a preprogrammed manner (Burdet *et al.*, 2001). Such feedforward control strategy (Winter *et al.*, 1998; Maurer, 2004) has the clear advantage of avoiding the risk of delay-induced instability but, on the other, it forces a trade-off between task-related errors and energetic costs. Moreover, accepting such high energetic costs seems to be incompatible with the minimum intervention principle, which has been suggested as a general, rational strategy for many biological systems (Todorov & Jordan, 2003). As a matter of fact, the intermittent control strategy for defeating instability and shaping purposive actions is clearly in favor of the minimum intervention principle, by exploiting the natural dynamics arising from the interaction between the human body and the external environment. At the same time, this strategy agrees as well with the general principles of biological autonomy advocated by Francisco Varela (Varela, 1979) in the framework of enactivist theories.

In any case, the intermittent control strategy is a general approach that can be articulated in a variety of versions of intermittent controllers: one version assumes anticipatory ballistic bias control, mathematically modeled with a state predictor for compensating feedback delay (Loram *et al.*, 2011, 2012; Gawthrop *et al.*, 2011); in a second version, off-loop phases are meant to represent a sensory dead-zone (Insperger & Milton, 2014); a third version has been characterized as *act-and-wait control* (Insperger & Stepan, 2010); another version is the one adopted in this study (Bottaro *et al.*, 2008; Asai *et al.*, 2009; Suzuki *et al.*, 2012), namely the state-space intermittent feedback strategy. The latter formulation exploits the fact that the state point of the inverted pendulum transiently approaches the upright position along a stable manifold of an unstable saddle-type equilibrium of the off-system; moreover, the key feature of this control strategy is that,

although the off- and on-systems are both unstable, the combination of the two, according to the switching mechanism, can achieve bounded stability, with a limit cycle oscillation that represents postural sway during quiet stance, even in the absence of motor noise. Another remarkable characteristic of the model is the small joint impedance that originates from the null feedback gains in the off-phase and the small feedback gains in the on-phase: this feature leads to joint flexibility that induces power-law-like postural sway when driven by tiny additive torque noise corresponding to the hemodynamic perturbations during stance (Suzuki *et al.*, 2012).

The dual balancing task introduces two additional issues to the discussion above on the rationale of intermittent control: the issue of dual task, in general, and the more specific issue of anticipatory postural adjustments (APA's). A dual task can be defined as the concurrent performance of two tasks that can be executed independently and have distinct and separate goals. It is well known that when attempting to perform two tasks at the same time, the tasks often interfere with each other. Typically such interference has been studied by using the refractory period paradigm (Luck, 1998) and has been modeled in different ways in terms of how to manage the increased attentional load, e.g. the central bottleneck model (Pashler, 1984) or the central capacity sharing model (Tombu & Jolicoeur, 2003). The dual balancing task investigated in this work, which is just an example of equilibrium skills exhibited in the circus, in our opinion is a different type of challenge, primarily because for all balancing tasks the issue is not accuracy per se but success/failure of the action, namely avoiding the fall (of the body, the stick etc.). In the specifically investigated dual balancing task the simulations demonstrate that two independent state-space intermittent task controllers appear to be robust enough to adapt their dynamic behavior, due to the mutual dynamic interaction, in such a way to succeed maintaining the dual bounded stability. Such *functional synergy* emerges in spite of the strong differences between the two balancing paradigms: the state-spaces are different, the sensory feedback channels are different (primarily visual for stick balancing and proprioceptive in upright standing), the number of degrees of freedom is different, the recruited groups of muscles are different. Consider that both balance task controllers have an important central/cognitive component but, different from the typical attentional tasks addressed in the investigation of dual task interference, such cognitive component is strongly grounded in an embodied cognitive framework: more specifically, it is based on

the exploitation of the dynamic affordance provided by the saddle-like instability of an inverted pendulum, whether a stick or the human body.

Modeling the CIP-like device as a single inverted pendulum (SIP) is obviously accurate enough, whereas adopting the same paradigm for upright standing, with the implicit assumption that only ankle rotations are relevant for describing and explaining sway movements, is certainly a less accurate approximation. In particular it ignores hip motion and ankle-hip coordination that have been the focus of recent experimental and modeling studies (Aramaki *et al.*, 2001; Creath *et al.*, 2005; Zhang *et al.*, 2007): The range of variation of the angular displacement, velocity, and acceleration of the hip is comparable to that of the ankle, thus suggesting that the SIP model should be substituted by a two-link or DIP (Double Inverted Pendulum) model, involving the coordinated control of ankle and hip joints. In particular, it has been found that the acceleration profiles of the two joints are strongly characterized by anti-phase correlation and it was proposed that DIP control could be characterized as an optimal bi-axial active controller with the goal of minimizing the acceleration of the global CoM (Suzuki *et al.*, 2015). However, the simulation study in the previous section involving a DIP mechanical model stabilized by a state-space intermittent controller (Morasso *et al.*, 2019) demonstrated that there is no need to introduce a bi-axial optimization process because the state-space intermittent controller applied to the VIP (Virtual Inverted Pendulum that links the ankle to the variable CoM) can fully explain ankle-hip coordination.

As regards the issue of APAs, for understanding dual balancing tasks, we should take into account that different types of APAs, that represent generally feed-forward control processes, can be defined. The traditional group of APAs occurs when a standing person performs an action leading to a postural perturbation or expects an external postural perturbation, inducing changes in the activation levels of postural muscles that can be observed prior to the perturbation time (Belen'kiĭ *et al.*, 1967; Massion, 1992), typically about 100 ms prior to the movement initiation or the perturbation time (Aruin & Latash, 1995). A second class of APAs occurs when a person prepares to make a whole-body action that may destabilize the standing posture, such as picking up a load from the floor and placing it on a table. At a first look either type of APAs might seem to be irrelevant for the paradigm investigated in this study because APAs are typically feed-forward processes whereas the dual balancing task implies dual feedback control. However, it is an intriguing issue, to be addressed in future studies, to consider *hybrid* experimental

situations, approximating complex tasks or task sequences in real life, where the two control paradigms (feedforward anticipation and intermittent feedback stabilization) may need to be integrated and coordinated by the brain.

This work has been submitted and is under review (P. Morasso+, A. Cherif+, J. Zenzeri. “State space intermittent feedback stabilization of a dual balancing task”. Under review for Scientific Reports).

+ equal contribution

Chapter 5

Pathological disturbance

5.1 Sensory dysfunction in cervical dystonia

After considering the effect of external perturbations and self-generated disturbances on healthy central nervous system, we get to the consideration of a very complex system. This section shows the effect, on upper limb sensorimotor control, of a disturbance that is internally triggered due to a neurological condition, cervical dystonia. This study looks into sensory function in both the affected district (the neck) and one unaffected district (the wrist) in subjects with cervical dystonia. It is also a representative example of how robotics can significantly improve diagnosis and consequently treatment of neurological conditions affecting movement in a direct or indirect way.

5.1.1 *Introduction*

Cervical dystonia (CD) is a common adult-onset idiopathic isolated dystonia that is characterized by involuntary muscle contractions causing twisted postures of the head and neck. Recent evidence suggests that CD is a network disorder involving the basal ganglia, the cerebellum and their interconnected cortical and subcortical structures (Prudente *et al.*, 2014). The key nodes in the malfunctioning cerebral network may differ between different CD phenotypes with tremor as an additional phenotypic feature of CD due to abnormal cerebellar processing (Avanzino, 2012; Prudente *et al.*, 2014; Antelmi *et al.*, 2017; Avanzino *et al.*, 2018*b*).

Smeared digit representations in primary somatosensory cortex (Bara-Jimenez *et al.*, 1998; Nelson *et al.*, 2009) are associated with a generalized somatosensory deficit in CD that also involves non-dystonic muscles (Avanzino *et al.*, 2015). Temporal or spatial forms of somatosensory perception such as tactile temporal discrimination thresholds (TDt) (Conte *et al.*, 2017); spatial grating sensitivity (Sanger *et al.*, 2001) and proprioception are all impaired in CD (Putzki *et al.*, 2006; Avanzino *et al.*, 2015).

Proprioception is essential for motor control (Sainburg *et al.*, 1995; Konczak *et al.*, 2012; Cuppone *et al.*, 2016). It relies on a network that includes the cerebellum and somatosensory cortex, which both are likely involved in defective processing of proprioceptive afferents in CD (Kaji *et al.*, 1995).

It is unknown if the different phenotypes of CD exhibit different levels of somatosensory impairment. If cerebellum is primarily involved in the expression of tremor in CD, then we would expect that tactile and proprioceptive dysfunction differentiates between CD with and without tremor. To address this knowledge gap, we assessed in CD patients with and without tremor 1) tactile temporal discrimination thresholds of the non-dystonic forearm and 2) proprioceptive acuity in both the dystonic (neck) and non-dystonic body segments (forearm/hand) using a joint position-matching task.

5.1.2 *Methods*

5.1.2.1 Participants and ethical approval

24 patients (11 males, 58.6 ± 11.4 years) affected by idiopathic isolated cervical dystonia were recruited from the outpatients of the Movement Disorders clinic of the Department of Neuroscience, University of Genoa. The following exclusion criteria were applied: (a) presence of psychiatric abnormalities that may affect cognitive functions such as schizophrenia and major depressive disorders, (b) presence of sensory/somatic abnormalities, (c) treatment with botulinum toxin in the past 3 months; (d) cognitive deficits (Mini-Mental State Examination score < 24). Twenty-two healthy controls (HC, 8 males, mean ± SD age 59.2 ± 10.7 years) were recruited as age-matched control group for the study.

Head tremor was assessed while patients sat on a comfortable chair holding their heads either held in neutral position or turned it to the right and the left side. Rest tremor, postural tremor and kinetic tremor localized in non-dystonic body segments were evaluated with ad-hoc manoeuvres. Patients were divided into two groups: dystonic patients with (CD-T) and without tremor (CD-NT). Dystonic patients with tremor were sub-classified as (i) patients with *dystonic tremor* if they had head tremor with irregular amplitude and superimposed jerks, as (ii) patients with *tremor associated with dystonia* if

they presented tremor in non-dystonic body segments and as (iii) patients with *dystonic tremor and tremor associated with dystonia* if they had both (Deuschl *et al.*, 2008).
We adopted the Fahn-Tolosa-Marin Tremor Rating Scale(Fahn *et al.*, 1988) and the Toronto Western Spasmodic Torticollis Rating Scale (Consky *et al.*, 1990) for rating severity of tremor and of cervical dystonia respectively. All patients had received treatment with botulinum toxin at least not < 3 months before the study.
All subjects were right-handed and gave written informed consent for participation in the study. The study was approved by the local ethics committee (Protocol number 311REG2014 approved on 09/12/2015) and was conducted in accordance with the Declaration of Helsinki.

5.1.2.2 Experimental protocol

The study was a single-centre observational controlled study. Participants attended our laboratories for a single evaluation consisting of: (a) a clinical evaluation assessing the severity of the disease and severity of tremor if present; (b) evaluation of somatosensory temporal discrimination threshold; (c) evaluation of proprioceptive acuity in the cervical segment (dystonic segment for CD patients) via joint position-matching task, using a motion capture system; (d) evaluation of proprioceptive acuity in the forearm segment (non-dystonic segment for CD patients) via a joint position-matching task, using a robotic wrist exoskeleton.

5.1.2.3 Tactile temporal discrimination task

Tactile temporal discrimination acuity was tested in the forearm by delivering square wave electrical pulses with a constant current stimulator (Digitimer Limited, D360, Welwyn Garden City, UK). The stimulation intensity was defined for each subject by delivering a series of stimuli at increasing intensity from 2 mA in steps of 1 mA; the intensity used for this task was the minimal intensity perceived by the subject in 10 over 10 consecutive stimuli. Paired stimuli were applied starting with an inter-stimulus interval (ISI) of 0 ms (simultaneous pair) and progressively increasing the ISIs (in 10 ms steps). Twenty- four ISIs (from 0 to 23 ms) were included in our experimental protocol. During the test the ISIs were applied in a random sequence and subjects had to report whether they perceived a single stimulus or 2 temporally separated stimuli.

5.1.2.4 Cervical joint position-matching task

In order to assess proprioceptive acuity in the dystonic segment, a position-matching task was used (Figure 5. 1A). Subjects sat on a chair and head movements were tracked using a 6-camera optoelectronic camera system (Qualisys Motion Capture System (Sweden)). Data were captured at a frequency of 120 Hz. Infrared light reflective markers were placed on the acromion processes, the sternum and on T1's spinous process. In addition, markers were placed on the front, back and the lateral sides of a helmet worn by the participant. After a baseline acquisition, in which subjects maintained the head in their neutral position (i.e., the dystonic head position), the maximal active head rotations around the vertical (head rotation) and sagittal (head lateral bending) axes were determined. These values were used to obtain maximal range of motion (RoM) around these axes.

For proprioceptive acuity testing, the head was passively displaced by the experimenter while subjects were blindfolded. After displacement, the subject's head was moved back to neutral position. Then subjects actively reproduced the same head position as accurately as possible. Each position at approximately 50% and 75% of active RoM was repeated 3 times. The order of movement amplitude (50% and 75% of RoM) and the type of joint displacement were randomized.

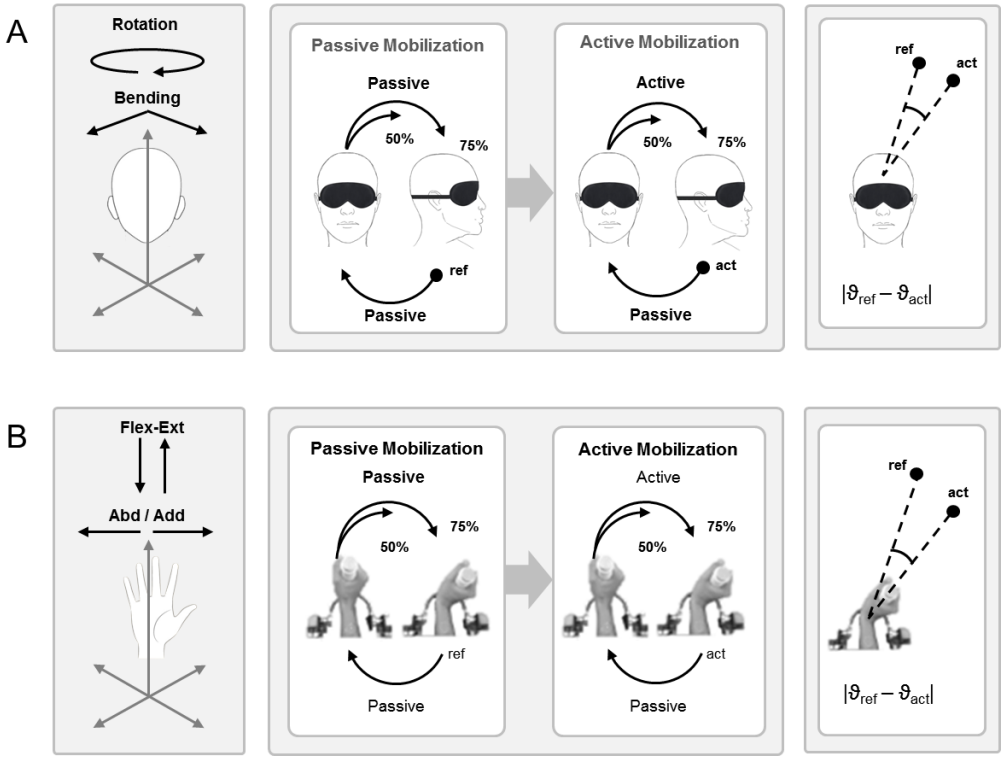

Figure 5. 1 Experimental paradigm. Proprioceptive acuity was assessed in both the affected (head/neck) and unaffected body segments (forearm/wrist) using a joint position-matching task. The head (A) or the wrist (B) was passively displaced to distinct joint positions by the experimenter (head lateral rotation; head lateral bending) or through a robotic exoskeleton (wrist flexion-extension; wrist abduction-adduction). Targets distances were chosen as 75% and 50% of the subject's active RoM. Then participants actively reproduced the experienced joint position, which was tracked by a motion capture system for the head or by encoders of the robotic exoskeleton for the wrist. The absolute joint position matching error between passive (ϑ_{ref}) and active (ϑ_{act}) mobilization performance served as a marker of proprioceptive acuity.

5.1.2.5 Wrist joint position-matching task

In order to assess the wrist proprioceptive acuity, a robot-based ipsilateral joint position-matching procedure was used (Cappello *et al.*, 2015; Marini *et al.*, 2016, 2018) (Figure 5. 1B and Figure 2. 1). The wrist robot allowed movements along three degrees of freedom - Flexion/Extension (Flex/Ext), Abduction/Adduction (Abd/Add) and Pronation/Supination (P/S) - of the human forearm/wrist. It is powered by four brushless motors that compensate for the weight and inertia of the device during movements. Angular rotations around the three axes were measured by means of high resolution incremental encoders with 0.17° of overall accuracy. Subjects were seated holding the robot handle with their dominant hand, keeping a 90° angle between the arm and the forearm. Subject's dominant forearm was strapped to the support to ensure the same wrist positioning across the different trials and to avoid joints misalignment or unwanted movement during task

execution. Participants' wrist joint was moved by the robot from the neutral anatomical position (0° of Flex/Ext, 0° of Abd/Add and 0° of P/S) to a reference position (target), holding it for three seconds, and then was moved back to the neutral position. Subsequently, participants were asked to actively move the wrist to the previously experienced target position. Participants did not receive any feedback or any force assistance from the robot during testing. Targets were located along 8 directions: Flexion, Extension, Abduction, Adduction and directions involving combined movements (2DoF; Flex+Abd, Flex+Add, Ext+Abd, Ext+Add). Angular rotations along the P/S axis were not performed. Targets distances were chosen as 75% and 50% of the subject's wrist active RoM previously recorded by the robot. Proprioceptive targets were presented 5 times for each direction, for a total of 80 randomized trials. Wrist joint rotations were recorded by the robot's encoders at a frequency of 100Hz; acquired signals were post-processed using a Savitzky-Golay low-pass filter (cut-off frequency of 10 Hz) and converted into angular displacements.

5.1.2.6 Data analysis

For the tactile temporal discrimination task, we derived the threshold (TDt) as the first inter-stimuli time interval of 3 consecutive ISIs at which patients recognized the stimuli as temporally separated (Scontrini *et al.*, 2009). For both joint position-matching tasks, we computed the matching errors for the head and the wrist positions as the absolute difference between the reference and matched joint positions. To account for the abnormal head postures in cervical dystonia (De Beyl & Salvia, 2009), matching error for the head was expressed as percentage of the maximal active individual RoM. Subsequently, for each subject, we averaged the matching errors across joint positions and workspaces to obtain a global measure of proprioceptive acuity (proprioceptive acuity index, PAI) for both the head and the wrist.

Mann-Whitney tests and Chi square tests were used to compare clinical and demographic data between patients with and without tremor. Because data related to TDt and matching errors were normally distributed, parametric tests were applied. TDt values in patients and healthy controls were compared by means of a one-way ANOVA with the factor GROUP (HC, CD-T, CD-NT) as main factor. Age and sex were entered as covariates. For testing differences between groups for both matching errors we performed two

separate three-way RM-ANCOVA with the factor GROUP (HC, CD-T, CD-NT) as between subjects factor and JOINT POSITION (head lateral rotation and head lateral bending; or wrist Flex/Ext, Abd/Add, 2DoF) and WORKSPACE (75% RoM, 50% RoM) as within-subjects factors. Age and sex were entered as covariates to account for the known differences in demographics in CD patients with and without tremor (Defazio *et al.*, 2015; Norris *et al.*, 2016).

To understand the possible linkage between tactile and proprioceptive acuity measures we computed Pearson correlation coefficient between TDt and PAI for the head and the wrist. To understand the possible linkage between proprioceptive acuity measures of the dystonic and non-dystonic body segments we computed Pearson correlation coefficient between PAI of the head and the wrist. Finally, we computed Spearman's correlation coefficient to assess any correlation between TDt, PAI at the joint position-matching tasks and severity of dystonia, tremor severity and duration of the disease in CD patients. Bonferroni post-hoc test was used for post-hoc analyses following the ANOVA. P-values of 0.05 were considered as threshold for statistical significance. Effect size was reported as Cohen's *d*.

5.1.3 *Results*

Based on clinical examination we recruited 12 dystonic patients with tremor and 12 without tremor. All patients had latero- or torticollis. Among patients with tremor, 6 had dystonic tremor and 6 had both dystonic tremor and tremor associated with dystonia. Dystonic tremor was observed especially when patients were asked to turn the head or during the maintenance of a posture. Tremor associated with dystonia occurred in upper limbs especially during the maintenance of a posture. Demographic and clinical characteristics are reported in Table 5. 1. There were significant differences in demographic characteristics among patients with and without tremor, consistently with literature (Defazio *et al.*, 2015; Norris *et al.*, 2016). Indeed, age in the CD-T group was higher ($p=0.045$) with a higher proportion of females (Chi-square=35.50; $p<0.001$) than in CD-NT group. There were no significant differences in disease severity ($p=0.37$) and disease duration ($p=0.31$).

Patients with dystonia (CD-NT)					Patients with dystonia and tremor (CD-T)							
Case	**Gender**	**Age**	**Disease duration**	**TWTRS**	**Case**	**Gender**	**Age**	**Disease duration**	**TWTRS**	**DT**	**TAWD**	**TRS**
1	M	33	8	7	1	F	47	22	12	X		6
2	M	53	7	21	2	F	72	9	13	X		7
3	M	44	10	16	3	F	68	10	15	X	hands	10
4	M	60	12	19	4	F	61	17	23	X	hands	9
5	F	40	4	15	5	F	60	6	10	X	hands	10
6	M	65	45	22	6	M	65	13	14	X		6
7	M	63	1	6	7	M	68	35	19	X		7
8	M	58	2	14	8	F	69	11	13	X		5
9	F	53	2	11	9	F	69	18	13	X	hands	21
10	F	40	5	14	10	M	68	5	15	X		3
11	F	49	8	18	11	F	58	30	20	X		6
12	F	72	25	12	12	F	72	9	21	X		9
Mean		**52.5**	**10.7**	**14.5**			**64.7**	**15.4**	**16.5**			**8.3**
SD		**11.7**	**12.5**	**5.1**			**7.2**	**7.2**	**4.5**			**7.2**

Table 5. 1 Clinical characteristics of Cervical Dystonia patients. M=male; F=female; Age and disease duration are measured in years; DT: dystonic tremor; SD: standard deviation; TAWD: tremor associated with dystonia; TRS: Fahn-Tolosa-Marin tremor rating scale; TWSTRS: Toronto western spasmodic torticollis rating scale; X: indicates presence of dystonic tremor.

5.1.3.1 Tactile temporal discrimination task

All patients underwent the tactile temporal discrimination task. TDt values are reported in Figure 5. 2. TDt values in the non-dystonic forearm were higher in patients than in healthy controls. RM ANCOVA showed a significant effect of GROUP ($F(2, 43) = 4.5$; $p = 0.017$), that remained significant after having entered age and sex as covariates [GROUP ($F(2, 41) = 4.44$; $p = 0.018$)]. Post-hoc analysis revealed that TDt values were lower in HC than in both CD-T ($p=0.010$, Cohen's $d= 0.99$) and CD-NT ($p=0.045$ Cohen's $d= 0.74$) with no differences between CD-T and CD-NT ($p=0.59$, Cohen's $d= 0.19$).

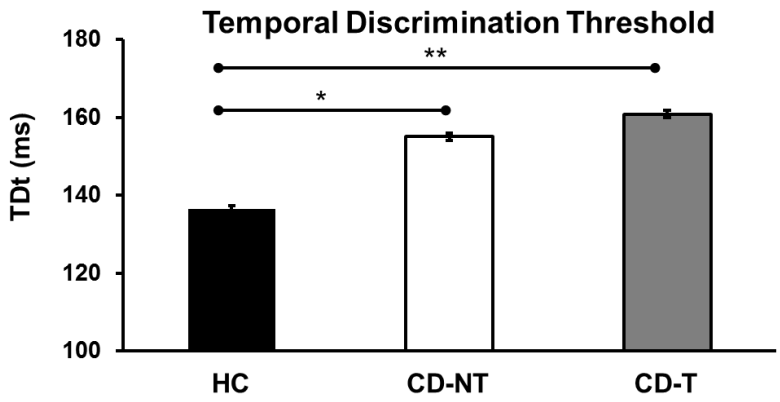

Figure 5. 2 Tactile temporal discrimination thresholds (TDt) in patients with cervical dystonia with (CD-T) and without tremor (CD-NT) and in healthy controls (HC). Each column represents mean value; the bars represent standard error. Asterisks indicate significant differences between groups (*p < 0.05; **p < 0.01).

5.1.3.2 Cervical joint position-matching task

One subject in the CD-T group was excluded from the analysis because of missing data. Two subjects (1 subject each in the CD-T and the CD-NT groups) did not perform the task because of inability to perform it or voluntary decision not to participate. Mean matching error for each group is shown in Figure 5. 3. Patients with CD and tremor exhibited an increased matching error respect to both healthy controls and patients with CD without tremor. Indeed RM-ANCOVA showed a main effect of GROUP ($F(2, 40) = 7.38$; $p = 0.002$), that remained significant after having entered age and sex as covariates [GROUP ($F(2, 38) = 6.70$; $p = 0.003$)]. Post-hoc analysis revealed that matching error was larger in CD-T patients than HCs ($p < 0.001$, Cohen's $d = 1.27$) and CD-NT patients ($p = 0.036$, Cohen's $d = 0.84$). There were no differences between CD-NT patients and HCs ($p = 0.17$, Cohen's $d = 0.73$). No other significant main effects of JOINT POSITION and WORKSPACE or interactions between the main factors were found.

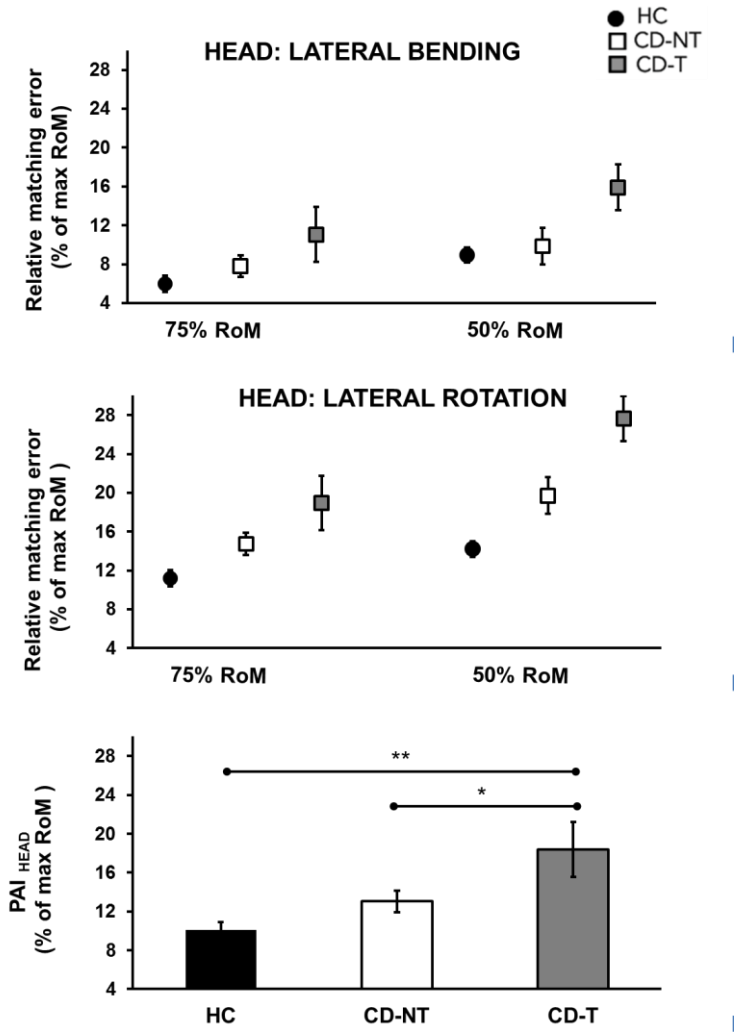

Figure 5. 3 Relative matching error for the cervical joint position-matching task. Mean matching error recorded for different movements (head lateral rotation and head lateral bending) in different workspaces (75% RoM and 50% RoM) is reported. In the bottom panel, columns represent the proprioceptive acuity index (PAI = averaged matching errors across joint positions and workspaces) for the head. CD-T: cervical dystonia with tremor; CD-NT: cervical dystonia without tremor; HC: healthy controls. Bars represent standard error. Asterisks indicate significant differences between groups (*$p < 0.05$; **$p < 0.01$).

5.1.3.3 Wrist joint position-matching task

Data collected from two subjects (1 subject each in the CD-T and the CD-NT group) were excluded from the analysis because there were missing data. Five subjects (3 subjects in the HC group, 1 subject in the CD-T group and 1 subject in the CD-NT group) did not perform the task because of orthopaedic problems at the wrist or voluntary decision not to participate. Mean matching error for each group is shown in Figure 5. 4. Patients with CD and tremor exhibited an increased matching error respect to both healthy controls and patients with CD without tremor. Indeed RM-ANCOVA showed a

main effect of GROUP ($F(2, 36) = 7.88$; $p = 0.001$), that remained significant after having entered age and sex as covariates [GROUP ($F(2, 34) = 6.71$; $p = 0.003$)]. Post-hoc analysis revealed that matching error was larger in CD-T patients than HCs ($p < 0.001$, Cohen's $d = 1.27$) and CD-NT patients ($p = 0.027$, Cohen's $d = 0.84$). There were no differences between CD-NT patients and healthy controls ($p = 0.19$ Cohen's $d = 0.72$). No other significant main effects of JOINT POSITION and WORKSPACE or interactions between the main factors were found.

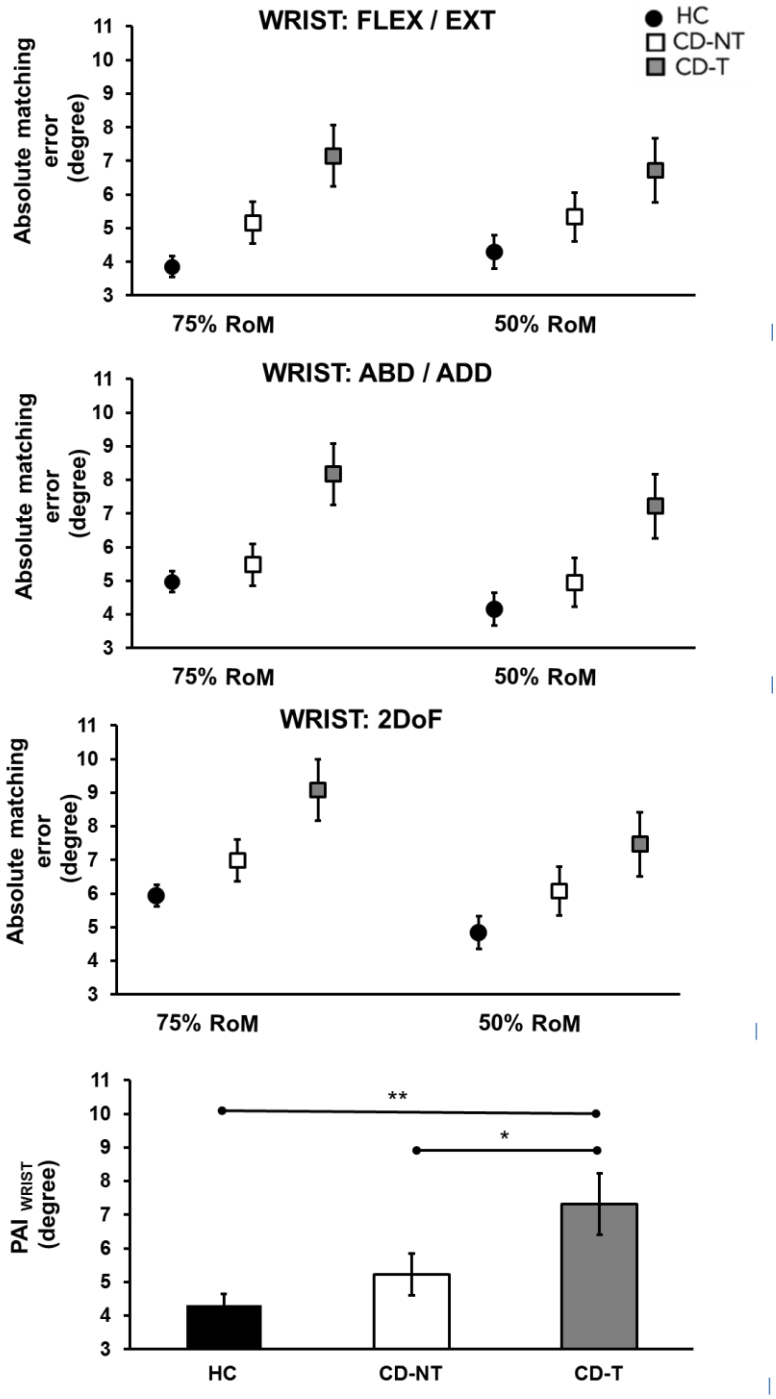

Figure 5. 4 Absolute matching error for the wrist joint position-matching task. Mean matching error is reported for different movements (Flexion/Extension, Adduction/Abduction and 2DoF) in different workspaces (75% RoM and 50% RoM). Two degree-of-freedoms (2DoF) corresponded to the following movements: Flexion+Abduction, Flexion+Adduction, Extension+Abduction, Extension+Adduction. In the bottom panel, columns represent mean proprioceptive acuity index (PAI = averaged matching errors across joint positions and workspaces) for the wrist. CD-T: cervical dystonia with tremor; CD-NT: cervical dystonia without tremor; HC: healthy controls. Bars represent standard error. Asterisks indicate significant differences between groups (*$p < 0.05$; **$p < 0.01$).

5.1.3.4 Distribution of tactile and proprioceptive acuity measures in cervical dystonia patients

To appreciate the relevance of tactile and proprioceptive dysfunction in CD patients with and without tremor, individual data at the different somatosensory assessment tasks are illustrated in Figure 5. 5. For tactile discrimination, there were no discernible differences between the two CD phenotypes. 75% of the CD-T patients and 58% in the CD-NT group exhibited TDt values in the fourth quartile of the control group or above and 17% in CD-T and 25% in CD-NT groups had elevated TDt values above the observed maximum of the control participants (Figure 5. 5A). For proprioceptive acuity of the head, 70% of the CD-T patients were in the fourth quartile of the control group or above and 50% of those patients showed values above the observed maximum of the control group (Figure 5. 5B). In contrast, 40% of the CD-NT patients were in the fourth quartile of the control group or above and only 18% of those patients exhibited matching errors above the observed maximum of the controls. For proprioceptive acuity of the non-dystonic wrist, 90% of the CD-T patients were in the fourth quartile of the control group or above and 50% of those patients showed values above the control group maximum (Figure 5. 5C). Differently, 60% of the CD-NT patients were in the fourth quartile of the control group or above and only 20% of those patients exhibited matching errors above the observed maximum of the controls.

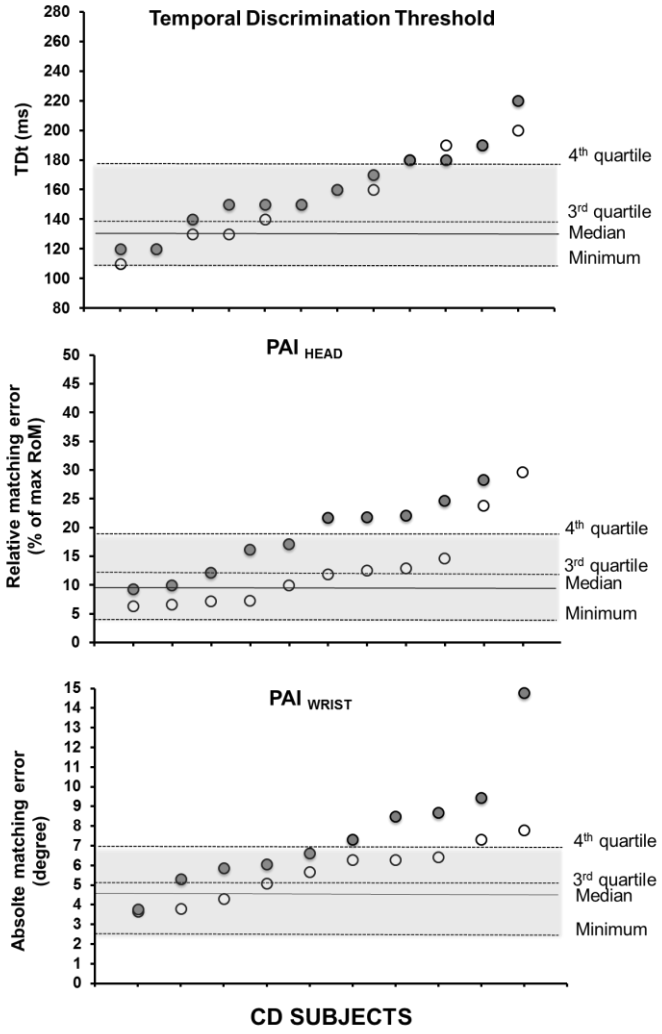

Figure 5. 5 Temporal discrimination threshold (A) and proprioceptive acuity index (PAI) for the head (B) and the wrist (C) of each participant. CD-T: cervical dystonia with tremor; CD-NT: cervical dystonia without tremor; HC: healthy controls. For each graph, data are sorted in ascending order. The shaded area represents respective range of the control group.

5.1.3.5 Correlation between tactile and proprioceptive acuity measures

We found no clear relationship between the tactile and proprioceptive acuity measures. The correlations between TDt values and the mean matching error for cervical ($r = 0.16$; $p = 0.28$) and wrist position-matching tasks ($r = 0.27$; $p= 0.10$) were not significant. In contrast, wrist and head proprioceptive acuity are related as evidenced by a positive significant correlation between the PAI for the head and the wrist ($r = 0.50$; $p= 0.002$).

5.1.3.6 Correlation between somatosensory deficits and clinical markers

No significant correlation was found (p always > 0.05) between TDt, the PAI of the head and wrist and disease severity, disease duration, tremor severity in both CD groups, suggesting that somatosensory deficits are independent of the severity and duration of motor symptoms.

5.1.4 *Discussion*

This is the first study that systematically examined tactile and proprioceptive function in patients with cervical dystonia manifesting or not tremor. The main findings of the present study are the following: first, tactile temporal discrimination thresholds were significantly higher in both CD groups compared to controls. Second, the joint position-matching errors, as a measure of proprioceptive acuity, were abnormal only in the CD group with tremor, both in the dystonic and non-dystonic body segments. That is, tactile abnormalities were a shared dysfunction of both CD phenotypes, while proprioceptive dysfunction was observed in CD patients with tremor. Third, we found no evidence that linked proprioceptive dysfunctions to clinical markers, such as severity scores and disease duration.

Our finding of increased tactile temporal discrimination thresholds in patients with CD is consistent with earlier works. Abnormal TDt has been described in unaffected first-degree relatives as well as in dystonic patients (Hutchinson *et al.*, 2014). A comprehensive model of the neural circuits involved in normal temporal discrimination suggests the basal ganglia as part of a network that integrates multimodal sensory information and selects salient events for on-line behaviour modulation through a dopamine-mediated alert system. Abnormal GABA-inhibitory activity within a cortico-subcortical network including basal ganglia, superior colliculus and primary somatosensory cortex are believed to be responsible for increased TDt (Conte *et al.*, 2017).

There is converging evidence that other structures likely involved in the dystonic network are not critical for this perceptual process. For example, theta-burst stimulation over primary somatosensory cortex induced changes in TDt in healthy subjects, whereas no

changes in TDt were observed after neuromodulation of lateral cerebellum and the dorsolateral prefrontal cortex (Conte *et al.*, 2012). We found elevated tactile discrimination thresholds in both CD subgroups with and without tremor (see Figure 5. 2), suggesting that tactile dysfunction is a universal feature of CD and the CD with tremor is not a differentiating phenotype in that respect.

We examined proprioceptive acuity through a position-matching test in both dystonic and non-dystonic body segments of CD patients. We found that the position matching error for both the head and the wrist can be high in CD. Previous works focusing on either dystonic or non-dystonic muscle systems had already shown that proprioceptive deficits in CD are expressed in dystonic and non-dystonic body segments. For example, a recent report already suggested that the head position matching error is increased in CD patients when compared to controls, with CD participants systematically overshooting the target position (De Pauw *et al.*, 2017) and that position sense of the non-dystonic index finger is abnormal in CD (Putzki *et al.*, 2006). Our data further show that deficits in proprioceptive acuity in different body segments correlate positively with each other indicating that a larger head position error tends to be associated with larger wrist position error. Noteworthy, botulinum toxin injections to the neck muscles have no systematic effect on improving head proprioception (De Pauw *et al.*, 2018).

The exact pathophysiological mechanism underlying abnormal proprioceptive acuity in focal dystonia is still not clear. However, it is known that the proprioceptive dysfunction is not due to structural abnormalities of peripheral muscle spindles (Swash & Fox, 1976). Moreover, the tonic vibration reflex (i.e., the electromyographic response evoked by muscle vibration) is normal in different forms of focal dystonia, while the perception of arm movement during the tonic vibration reflex is abnormal (Kaji *et al.*, 1995; Grunewald *et al.*, 1997). In addition, the perception for illusory movements when muscles of an immobilized arm are vibrated is abnormal in CD (Rome & Grünewald, 1999; Frima *et al.*, 2008). Therefore, abnormal perception for illusory movements while the tonic vibration reflex is preserved, suggests a central rather than a peripheral misprocessing of proprioceptive inputs in focal dystonia.

For the cervical joint position-matching task, another potential source of head position error could be abnormal information about head acceleration from the vestibular system. However, there is no empirical evidence suggesting that vestibular dysfunction contributes to the motor symptoms in CD. Vestibular-evoked myogenic potentials in both

the neck and extraocular muscles in patients with CD are not altered even after long disease or treatment durations (Rosengren *et al.*, 2010).

A main finding of our study is that CD patients with tremor exhibit a more severe dysfunction of the joint position sense. At a group level, only the CD with tremor subgroup showed significant differences in head and wrist position sense acuity when compared to controls and a significant difference emerged also between CD patients with and without tremor (see Figure 5. 3 and Figure 5. 4). This raises the question of the underlying neural dysfunction that may differentiate this subgroup from people who have CD but no tremor. Given our knowledge on central structures involved in proprioceptive processing and given what we know about the origin of tremor in CD, one can put forward the hypothesis that a dysfunction of the cerebellum may account for both the expression of tremor and of deficits in proprioception. We will review empirical evidence in favour of this hypothesis.

First, dystonic tremor very likely has a cerebellar component. For example, brain imaging data of people with laryngeal dystonia with or without voice tremor have a similarly increased activation in a network comprising the sensorimotor cortex, the inferior frontal and superior temporal gyri, putamen and ventral thalamus. However, those with voice tremor showed additional functional alterations in the cerebellum (lobule VIIa) and the medial frontal gyrus (Kirke *et al.*, 2017). Furthermore, a structural MRI study showed cerebellar abnormalities in 14% of all patients with predominant CD (Batla *et al.*, 2015). Out of these patients, 65% were affected by concomitant tremor. In addition, eye blink classical conditioning and motor adaption, both skills strongly dependent on cerebellar functional integrity, were found to be impaired in patients with CD and tremor, whereas they are normal in CD patients without tremor (Antelmi *et al.*, 2017; Avanzino *et al.*, 2018*b*). Second, genetic silencing of olivo-cerebellar projections in a new rodent model of dystonia led to abnormal firing of the deep cerebellar nuclei, as well as dystonic posturing and a high- frequency tremor (White & Sillitoe, 2017). Third, recent imaging data suggest that cerebellar dysplasia underlies developmental coordination disorder (Mariën *et al.*, 2010). While these children exhibit a range of motor problems ranging from balance instability to problems in handwriting, they also display increased joint position error variability in the same wrist-position matching task (Tseng *et al.*, 2018) that we applied in this study, underlining a cerebellar contribution in proprioception.

Indeed, cerebellar function has recently been reconsidered from a sensory point of view and a role of the cerebellum as "movement sensor" (Therrien & Bastian, 2019) in the "optimization of sensory data acquisition" (Proville *et al.*, 2014) has been suggested. Following this hypothesis, cerebellar effects on movement may be an indirect consequence of disrupting the sensory data on which motor behaviour depends (Bower, 1997). This prediction is also consistent with evidence that cerebellar patients have difficulty discriminating proprioceptive stimuli (Tinazzi *et al.*, 2013) and that a significant component of cerebellar ataxia results from the inability of patients to perceive environmental instabilities (Schlerf *et al.*, 2013).

All these data suggest a role of the cerebellum in dystonic tremor as well as in abnormal proprioceptive function. However, the presence of tremor cannot be regarded as the unique biomarker capable to differentiate between CD patients with or without altered proprioceptive function. Between 18% to 20% of the participants in the CD-NT group exhibited proprioceptive acuity index values that were above the maximum of controls, indicating that proprioceptive dysfunction is also observed in CD without tremor (see Figure 5. 5). Thus, based on our data one can conclude that the degree of proprioceptive dysfunction is more frequent and more pronounced in CD with tremor.

These findings also provide new insights into the pathophysiology of CD as they imply that focal dystonia and dystonic tremor arise from the interaction of two distinct networks both processing somatosensory afferent information for motor control. One network would involve the somatosensory cortex-basal ganglia-thalamo-cortical loop, while the second network comprises somatosensory and motor cortex, the cerebellum and its efferent projections (see Figure 5. 6). Noteworthy, the thalamus receives inputs from the spinal cord and from both the basal ganglia and the cerebellum in its sensory and motor nuclei respectively, acting as "drivers" and "modulators" of thalamo-cortical projections (Bosch-Bouju *et al.*, 2013). Thus, thalamic activity may play a role within both the two networks. In CD, one or both networks may give rise to two distinct abnormal neural processes: first, an abnormal gating mechanism involving the basal ganglia. The activity within direct and indirect pathways of the basal ganglia could be part of such gating mechanism that modulates upstream excitatory output at the motor cortex. Instability in this network would contribute to the onset of involuntary muscle spasms. A second pathophysiological mechanism relates to the abnormal processing of proprioceptive information in the cortico-cerebellar loop, in which altered or biased head position signals

may affect the feedback control of the head, ultimately leading to abnormal postures and oscillations (i.e. tremor) of the effector system. That is, the distinct motor symptoms (with and without tremor) and differences in somatosensory impairment (altered position sense or not) in CD could be understood as the manifestations of faulty processing within two distinct neural networks that ultimately converge on the same motor cortical target.

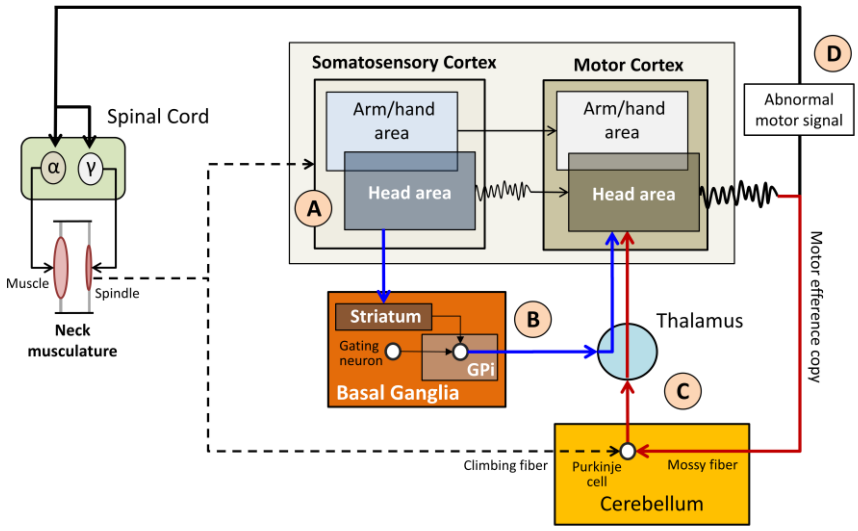

Figure 5. 6 Simplified diagram of the sensorimotor networks involved in cervical. (A) "Smeared" overlapping somatosensory representations of the arm/hand and head area provide imprecise, noisy feedback to the motor cortex. (B) The striatum receives afferents from somatosensory cortex. An impaired gating mechanism leads to unstable inhibitory output via Globus Pallidus Externus that affects excitatory output of motor cortex. (C). Abnormal motor cortical signals affect α motorneurons, but also γ motorneurons, which up-regulate spindle sensitivity. This, in turn, leads to abnormal proprioceptive feedback to the somatosensory cortex and the cerebellum. The cerebellum modulates muscle tone based on altered propriospinal feedback, which further impacts volitional motor control. (D) The converging inputs from somatosensory cortex, the cortico-basal ganglia and the cortico-cerebellar loop all modulate motor cortex and lead to abnormal feedback and feed-forward control of the head.

Several limitations of the study deserve attention. First, we lacked a quantitative assessment of head tremor, which would provide data of the extent and variability of tremor in both groups (CD-T and CD-NT). Second, both the wrist/head position-matching tests require participants to match a remembered position and, thus, rely on working memory. However, there is no conclusive evidence that working memory is affected in CD (Romano *et al.*, 2014) and no evidence supports the hypothesis that working memory can differentiate between CD with and without tremor. Finally, we did not record flexion/extension movements in the sagittal plane, because our CD patients

presented with latero- or torticollis, which are the most two common forms of cervical dystonia. Based on our current knowledge, one would expect to observe proprioceptive deficits for this joint degree of freedom albeit likely to a lesser degree.

Our findings suggest that pathophysiology in CD patients is characterized by two abnormal neural processes: first, an abnormal gating mechanism that could contribute to triggering involuntary muscle spasms and second, an abnormal processing of proprioceptive information that may also affect the feedback control of head postures. The proprioceptive deficit is most expressed in CD with tremor. Our findings can translated into clinical practice as they inform the design and implementation of invasive and non-invasive neuromodulation protocols for patients with CD (Pelosin *et al.*, 2013; Avanzino *et al.*, 2018*a*). At present, rehabilitation protocols and neuromodulation treatments have been scarcely effective in treating dystonic symptoms (Prudente *et al.*, 2018; van den Dool *et al.*, 2019), possibly because the pathophysiological mechanism underlying the different phenotypes of CD are not routinely addressed in individual patients.

This work has been published on Neurology (Avanzino *et al.*, 2020).

Conclusions

The case of cervical dystonia, described in Chapter 5, is a clear example of how important assessment is: possibly adequate treatments are missing because the physiological and pathological mechanisms underlying sensorimotor control are not routinely addressed in clinical practice. This study showed how sensory function is crucial but in the future it would be useful to investigate the effect of a sensory training (Ostry & Gribble, 2016; Cuppone *et al.*, 2016, 2018) on this neurological condition.

The relevance of proprioception in motor control and learning is evident also in healthy humans. In Chapter 3 we showed that stiffness control is associated with worse robustness and learning. This kind of behavior can be attributed to sensitiveness while moving or co-activating: proprioception becomes markedly less sensitive during co-activation across joints and passive spindles are more sensitive to movements than when fusimotor neurons are contracting (Wise *et al.*, 1999; Loram *et al.*, 2009*b*; Proske & Gandevia, 2012). However, using the "good strategy", i.e. force accuracy control, the combination of higher reliance on proprioception with "disturbance training" is able to lead to a better learning and better robustness. This is in line with recent findings showing that variability may facilitate learning and thus sensorimotor recovery (Ranganathan & Newell, 2013; Wu *et al.*, 2014). These are results to exploit in sensorimotor neurorehabilitation, designing robotic rehabilitation protocols that introduce variability in the task during the training phase.

Asking participants to use the force accuracy strategy, we found that control is non-linear and we associated this non-linearity with intermittent control (3.3). It is an intriguing issue, to be addressed in future studies, to consider how learning affects intermittency. Chapter 4 provides one possible starting point approximating complex tasks or task sequences in real life and evaluating how two control paradigms, i.e. feedforward anticipation and intermittent feedback stabilization, may need to be integrated and coordinated by the brain.

In a neurorehabilitation perspective, we started recruiting subjects with Parkinson's disease for the study about intermittency in postural control (3.3) because degeneration of the basal ganglia's dopaminergic pathway causes Parkinson's disease, and abnormal refractoriness has been shown in Parkinson's disease patients (off dopaminergic medication) when compared to healthy controls (Harrison *et al.*, 1995; Samii *et al.*, 2004). It has been hypothesised that functional deficits in Parkinson's disease, including, freezing and postural rigidity, are related to deficits in the intermittent control process fundamental to human motor control (Harrison *et al.*, 1995). Because Parkinson's disease patients have only been tested in simple, discrete, reaction time tasks we do not know whether or not intermittent control abnormalities in Parkinson's disease patients generalize to the control of sustained movements like human balance. Gaining knowledge about abnormal refractoriness in Parkinson's disease (and other neurological conditions) may provide insight into the mechanistic properties of the proposed neural substrates of the intermittent control and open a new pathway for rehabilitation.

Restoration of function related to sensorimotor integration requires reeducation of the central processes of perception and selection which drive motor control. The approach that can exploit the results of this thesis is the computational neurorehabilitation. In fact it consists of mathematically modeling the mechanisms underlying the rehabilitation process, with the aim of understanding the biological details of recovery and of optimizing the individual treatment of patients. Each model is characterized by three features: (i) it uses, as an input, a quantitative description of the sensorimotor activity obtained by simulations or by the interaction with robots; (ii) it is based on the description of computational mechanisms of activity-dependent plasticity; and (iii) it produces, as an output, quantitative values of functional outcomes.

Integrating models of sensorimotor control during robotic neurorehabilitation, might lead to robots that are fully adaptable to the level of impairment of the patient and able to change their behavior accordingly to the patient's intention.

This is one of the goals for the development of Wristbot, our robot for wrist rehabilitation. During these three years I contributed in the advancements of the device with the idea to maximize its effects combining it with proper assessment and training protocols, based on motor control paradigms. The dream is to make it available for the highest possible number of patients, launching it into the market in the near future.

References

Allum JH., Bloem B., Carpenter M. & Honegger F (2001). Differential diagnosis of proprioceptive and vestibular deficits using dynamic support-surface posturography. *Gait Posture* **14,** 217–226.

Alvarez-Otero R & Perez-Fernandez N (2017). The limits of stability in patients with unilateral vestibulopathy. *Acta Otolaryngol* **137,** 1051–1056.

Antelmi E, Erro R, Rocchi L, Liguori R, Tinazzi M, Di Stasio F, Berardelli A, Rothwell JC & Bhatia KP (2017). Neurophysiological correlates of abnormal somatosensory temporal discrimination in dystonia. *Mov Disord* **32,** 141–148.

Aramaki Y, Nozaki D, Masani K, Sato T, Nakazawa K & Yano H (2001). Reciprocal angular acceleration of the ankle and hip joints during quiet standing in humans. *Exp Brain Res* **136,** 463–473.

Arsan T, Gawthrop PJ & Ronco E (1999). Open-loop intermittent feedback control: Practical continuous-time GPC. *IEE Proc - Control Theory Appl* **146,** 426–434.

Aruin AS & Latash ML (1995). The role of motor action in anticipatory postural adjustments studied with self-induced and externally triggered perturbations. *Exp brain Res* **106,** 291–300.

Asai Y, Tasaka Y, Nomura K, Nomura T, Casadio M & Morasso P (2009). A model of postural control in quiet standing: Robust compensation of delay-induced instability using intermittent activation of feedback control. *PLoS One* **4,** e6169.

Asai Y, Tateyama S & Nomura T (2013). Learning an Intermittent Control Strategy for Postural Balancing Using an EMG-Based Human-Computer Interface ed. Balasubramaniam R. *PLoS One* **8,** e62956.

van Asseldonk EHF, Buurke JH, Bloem BR, Renzenbrink GJ, Nene A V., van der Helm FCT & van der Kooij H (2006). Disentangling the contribution of the paretic and non-paretic ankle to balance control in stroke patients. *Exp Neurol* **201,** 441–451.

Avanzino L (2012). How does the cerebellum contribute to the pathophysiology of dystonia? *Basal Ganglia* **2,** 231–235.

Avanzino L+, Cherif A+, Crisafulli O, Carbone F, Zenzeri J, Morasso P, Abbruzzese G,

Pelosin E & Konczak J (2020). Tactile and proprioceptive dysfunction differentiates cervical dystonia with and without tremor. *Neurology*; DOI: 10.1212/WNL.0000000000008916.

Avanzino L, Fiorio M & Conte A (2018*a*). Actual and Illusory Perception in Parkinson's Disease and Dystonia: A Narrative Review. *Front Neurol* **9,** 584.

Avanzino L, Ravaschio A, Lagravinese G, Bonassi G, Abbruzzese G & Pelosin E (2018*b*). Adaptation of feedforward movement control is abnormal in patients with cervical dystonia and tremor. *Clin Neurophysiol* **129,** 319–326.

Avanzino L, Tinazzi M & Fiorio M (2015). Sensory-motor integration in focal dystonia. *Neuropsychologia* **79,** 288–300.

Avila Mireles EJ, Zenzeri J, Squeri V, Morasso P & De Santis D (2017). Skill learning and skill transfer mediated by cooperative haptic interaction. *IEEE Trans Neural Syst Rehabil Eng*; DOI: 10.1109/TNSRE.2017.2700839.

Bakker M, Allum JHJ, Visser JE, Grüneberg C, van de Warrenburg BP, Kremer BHP & Bloem BR (2006). Postural responses to multidirectional stance perturbations in cerebellar ataxia. *Exp Neurol* **202,** 21–35.

Baloh RW, Jacobson KM, Beykirch K & Honrubia V (1998). Static and Dynamic Posturography in Patients With Vestibular and Cerebellar Lesions. *Arch Neurol* **55,** 649.

Bara-Jimenez W, Catalan MJ, Hallett M & Gerloff C (1998). Abnormal somatosensory homunculus in dystonia of the hand. *Ann Neurol* **44,** 828–831.

Batla A, Sánchez MC, Erro R, Ganos C, Stamelou M, Balint B, Brugger F, Antelmi E & Bhatia KP (2015). The role of cerebellum in patients with late onset cervical/segmental dystonia?–Evidence from the clinic. *Parkinsonism Relat Disord* **21,** 1317–1322.

Bays PM & Wolpert DM (2007). Computational principles of sensorimotor control that minimize uncertainty and variability. *J Physiol* **578,** 387–396.

Belen'kiĭ VE, Gurfinkel' VS & Pal'tsev EI (1967). Control elements of voluntary movements. *Biofizika* **12,** 135–141.

Benjuya N, Melzer I & Kaplanski J (2004). Aging-Induced Shifts From a Reliance on Sensory Input to Muscle Cocontraction During Balanced Standing. *Journals Gerontol Ser A Biol Sci Med Sci* **59,** M166–M171.

Berniker M & Kording K (2011). Bayesian approaches to sensory integration for motor

control. *Wiley Interdiscip Rev Cogn Sci* **2,** 419–428.

Bernstein N (1966). *The co-ordination and regulation of movements*. Pergamon Press.

Bernstein N (1996). *Dexterity and Its Development*. M. L. Latash & M. T. Turvey (Eds.).

De Beyl DZ & Salvia P (2009). Neck movement speed in cervical dystonia. *Mov Disord* **24,** 2267–2271.

Bittar RSM, Santos MD & Mezzalira R (2016). Glucose metabolism disorders and vestibular manifestations: evaluation through computerized dynamic posturography. *Braz J Otorhinolaryngol* **82,** 372–376.

Bizzi E, Accornero N, Chapple W & Hogan N (1982). Arm trajectory formation in monkeys. *Exp Brain Res* **46,** 139–143.

Black FO, Shupert CL, Horak FB & Nashner LM (1988). Chapter 23 Abnormal postural control associated with peripheral vestibular disorders. *Prog Brain Res* **76,** 263–275.

Błaszczyk JW, Orawiec R, Duda-Kłodowska D & Opala G (2007). Assessment of postural instability in patients with Parkinson's disease. *Exp Brain Res* **183,** 107–114.

Bosch-Bouju C, Hyland BI & Parr-Brownlie LC (2013). Motor thalamus integration of cortical, cerebellar and basal ganglia information: implications for normal and parkinsonian conditions. *Front Comput Neurosci* **7,** 163.

Bottaro A, Casadio M, Morasso PG & Sanguineti V (2005). Body sway during quiet standing: Is it the residual chattering of an intermittent stabilization process? *Hum Mov Sci* **24,** 588–615.

Bottaro A, Yasutake Y, Nomura T, Casadio M & Morasso P (2008). Bounded stability of the quiet standing posture: An intermittent control model. *Hum Mov Sci* **27,** 473–495.

Bower JM (1997). Control of Sensory Data Acquisition. *Int Rev Neurobiol* **41,** 489–513.

Broeks JG, Lankhorst GJ, Rumping K & Prevo AJ (1999). The long-term outcome of arm function after stroke: results of a follow-up study. *Disabil Rehabil* **21,** 357–364.

Burdet E & Milner TE (1998). Quantization of human motions and learning of accurate movements. *Biol Cybern* **78,** 307–318.

Burdet E, Osu R, Franklin DW, Milner TE & Kawato M (2001). The central nervous system stabilizes unstable dynamics by learning optimal impedance. *Nature* **414,** 446–449.

Buster TW, Chernyavskiy P, Harms NR, Kaste EG & Burnfield JM (2016).

Computerized dynamic posturography detects balance deficits in individuals with a history of chronic severe traumatic brain injury. *Brain Inj* **30,** 1249–1255.

Butler RJ, Crowell HP & Davis IMC (2003). Lower extremity stiffness: Implications for performance and injury. *Clin Biomech* **18,** 511–517.

Bye RT & Neilson PD (2008). The BUMP model of response planning: Variable horizon predictive control accounts for the speed–accuracy tradeoffs and velocity profiles of aimed movement. *Hum Mov Sci* **27,** 771–798.

Cabrera JL & Milton JG (2002). On-off intermittency in a human balancing task. *Phys Rev Lett* **89,** 158702.

Campbell SA (2007). Time Delays in Neural Systems. In, pp. 65–90. Springer, Berlin, Heidelberg.

Cappello L, Elangovan N, Contu S, Khosravani S, Konczak J & Masia L (2015). Robot-aided assessment of wrist proprioception. *Front Hum Neurosci* **9,** 198.

Carpenter MG, Murnaghan CD & Inglis JT (2010). Shifting the balance: Evidence of an exploratory role for postural sway. *Neuroscience* **171,** 196–204.

Casadio M, Morasso PG & Sanguineti V (2005). Direct measurement of ankle stiffness during quiet standing: Implications for control modelling and clinical application. *Gait Posture* **21,** 410–424.

Cherif A, Loram I & Zenzeri J (2019). Effect of motor and sensory noise in the control of upright standing. In *Progress in Brain Research*, pp. 319–327. Elsevier B.V.

Chong RKY, Horak FB, Frank J & Kaye J (1999). Sensory Organization for Balance: Specific Deficits in Alzheimer's but not in Parkinson's Disease. *Journals Gerontol Ser A Biol Sci Med Sci* **54,** M122–M128.

Le Clair K & Riach C (1996). Postural stability measures: what to measure and for how long. *Clin Biomech* **11,** 176–178.

Clapp S & Wing AM (1999). Light touch contribution to balance in normal bipedal stance. *Exp Brain Res* **125,** 521–524.

Coderre AM, Amr Abou Zeid AA, Dukelow SP, Demmer MJ, Moore KD, Demers MJ, Bretzke H, Herter TM, Glasgow JI, Norman KE, Bagg SD & Scott SH (2010). Assessment of Upper-Limb Sensorimotor Function of Subacute Stroke Patients Using Visually Guided Reaching. *Neurorehabil Neural Repair* **24,** 528–541.

Collins JJ & De Luca CJ (1993). Open-loop and closed-loop control of posture: A random-walk analysis of center-of-pressure trajectories. *Exp Brain Res* **95,** 308–318.

Consky E, Basinski A, Belle L, Ranawaya R & Lang A (1990). The Toronto Western Spasmodic Torticollis Rating Scale (TWSTRS): assessment of validity and inter-rater reliability. *Neurology* **40,** 445.

Conte A, McGovern EM, Narasimham S, Beck R, Killian O, O'Riordan S, Reilly RB & Hutchinson M (2017). Temporal Discrimination: Mechanisms and Relevance to Adult-Onset Dystonia. *Front Neurol* **8,** 625.

Conte A, Rocchi L, Nardella A, Dispenza S, Scontrini A, Khan N & Berardelli A (2012). Theta-Burst Stimulation-Induced Plasticity over Primary Somatosensory Cortex Changes Somatosensory Temporal Discrimination in Healthy Humans. *PLoS One* **7,** e32979.

Craik KJW (1947). Theory of the human operator in control systems. I. the operator as an engineering system. *Br J Psychol* **38,** 56–61.

Creath R, Kiemel T, Horak F, Peterka R & Jeka J (2005). A unified view of quiet and perturbed stance: simultaneous co-existing excitable modes. *Neurosci Lett* **377,** 75–80.

Cuppone AV, Semprini M & Konczak J (2018). Consolidation of human somatosensory memory during motor learning. *Behav Brain Res* **347,** 184–192.

Cuppone AV, Squeri V, Semprini M, Masia L & Konczak J (2016). Robot-assisted proprioceptive training with added vibro-tactile feedback enhances somatosensory and motor performance. *PLoS One* **11,** e0164511.

Defazio G, Conte A, Gigante AF, Fabbrini G & Berardelli A (2015). Is tremor in dystonia a phenotypic feature of dystonia? *Neurology* **84,** 1053–1059.

Deuschl G, Bain P & Brin M (2008). Consensus Statement of the Movement Disorder Society on Tremor. *Mov Disord* **13,** 2–23.

Diener H., Dichgans J, Bacher M & Gompf B (1984). Quantification of postural sway in normals and patients with cerebellar diseases. *Electroencephalogr Clin Neurophysiol* **57,** 134–142.

van den Dool J, Visser B, Koelman JH, Engelbert RH & Tijssen MA (2019). Long-Term Specialized Physical Therapy in Cervical Dystonia: Outcomes of a Randomized Controlled Trial. *Arch Phys Med Rehabil*; DOI: 10.1016/J.APMR.2019.01.013.

Emken JL, Benitez R, Sideris A, Bobrow JE & Reinkensmeyer DJ (2007). Motor Adaptation as a Greedy Optimization of Error and Effort. *J Neurophysiol* **97,** 3997–4006.

Fahn S, Tolosa E & Marin C (1988). Parkinson's Disease and Movement Disorders: Clinical Rating scale for Tremor. *Park Dis Mov Disord*225–234.

Faisal AA, Selen LPJ & Wolpert DM (2008). Noise in the nervous system. *Nat Rev Neurosci* **9,** 292–303.

Feldman AG (1966). Functional tuning of the nervous system during control of movement or maintenance of a steady posture. *Biophysics (Oxf)* **11,** 766–775.

Feldman AG & Levin MF (1995). The origin and use of positional frames of reference in motor control. *Behav Brain Sci* **18,** 723.

Fetsch CR, Turner AH, DeAngelis GC & Angelaki DE (2009). Dynamic Reweighting of Visual and Vestibular Cues during Self-Motion Perception. *J Neurosci* **29,** 15601–15612.

Finley JM, Bastian AJ & Gottschall JS (2013). Learning to be economical: the energy cost of walking tracks motor adaptation. *J Physiol* **591,** 1081–1095.

Fletcher JR, Pfister TR & MacIntosh BR (2013). Energy cost of running and Achilles tendon stiffness in man and woman trained runners. *Physiol Rep* **1,** e00178.

Frank MJ (2006). Hold your horses: A dynamic computational role for the subthalamic nucleus in decision making. *Neural Networks* **19,** 1120–1136.

Frank MJ (2011). Computational models of motivated action selection in corticostriatal circuits. *Curr Opin Neurobiol* **21,** 381–386.

Frima N, Nasir J & Grünewald RA (2008). Abnormal vibration-induced illusion of movement in idiopathic focal dystonia: An endophenotypic marker? *Mov Disord* **23,** 373–377.

Gage WH, Winter DA, Frank JS & Adkin AL (2004). Kinematic and kinetic validity of the inverted pendulum model in quiet standing. *Gait Posture* **19,** 124–132.

Gandelman-Marton R, Arlazoroff A & Dvir Z (2016). Postural stability in patients with different types of head and neck trauma in comparison to healthy subjects. *Brain Inj* **30,** 1612–1616.

Gatev P, Thomas S, Kepple T & Hallett M (1999). Feedforward ankle strategy of balance during quiet stance in adults. *J Physiol* **514,** 915–928.

Gawthrop P, Gollee H & Loram I (2014*a*). Intermittent Control in Man and Machine. *arXiv Prepr arXiv14073543*.

Gawthrop P, Loram I, Gollee H & Lakie M (2014*b*). Intermittent control models of human standing: Similarities and differences. *Biol Cybern* **108,** 159–168.

Gawthrop P, Loram I, Lakie M & Gollee H (2011). Intermittent control: A computational theory of human control. *Biol Cybern* **104,** 31–51.

Gawthrop PJ & Wang L (2007). Intermittent model predictive control. *Proc Inst Mech Eng Part I J Syst Control Eng* **221,** 1007–1018.

Gawthrop PJ & Wang L (2009). Event-driven intermittent control. *Int J Control* **82,** 2235–2248.

Ghai S, Ghai I & Effenberg AO (2017). Effects of dual tasks and dual-task training on postural stability: a systematic review and meta-analysis. *Clin Interv Aging* **12,** 557–577.

Di Giulio I, Baltzopoulos V, Maganaris CN & Loram ID (2013). Human standing: does the control strategy preprogram a rigid knee? *J Appl Physiol* **114,** 1717–1729.

Grunewald R, Yoneda Y, Shipman JM & Sagar HJ (1997). Idiopathic focal dystonia: a disorder of muscle spindle afferent processing? *Brain* **120,** 2179–2185.

Hardwick RM, Rottschy C, Miall RC & Eickhoff SB (2013). A quantitative meta-analysis and review of motor learning in the human brain. *Neuroimage* **67,** 283–297.

Harrison J, Henderson L & Kennard C (1995). Abnormal refractoriness in patients with Parkinson's disease after brief withdrawal of levodopa treatment. *J Neurol Neurosurg Psychiatry* **59,** 499–506.

Hatem SM, Saussez G, Della Faille M, Prist V, Zhang X, Dispa D & Bleyenheuft Y (2016). Rehabilitation of Motor Function after Stroke: A Multiple Systematic Review Focused on Techniques to Stimulate Upper Extremity Recovery. *Front Hum Neurosci* **10,** 442.

Hebb DO (1962). *The organization of behavior: a neuropsychological theory*, Science Ed.

Hebert JR & Manago MM (2017). Reliability and Validity of the Computerized Dynamic Posturography Sensory Organization Test in People with Multiple Sclerosis. *Int J MS Care* **19,** 151–157.

Hermens HJ, Freriks B, Merletti R, Stegeman D, Blok J, Rau G, Disselhorst-Klug C & Hägg G (1999). European Recommendations for Surface ElectroMyoGraphy. *Roessingh Res Dev*8–11.

Hikosaka O, Nakamura K, Sakai K & Nakahara H (2002). Central mechanisms of motor skill learning. *Curr Opin Neurobiol* **12,** 217–222.

Hogan N (1984). Adaptive Control of Mechanical Impedance by Coactivation of

Antagonist Muscles. *IEEE Trans Automat Contr* **29,** 681–690.

Horak FB & Nashner LM (1986). Central programming of postural movements: adaptation to altered support-surface configurations. *J Neurophysiol* **55,** 1369–1381.

Horak FB, Nashner LM & Diener HC (1990). Postural strategies associated with somatosensory and vestibular loss. *Exp Brain Res* **82,** 167–177.

Huisinga J, Mancini M, Veys C, Spain R & Horak F (2018). Coherence analysis of trunk and leg acceleration reveals altered postural sway strategy during standing in persons with multiple sclerosis. *Hum Mov Sci* **58,** 330–336.

Hutchinson M, Isa T, Molloy A, Kimmich O, Williams L, Molloy F, Moore H, Healy DG, Lynch T, Walsh C, Butler J, Reilly RB, Walsh R & O'Riordan S (2014). Cervical Dystonia: A Disorder of the Midbrain Network for Covert Attentional Orienting. *Front Neurol* **5,** 54.

Iandolo R, Marini F, Semprini M, Laffranchi M, Mugnosso M, Cherif A, De Michieli L, Chiappalone M, Zenzeri J, Iandolo R, Marini F, Semprini M, Laffranchi M, Mugnosso M, Cherif A, De Michieli L, Chiappalone M & Zenzeri J (2019). Perspectives and Challenges in Robotic Neurorehabilitation. *Appl Sci* **9,** 3183.

Inoue Y & Sakaguchi Y (2014). Periodic change in phase relationship between target and hand motion during visuo-manual tracking task: Behavioral evidence for intermittent control. *Hum Mov Sci* **33,** 211–226.

Insperger T & Milton J (2014). Sensory uncertainty and stick balancing at the fingertip. *Biol Cybern* **108,** 85–101.

Insperger T, Milton J & Stépán G (2013). Acceleration feedback improves balancing against reflex delay. *J R Soc Interface* **10,** 20120763.

Insperger T & Stepan G (2010). On the dimension reduction of systems with feedback delay by act-and-wait control. *IMA J Math Control Inf* **27,** 457–473.

Inzelberg R, Flash T, Schechtman E & Korczyn AD (1995). Kinematic properties of upper limb trajectories in idiopathic torsion dystonia. *J Neurol Neurosurg Psychiatry* **58,** 312–319.

Jacono M, Casadio M, Morasso PG & Sanguineti V (2004). The sway-density curve and the underlying postural stabilization process. *Motor Control* **8,** 292–311.

Jeka JJ & Lackner JR (1994). Fingertip contact influences human postural control. *Exp brain Res* **100,** 495–502.

Jordan MI (1996). Chapter 2 Computational aspects of motor control and motor learning.

Handb Percept Action **2,** 71–120.

Kaji R, Rothwell JC, Katayama M, Ikeda T, Kubori T, Kohara N, Mezaki T, Shibasaki H & Kimura J (1995). Tonic vibration reflex and muscle afferent block in writer's cramp. *Ann Neurol* **38,** 155–162.

van de Kamp C, Gawthrop PJ, Gollee H, Lakie M & Loram ID (2013*a*). Interfacing sensory input with motor output: does the control architecture converge to a serial process along a single channel? *Front Comput Neurosci* **7,** 55.

van de Kamp C, Gawthrop PJ, Gollee H & Loram ID (2013*b*). Refractoriness in Sustained Visuo-Manual Control: Is the Refractory Duration Intrinsic or Does It Depend on External System Properties? *PLoS Comput Biol* **9,** e1002843.

Kandel ER, Schwartz JH & Jessell TM (2000). *Principles of neural science*. McGraw-Hill, Health Professions Division.

Kato T, Yamamoto S, Miyoshi T, Nakazawa K, Masani K & Nozaki D (2014). Anti-phase action between the angular accelerations of trunk and leg is reduced in the elderly. *Gait Posture* **40,** 107–112.

Kelly AMC & Garavan H (2005). Human functional neuroimaging of brain changes associated with practice. *Cereb Cortex* **15,** 1089–1102.

Kiemel T, Oie KS & Jeka JJ (2002). Multisensory fusion and the stochastic structure of postural sway. *Biol Cybern* **87,** 262–277.

Kirke DN, Battistella G, Kumar V, Rubien-Thomas E, Choy M, Rumbach A & Simonyan K (2017). Neural correlates of dystonic tremor: a multimodal study of voice tremor in spasmodic dysphonia. *Brain Imaging Behav* **11,** 166–175.

Kiss R, Brueckner D & Muehlbauer T (2018). Effects of Single Compared to Dual Task Practice on Learning a Dynamic Balance Task in Young Adults. *Front Psychol* **9,** 311.

Kok P, Brouwer GJ, van Gerven MAJ & de Lange FP (2013). Prior Expectations Bias Sensory Representations in Visual Cortex. *J Neurosci* **33,** 16275–16284.

Konczak J, Sciutti A, Avanzino L, Squeri V, Gori M, Masia L, Abbruzzese G & Sandini G (2012). Parkinson's disease accelerates age-related decline in haptic perception by altering somatosensory integration. *Brain* **135,** 3371–3379.

van der Kooij H, Jacobs R, Koopman B & van der Helm F (2001). An adaptive model of sensory integration in a dynamic environment applied to human stance control. *Biol Cybern* **84,** 103–115.

van der Kooij H & de Vlugt E (2007). Postural Responses Evoked by Platform Pertubations Are Dominated by Continuous Feedback. *J Neurophysiol* **98,** 730–743.

Körding KP & Wolpert DM (2006). Probabilistic mechanisms in sensorimotor control. *Novartis Found Symp* **270,** 191–198; discussion 198-202, 232–237.

Kuo AD & Zajac FE (1993). Human standing posture: multi-joint movement strategies based on biomechanical constraints. *Prog Brain Res* **97,** 349–358.

Lang CE & Beebe JA (2007). Relating Movement Control at 9 Upper Extremity Segments to Loss of Hand Function in People with Chronic Hemiparesis. *Neurorehabil Neural Repair* **21,** 279–291.

Lang CE, Bland MD, Bailey RR, Schaefer SY & Birkenmeier RL (2013). Assessment of upper extremity impairment, function, and activity after stroke: foundations for clinical decision making. *J Hand Ther* **26,** 104–115.

Lashley KS (1930). Basic neural mechanisms in behavior. *Psychol Rev* **37,** 1–24.

Lee Y-W, Lee H, Chung I-S & Yi H-A (2017). Relationship between postural instability and subcortical volume loss in Alzheimer's disease. *Medicine (Baltimore)* **96,** e7286.

Li C-SR, Padoa-Schioppa C & Bizzi E (2001). Neuronal Correlates of Motor Performance and Motor Learning in the Primary Motor Cortex of Monkeys Adapting to an External Force Field. *Neuron* **30,** 593–607.

Liu LY, Li Y & Lamontagne A (2018). The effects of error-augmentation versus error-reduction paradigms in robotic therapy to enhance upper extremity performance and recovery post-stroke: a systematic review. *J Neuroeng Rehabil* **15,** 65.

Loram I (2015). Postural control and sensorimotor integration. *Grieve's Mod Musculoskelet Physiother*.

Loram I, Cunningham R, Zenzeri J & Gollee H (2016). Intermittent control of unstable multivariate systems with uncertain system parameters. In *2016 38th Annual International Conference of the IEEE Engineering in Medicine and Biology Society (EMBC)*, pp. 17–20. IEEE.

Loram ID, Gollee H, Lakie M & Gawthrop PJ (2011). Human control of an inverted pendulum: Is continuous control necessary? Is intermittent control effective? Is intermittent control physiological? *J Physiol* **5892,** 307–324.

Loram ID, van de Kamp C, Gollee H & Gawthrop PJ (2012). Identification of intermittent control in man and machine. *J R Soc Interface* **9,** 2070–2084.

Loram ID, Kelly SM & Lakie M (2001). Human balancing of an inverted pendulum: Is sway size controlled by ankle impedance? *J Physiol* **532,** 879–891.

Loram ID & Lakie M (2002*a*). Direct measurement of human ankle stiffness during quiet standing: the intrinsic mechanical stiffness is insufficient for stability. *J Physiol* **545,** 1041–1053.

Loram ID & Lakie M (2002*b*). Human balancing of an inverted pendulum: position control by small, ballistic-like, throw and catch movements. *J Physiol* **540,** 1111–1124.

Loram ID, Lakie M & Gawthrop PJ (2009*a*). Visual control of stable and unstable loads: what is the feedback delay and extent of linear time-invariant control? *J Physiol* **587,** 1343–1365.

Loram ID, Lakie M, Di Giulio I & Maganaris CN (2009*b*). The Consequences of Short-Range Stiffness and Fluctuating Muscle Activity for Proprioception of Postural Joint Rotations: The Relevance to Human Standing. *J Neurophysiol* **102,** 460–474.

Luck SJ (1998). Sources of Dual-Task Interference: Evidence From Human Electrophysiology. *Psychol Sci* **9,** 223–227.

Maggioni S, Melendez-Calderon A, van Asseldonk E, Klamroth-Marganska V, Lünenburger L, Riener R & van der Kooij H (2016). Robot-aided assessment of lower extremity functions: a review. *J Neuroeng Rehabil* **13,** 72.

Malina RM, Bouchard C & Bar-Or O (2004). *Growth, maturation, and physical activity*. Human Kinetics.

Mariën P, Wackenier P, De Surgeloose D, De Deyn PP & Verhoeven J (2010). Developmental Coordination Disorder: Disruption of the Cerebello-Cerebral Network evidenced by SPECT. *The Cerebellum* **9,** 405–410.

Marini F, Ferrantino M & Zenzeri J (2018). Proprioceptive identification of joint position versus kinaesthetic movement reproduction. *Hum Mov Sci* **62,** 1–13.

Marini F, Squeri V, Morasso P, Konczak J & Masia L (2016). Robot-aided mapping of wrist proprioceptive acuity across a 3D workspace. *PLoS One* **11,** 1–12.

Marsden CD, Merton PA, Morton HB, Rothwell JC & Traub MM (1981). Reliability and efficacy of the long-latency stretch reflex in the human thumb. *J Physiol* **316,** 47–60.

Masani K (2003). Importance of Body Sway Velocity Information in Controlling Ankle Extensor Activities During Quiet Stance. *J Neurophysiol* **90,** 3774–3782.

Massion J (1992). Movement, posture and equilibrium: interaction and coordination.

Prog Neurobiol **38,** 35–56.

Matheson IBC & Lee J (1970). Reaction of chemical acceptors with singlet oxygen produced by direct laser excitation. *Chem Phys Lett* **7,** 475–476.

Matthews PBC (1959). The dependence of tension upon extension in the stretch reflex of the soleus muscle of the decerebrate cat. *J Physiol* **147,** 521–546.

Maurer C (2004). A New Interpretation of Spontaneous Sway Measures Based on a Simple Model of Human Postural Control. *J Neurophysiol* **93,** 189–200.

Mergner T, Maurer C & Peterka RJ (2002). Sensory contributions to the control of stance: a posture control model. *Adv Exp Med Biol* **508,** 147–152.

Merton PA (1953). Speculations on the Servo-Control of Movement. In, pp. 247–260. John Wiley & Sons, Ltd.

Milner T & Cloutier C (1993). Compensation for mechanically unstable loading in voluntary wrist movement. *Exp Brain Res* **94,** 522–532.

Milton J, Meyer R, Zhvanetsky M, Ridge S & Insperger T (2016). Control at stability's edge minimizes energetic costs: Expert stick balancing. *J R Soc Interface*; DOI: 10.1098/rsif.2016.0212.

Milton J, Townsend JL, King MA & Ohira T (2009). Balancing with positive feedback: The case for discontinuous control. *Philos Trans R Soc A Math Phys Eng Sci* **367,** 1181–1193.

Mok NW, Brauer SG & Hodges PW (2004). Hip strategy for balance control in quiet standing is reduced in people with low back pain. *Spine (Phila Pa 1976)* **29,** E107-12.

Morasso P, Casadio M, Mohan V, Rea F & Zenzeri J (2015). Revisiting the Body-Schema Concept in the Context of Whole-Body Postural-Focal Dynamics. *Front Hum Neurosci* **9,** 83.

Morasso P, Casadio M, De Santis D, Nomura T, Rea F & Zenzeri J (2014). Stabilization strategies for unstable dynamics. *J Electromyogr Kinesiol* **24,** 803–814.

Morasso P, Cherif A & Zenzeri J (2019). Quiet standing: The single inverted pendulum model is not so bad after all. *PLoS One* **14,** e0213870.

Morasso PG & Sanguineti V (2002). Ankle Muscle Stiffness Alone Cannot Stabilize Balance During Quiet Standing. *J Neurophysiol* **88,** 2157–2162.

Morasso PG & Schieppati M (1999). Can Muscle Stiffness Alone Stabilize Upright Standing ? *J Neurophysiol* **82,** 1622–1626.

Di Nardo W, Ghirlanda G, Cercone S, Pitocco D, Soponara C, Cosenza A, Paludetti G, Di Leo MA. & Galli I (1999). The Use of Dynamic Posturography to Detect Neurosensorial Disorder in IDDM Without Clinical Neuropathy. *J Diabetes Complications* **13,** 79–85.

Nashner LM & McCollum G (1985). The organization of human postural movements: A formal basis and experimental synthesis. *Behav Brain Sci* **8,** 135.

Navas F & Stark L (1968). Sampling or Intermittency in Hand Control System Dynamics. *Biophys J* **8,** 252–302.

Neilson PD & Neilson MD (2005). An overview of adaptive model theory: solving the problems of redundancy, resources, and nonlinear interactions in human movement control. *J Neural Eng* **2,** S279–S312.

Neilson PD, Neilson MD & O'Dwyer NJ (1988). Internal models and intermittency: A theoretical account of human tracking behavior. *Biol Cybern* **58,** 101–112.

Nelson AJ, Blake DT & Chen R (2009). Digit-specific aberrations in the primary somatosensory cortex in Writer's cramp. *Ann Neurol* **66,** 146–154.

Norris SA et al. (2016). Clinical and demographic characteristics related to onset site and spread of cervical dystonia. *Mov Disord* **31,** 1874–1882.

Ondo W, Warrior D, Overby A, Calmes J, Hendersen N, Olson S & Jankovic J (2000). Computerized posturography analysis of progressive supranuclear palsy: a case-control comparison with Parkinson's disease and healthy controls. *Arch Neurol* **57,** 1464–1469.

Ostry DJ & Gribble PL (2016). Sensory Plasticity in Human Motor Learning. *Trends Neurosci* **39,** 114–123.

Panzer VP, Bandinelli S & Hallett M (1995). Biomechanical assessment of quiet standing and changes associated with aging. *Arch Phys Med Rehabil* **76,** 151–157.

Pashler H (1984). Processing stages in overlapping tasks: evidence for a central bottleneck. *J Exp Psychol Hum Percept Perform* **10,** 358–377.

Patton JL, Wei YJ, Bajaj P & Scheidt RA (2013). Visuomotor learning enhanced by augmenting instantaneous trajectory error feedback during reaching. *PLoS One* **8,** e46466.

De Pauw J, Cras P, Truijen S, Mercelis R, Michiels S, Saeys W, Vereeck L, Hallemans A & De Hertogh W (2018). The effect of a single botulinum toxin treatment on somatosensory processing in idiopathic isolated cervical dystonia: an observational

study. *J Neurol* **265,** 2672–2683.

De Pauw J, Mercelis R, Hallemans A, Michiels S, Truijen S, Cras P & De Hertogh W (2017). Cervical sensorimotor control in idiopathic cervical dystonia: A cross-sectional study. *Brain Behav* **7,** e00735.

Pelosin E, Avanzino L, Marchese R, Stramesi P, Bilanci M, Trompetto C & Abbruzzese G (2013). KinesioTaping Reduces Pain and Modulates Sensory Function in Patients With Focal Dystonia. *Neurorehabil Neural Repair* **27,** 722–731.

Peterka RJ (2000). Postural control model interpretation of stabilogram diffusion analysis. *Biol Cybern* **82,** 335–343.

Peterka RJ (2002). Sensorimotor integration in human postural control. *J Neurophysiol* **88,** 1097–1118.

Piirtola M & Era P (2006). Force Platform Measurements as Predictors of Falls among Older People – A Review. *Gerontology* **52,** 1–16.

Pintelon R & Schoukens J (2001). Measurement of frequency response functions using periodic excitations, corrupted by correlated input/output errors. *IEEE Trans Instrum Meas* **50,** 1753–1760.

Proske U & Gandevia SC (2012). The Proprioceptive Senses: Their Roles in Signaling Body Shape, Body Position and Movement, and Muscle Force. *Physiol Rev* **92,** 1651–1697.

Proville RD, Spolidoro M, Guyon N, Dugué GP, Selimi F, Isope P, Popa D & Léna C (2014). Cerebellum involvement in cortical sensorimotor circuits for the control of voluntary movements. *Nat Neurosci* **17,** 1233–1239.

Prudente CN, Hess EJ & Jinnah HA (2014). Dystonia as a network disorder: What is the role of the cerebellum? *Neuroscience* **260,** 23–35.

Prudente CN, Zetterberg L, Bring A, Bradnam L & Kimberley TJ (2018). Systematic Review of Rehabilitation in Focal Dystonias: Classification and Recommendations. *Mov Disord Clin Pract* **5,** 237–245.

Pruszynski JA & Scott SH (2012). Optimal feedback control and the long-latency stretch response. *Exp Brain Res* **218,** 341–359.

Putzki N, Stude P, Konczak J, Graf K, Diener H & Maschke M (2006). Kinesthesia is impaired in focal dystonia. *Mov Disord* **21,** 754–760.

Rajachandrakumar R, Mann J, Schinkel-Ivy A & Mansfield A (2018). Exploring the relationship between stability and variability of the centre of mass and centre of

pressure. *Gait Posture* **63,** 254–259.

Ranganathan R & Newell KM (2013). Changing Up the Routine. *Exerc Sport Sci Rev* **41,** 64–70.

Reid VA, Adbulhadi H, Black KR, Kerrigan C & Cros D (2002). Using Posturography to Detect Unsteadiness in 13 Patients With Peripheral Neuropathy: A Pilot Study. *Neurol Clin Neurophysiol* **2002,** 2–8.

Riccio, GE; Newell, KM; Corcos D (1993). Variability and motor control. *Am J Respir Crit Care Med* **168,** 317–358.

Rogers MW, Wardman DL, Lord SR & Fitzpatrick RC (2001). Passive tactile sensory input improves stability during standing. *Exp Brain Res* **136,** 514–522.

Roh J, Cheung VCK & Bizzi E (2011). Modules in the brain stem and spinal cord underlying motor behaviors. *J Neurophysiol* **106,** 1363–1378.

Romano R, Bertolino A, Gigante A, Martino D, Livrea P & Defazio G (2014). Impaired cognitive functions in adult-onset primary cranial cervical dystonia. *Parkinsonism Relat Disord* **20,** 162–165.

Rome S & Grünewald RA (1999). Abnormal perception of vibration-induced illusion of movement in dystonia. *Neurology* **53,** 1794–1800.

Rosengren SM, Welgampola MS & Colebatch JG (2010). Vestibular evoked myogenic potentials: Past, present and future. *Clin Neurophysiol* **121,** 636–651.

Rossi-Izquierdo M, Basta D, Rubio-Rodríguez JP, Santos-Pérez S, Ernst A, Sesar-Ignacio Á, Alberte-Woodward M, Amo MG-D, Estany-Gestal A, Román-Rodríguez ES, Faraldo-García A, Zubizarreta-Gutiérrez A & Soto-Varela A (2014). Is posturography able to identify fallers in patients with Parkinson's disease? *Gait Posture* **40,** 53–57.

Saffer M, Kiemel T & Jeka J (2008). Coherence analysis of muscle activity during quiet stance. *Exp Brain Res* **185,** 215–226.

Saha DJ & Morasso P (2012). Stabilization Strategies for Unstable Dynamics. *PLoS One* **7,** e30301.

Sainburg RL, Ghilardi MF, Poizner H & Ghez C (1995). Control of limb dynamics in normal subjects and patients without proprioception. *J Neurophysiol* **73,** 820–835.

Sakaguchi Y, Tanaka M & Inoue Y (2015). Adaptive intermittent control: A computational model explaining motor intermittency observed in human behavior. *Neural Networks* **67,** 92–109.

Samii A, Nutt JG & Ransom BR (2004). Parkinson's disease. *Lancet* **363,** 1783–1793.

Sanger TD, Tarsy D & Pascual-Leone A (2001). Abnormalities of spatial and temporal sensory discrimination in writer's cramp. *Mov Disord* **16,** 94–99.

Sasagawa S, Shinya M & Nakazawa K (2014). Interjoint dynamic interaction during constrained human quiet standing examined by induced acceleration analysis. *J Neurophysiol* **111,** 313–322.

Sasagawa S, Ushiyama J, Kouzaki M & Kanehisa H (2009). Effect of the hip motion on the body kinematics in the sagittal plane during human quiet standing. *Neurosci Lett* **450,** 27–31.

Scheidt RA, Reinkensmeyer DJ, Conditt MA, Rymer WZ & Mussa-Ivaldi FA (2000). Persistence of Motor Adaptation During Constrained, Multi-Joint, Arm Movements. *J Neurophysiol* **84,** 853–862.

Schlerf JE, Xu J, Klemfuss NM, Griffiths TL & Ivry RB (2013). Individuals with cerebellar degeneration show similar adaptation deficits with large and small visuomotor errors. *J Neurophysiol* **109,** 1164–1173.

Scontrini A, Conte A, Defazio G, Fiorio M, Fabbrini G, Suppa A, Tinazzi M & Berardelli A (2009). Somatosensory temporal discrimination in patients with primary focal dystonia. *J Neurol Neurosurg Psychiatry* **80,** 1315–1319.

Scott SH (2004). Optimal feedback control and the neural basis of volitional motor control. *Nat Rev Neurosci* **5,** 532–544.

Scott SH (2012). The computational and neural basis of voluntary motor control and planning. *Trends Cogn Sci* **16,** 541–549.

Sertel M, Sakızlı E, Bezgin S, Savcun Demirci C, Yıldırım Şahan T & Kurtoğlu F (2017). The effect of single-tasks and dual-tasks on balance in older adults. *Cogent Soc Sci* **3,** 1330913.

Shadmehr R & Mussa-Ivaldi FA (1994). Adaptive representation of dynamics during learning of a motor task. *J Neurosci* **14,** 3208–3224.

Soest AJ "Knoek" van, Haenen WP & Rozendaal LA (2003). Stability of bipedal stance: the contribution of cocontraction and spindle feedback. *Biol Cybern* **88,** 293–301.

Suzuki Y, Morimoto H, Kiyono K, Morasso P & Nomura T (2015). Non-actively controlled double-inverted-pendulum-like dynamics can minimize center of mass acceleration during human quiet standing. In *2015 37th Annual International Conference of the IEEE Engineering in Medicine and Biology Society (EMBC)*, pp.

1432–1435. IEEE.

Suzuki Y, Nomura T, Casadio M & Morasso P (2012). Intermittent control with ankle, hip, and mixed strategies during quiet standing: A theoretical proposal based on a double inverted pendulum model. *J Theor Biol* **310,** 55–79.

Swash M & Fox KP (1976). Normal muscle spindles in idiopathic torsion dystonia. *J Neurol Sci* **27,** 525–527.

Tanabe H, Fujii K & Kouzaki M (2017). Intermittent muscle activity in the feedback loop of postural control system during natural quiet standing. *Sci Rep* **7,** 10631.

Termoz N, Halliday SE, Winter DA, Frank JS, Patla AE & Prince F (2008). The control of upright stance in young, elderly and persons with Parkinson's disease. *Gait Posture* **27,** 463–470.

Therrien AS & Bastian AJ (2019). The cerebellum as a movement sensor. *Neurosci Lett* **688,** 37–40.

Thoroughman KA & Shadmehr R (1999). Electromyographic Correlates of Learning an Internal Model of Reaching Movements. *J Neurosci* **19,** 8573–8588.

Tinazzi M, Morgante F, Peretti A, Mariotti C, Panzeri M, Fiorio M & Fasano A (2013). Impaired Temporal Processing of Tactile and Proprioceptive Stimuli in Cerebellar Degeneration. *PLoS One* **8,** e78628.

Todorov E & Jordan MI (2002). Optimal feedback control as a theory of motor coordination. *Nat Neurosci* **5,** 1226–1235.

Todorov E & Jordan MI (2003). A minimal intervention principle for coordinated movement. *Adv Neural Inf Process Syst*27–34.

Tombu M & Jolicoeur P (2003). A central capacity sharing model of dual-task performance. *J Exp Psychol Hum Percept Perform* **29,** 3–18.

Tseng Y-T, Tsai C-L, Chen F-C & Konczak J (2018). Wrist position sense acuity and its relation to motor dysfunction in children with developmental coordination disorder. *Neurosci Lett* **674,** 106–111.

Uimonen S, Laitakari K, Kiukaanniemi H & Sorri M (1995). Does posturography differentiate malingerers from vertiginous patients? *J Vestib Res* **5,** 117–124.

Varela FJ (1979). *Principles of biological autonomy*. North Holland.

Vince MA (1948). The intermittency of control movements and psychological refractory period. *Br J Psychol* **38,** 149.

Visser JE, Carpenter MG, van der Kooij H & Bloem BR (2008). The clinical utility of

posturography. *Clin Neurophysiol* **119,** 2424–2436.

White JJ & Sillitoe R V. (2017). Genetic silencing of olivocerebellar synapses causes dystonia-like behaviour in mice. *Nat Commun* **8,** 14912.

Williams NP, Roland PS & Yellin W (1997). Vestibular evaluation in patients with early multiple sclerosis. *Am J Otol* **18,** 93–100.

Winter DA, Patla AE, Prince F, Ishac M & Gielo-Perczak K (1998). Stiffness Control of Balance in Quiet Standing. *J Neurophysiol* **80,** 1211–1221.

Winters J, Stark L & Seif-Naraghi A-H (1988). An analysis of the sources of musculoskeletal system impedance. *J Biomech* **21,** 1011–1025.

Winward CE, Halligan PW & Wade DT (1999). Current practice and clinical relevance of somatosensory assessment after stroke. *Clin Rehabil* **13,** 48–55.

Wise AK, Gregory JE & Proske U (1999). The responses of muscle spindles to small, slow movements in passive muscle and during fusimotor activity. *Brain Res* **821,** 87–94.

Wolpert D, Ghahramani Z & Jordan M (1995). Are arm trajectories planned in kinematic or dynamic coordinates? An adaptation study. *Exp Brain Res* **103,** 460–470.

Wolpert DM, Diedrichsen J & Flanagan JR (2011). Principles of sensorimotor learning. *Nat Rev Neurosci* **12,** 739–751.

Wright WG, Ivanenko YP & Gurfinkel VS (2012). Foot anatomy specialization for postural sensation and control. *J Neurophysiol* **107,** 1513–1521.

Wu HG, Miyamoto YR, Castro LNG, Ölveczky BP & Smith MA (2014). Temporal structure of motor variability is dynamically regulated and predicts motor learning ability. *Nat Neurosci* **17,** 312–321.

Yin HH & Knowlton BJ (2006). The role of the basal ganglia in habit formation. *Nat Rev Neurosci* **7,** 464–476.

Yoshikawa N, Suzuki Y, Kiyono K & Nomura T (2016). Intermittent Feedback-Control Strategy for Stabilizing Inverted Pendulum on Manually Controlled Cart as Analogy to Human Stick Balancing. *Front Comput Neurosci*.

Zenzeri J, De Santis D & Morasso P (2014). Strategy switching in the stabilization of unstable dynamics. *PLoS One* **9,** e99087.

Zhang Y, Kiemel T & Jeka J (2007). The influence of sensory information on two-component coordination during quiet stance. *Gait Posture* **26,** 263–271.